BNL-82395-2009

Fate of Contaminants in Contact with West Valley Grouts

Mark Fuhrmann and Jeffrey Gillow

July 2009

Environmental Sciences Department/Environmental Research & Technology Division

Brookhaven National Laboratory
P.O. Box 5000
Upton, NY 11973-5000
www.bnl.gov

DISCLAIMER

Fate of Contaminants in Contact with West Valley Grouts

DRAFT

August 18, 2005

Revised July 22, 2009

Mark Fuhrmann[1] and Jeffrey Gillow[2]

Environmental Sciences Department

Brookhaven National Laboratory

Upton, NY 11973-5000

1. **Currently at U.S. Nuclear Regulatory Commission, Rockville, MD 20852**
   mark.fuhrmann@nrc.gov

2. **Currently at Arcadis, 630 Plaza Drive, Highlands Ranch, CO 80129**
   jeff.gillow@arcadis-us.com

Table of Contents

INTRODUCTION

The objective of the work described here is to determine to what extent a variety of contaminants, including fission products, actinides, and RCRA elements are sequestered by the two grout formulations. The conceptual model for this study is as follows: a large mass of grout having been poured into a high-level waste tank is in the process of aging and weathering for thousands of years. The waste remaining in the tank will contain radionuclides and other contaminants, much of which will adhere to tank walls and internal structures. The grout will encapsulate the contaminants. Initially the grout will be well sequestered, but over time rainwater and groundwater will gain access to it. Ultimately, the grout/waste environment will be an open system. In this condition water will move through the grout, exposing it to O_2 and CO_2 from the air and HCO_3^- from the groundwater. Thus we are considering an oxic environment containing HCO_3^-.

Initially the solubility of many contaminants, but not all, will be constrained by chemistry dominated by the grout, primarily by the high pH, around 11.8. This is controlled and buffered by the portland cement and blast furnace slag components of the grout, which by themselves maintain a solution pH of about 12.5. Slowly the pH will diminish as $Ca(OH)_2$ and KOH dissolve, are carried away by water, and $CaCO_3$ forms. As these conditions develop, the behavior of these elements comes into question. In our conceptual model, although the grout is formulated to provide some reducing capacity, in order to be conservative this mechanism is not considered. In addition to solubility constraints imposed by pH, the various contaminants may be incorporated into a variety of solid phases. Some may be incorporated into newly forming compounds as the grout sets and cures. Others (like soddyite, $(UO_2)_2SiO_4(H_2O)_2$) are the result of slower reactions but may become important over time as contaminants are exposed to evolving chemistry in the grout. Still other solid phases may form from reactions between the waste and grout components, not only the cementitious materials, but also the additives used in the grout. Another process that may exert some control on contaminant concentrations is adsorption onto solids within the grout. These may be additives such as the fluorapatite or zeolite that are substantial percentages of the grouts or they may be minerals, typically Ca-Al-Si materials, that form in the grout system as cement sets. In

addition, as the grout weathers over time, $CaCO_3$ minerals, such as calcite and aragonite, will form as a rind on the grout and as a fracture filling mineral. Some contaminants are likely to be incorporated into these minerals, to a greater or lesser extent, as they precipitate. For some elements, such as U, there is a significant literature exploring the incorporation into $CaCO_3$, but for others there is essentially no information. This is also the case for much of the chemical regime of the grouts. Initial conditions are at pH values around 12 and information is often sparse.

Objectives.

To develop information on the behavior of a wide range of contaminants that are present in the West Valley Tanks, an experimental program was conducted that explored contaminant sorption/desorption/solubility in the presence of the grout and individual components of the grout under alkaline conditions. As the grout ages and weathers over long times, the pH will decrease, weathering products (especially calcium carbonate minerals; calcite, aragonite and vaterite) will precipitate, and the chemistry of water flowing through the grout will be altered. The impact of these changing conditions on the fate of contaminants that were initially sequestered, was explored for U, Pu, Am, Cm and Np. Topics of this work were:

1) develop adsorption isotherms for 20 elements, including fission and activation products, actinides, and RCRA elements.
2) determine the behavior of actinides as the chemistry of the aging grout system is altered.
3) determine the relationships among pH, water chemistry, and water flow through the grout as it controls the fate of uranium.

Specific objectives were to:

1) Assess the sorption behavior of contaminants through isotherms
2) Determine if actinides, that had been sequestered in contact with the two grouts, return to solution as the grouts age.
3) Determine if actinides sequestered with the aged grouts return to solution on contact with increasing concentrations of $KHCO_3$.

4) Determine the behavior of actinides that have precipitated in a simulated grout pore water (without grout present), as the pH is lowered or $KHCO_3$ content is increased.
5) Determine the behavior of actinides in simulated grout pore water in contact with the components of the grout: portland cement, blast furnace slag, fly ash, zeolite, and fluorapatite.
6) Compare the concentrations of actinides in "new" and "aged" experiments as $KHCO_3$ is added.
7) Identify newly formed solid phases that influence concentrations in the batch experiments.
8) Determine pH, U and other elemental concentrations in column effluent relative to pore volumes flowing through the grout.

The addition of carbonate ions was used to drive the chemical system toward the presumed endpoint of a cementitious material (Berner, 1992); that is a heavily carbonated condition where the pH is substantially lower than the pH 12 of the initial grout. This approach allowed observation of elemental behavior under conditions expected over long times as: 1) carbonate in solution increases, 2) carbonate minerals develop, and 3) pH is lowered. $KHCO_3$ was used as a source of carbonate because K is a major element released during cement leaching. There was a concern about formation of low solubility U and K compounds, but geochemical modeling indicated that their formation was unlikely.

EXPERIMENTAL METHODS

Batch Experiments

RCRA Element Isotherms

Isotherm experiments for RCRA elements exposed to the grout materials were conducted as follows. For each element contact solutions were prepared at five concentrations, consisting of distilled/deionized water to which the tracer solutions were added. The starting volume was held constant at 55 mL, with the quantity of water being changed to accommodate the required volume of tracer. The tracers were made by dissolving

weighed quantities of soluble salts (reagent grade) of the various metals into distilled water to produce a high concentration (several thousand mg/L) stock solution of each element. Some of this solution was diluted 100-fold to produce a low concentration stock solution. Each tracer was added to the experiment to produce the contact solution as illustrated in Table 1, typically giving a 200-fold range in concentration. Reference solutions were also made using the same dilutions as the samples and were used for direct comparison of concentrations before and after exposure to the grout. For each experiment 2.00 g of the grout were added to each bottle. In addition to the experimental samples and the references, several blanks, consisting of different concentrations of just the spiked water, were treated as samples. For most elements, a kinetics experiment was run, for each grout, to determine the appropriate contact time. At the end of the experiments, aliquots were removed from each sample with 5 mL syringes, filtered through 0.2 μm surfactant free cellulose acetate (SFCA) syringe filters, acidified and analyzed by Inductively Coupled Plasma Optical Emission Spectroscopy (ICP). All analysis was done using NIST traceable standards from SPEX CertiPrep, Inc. Typically a wavelength calibration was done at the start of each run and the instrument was recalibrated after each 12 samples.

Table 1. Example of Dilutions and Tracer Concentrations in Experiments

Relative Concentration In Experiment	Water Volume (mL)	Nominal Tracer Concentration (mg/L)	Tracer Volume (mL)
1	54	55	1.00
10	55	5500	0.10
50	54.5	5500	0.50
100	54	5500	1.00
200	53	5500	2.00

For some elements isotherm experiments were conducted, not just on the grouts, but on the individual components of the grout as well. In these experiments, the same procedure, including liquid to solid ratio (25:1), was used. However, to reproduce the high pH chemistry of the grout/solution mixture, the contact solution for the individual

components was a mixture of 1.2g of $Ca(OH)_2$ and 0.47 g of KOH. This solution was filtered through a glass-fiber TCLP filter and stored in glass containers for only very short times before use. This solution composition was based on analysis of water in contact with the cement used in the grout mixture.

Radionuclide Isotherms

Isotherm experiments for radionuclides exposed to grout were set up in a manner similar to the RCRA elements. The liquid to solid ratio was the same but the approach to adding the tracers varied somewhat. In most cases, radionuclides were obtained in 10 μCi quantities from the supplier, although ^{99}Tc was 100 μCi, and ^{14}C was 1 mCi. These were diluted serially as needed, usually into three solution concentrations. In some cases, there were changes in this procedure to accommodate the behavior of different tracers and these are mentioned below.

Data Analysis For Isotherms

Data were entered into Excel spread sheets. To determine the quantity of the element of interest that was sorbed, measured solution concentrations from the experiments were subtracted from reference solution concentrations. The total mass of the sorbed element was determined and the mass per gram sorbed on the solid was calculated. Values of K_d were calculated for each sample by eq. 1 at steady-state.

$$K_d = [\text{element on solid}] / [\text{element in liquid}] \qquad \text{eq. 1}$$

They were also determined from the isotherms, which provide a better assessment of the K_d. Isotherm plots were generated by graphing the steady-state concentration of the element of interest remaining in solution (x-axis) against its concentration on the sorbing solid. For linear isotherms over the concentration range plotted, the slope is the K_d. For non-linear isotherms, Freundlich isotherms were generated. The Freundlich isotherm equation is:

$$A_i = K_f \ C_i^N \qquad \text{eq.2}$$

where A_i is the quantity of the element of interest that is sorbed on the solid, per gram of the solid.
K_f is the Freundlich constant
C_i is the concentration of the element of interest remaining in solution at steady-state and N is a constant.

To extract K_d, the Log values of the data were plotted with Log A_i on the y-axis and Log C_i on the x-axis. From this plot, the slope is N and the intercept is Log K_f. Essentially, this is a log transform of equation 2:

$$\text{Log } A_i = \text{Log } K_f + N \text{ Log } C_i \qquad \text{eq. 3}$$

Since $A_i/C_i = K_d$, then $K_f = K_d$ when N is close to 1.

Grout and Actinide Batch Experiments

Approach

The approach in the batch experiments was to determine actinide concentrations in solution as $KHCO_3$ is added and the pH, as a result, decreases from the high values maintained by the cement. The radionuclides studied were natural U, ^{237}Np, ^{239}Pu, ^{241}Am, and ^{244}Cm. While the groundwater at the site has HCO_3^- content between 0.0015 and 0.0035 M we have assumed that atmospheric CO_2 will be available to react with the grout. Consequently we have driven the system with additions of $KHCO_3$ up to about 0.1 M to obtain pH values expected for a weathered and leached concrete. We have examined this behavior for the actinides using the two grouts, their individual components, and a set of simulated pore water experiments in which the pH was decreased and the $KHCO_3$ content increased. These experiments, and geochemical speciation modeling with Geochemists Workbench, provide basic information on the solubility of these elements under conditions controlled by the various solids in which they are in contact.

Materials

Two grout formulations were prepared based on formulae provided by West Valley. For Grout 21, the composition was: 7.6% cement, 32.6% fly ash, 10% zeolite, 12.5% slag, and 37.2% water. For Grout 26, it was 8.9% cement, 42.2 % fly ash, 12.0% apatite, 13.0% slag, and 23.9% water. As instructed, the criteria for the mixture is based on a slump test and the quantity of water may be reduced to meet the slump test criterion of a circle of 10 to 12 inches diameter after 30 seconds. For Grout 26, a batch was made consisting of component weights that were 20 times their respective percentages. The slump test for this material resulted in a circle of 11.5 inches. For Grout 21, only 71% of the water was used and a circle of 10.8 inches was obtained. The grout was allowed to cure for 7 days and was then lightly crushed so that it passed through a # 20 (< 0.84mm) sieve. The material was stored under high purity nitrogen for future use. Some experiments used the individual components that went into producing the grout.

The contact solution used in the experiments was based on porewater taken from the cement used in the grout. It consisted of 1.20 g /L of $Ca(OH)_2$ and 0.47 g/L of KOH. After sitting overnight the solution was filtered through a glass-fiber filter under pressure and stored in a glass-stoppered bottle. This solution had a pH of 12.3.

Methods

The samples for some grout experiments were originally batch isotherm experiments used for K_d determinations, that were set up in spring of 2003. They contained 2 g of solid and 55 g of contact solution and tracer. They consisted of the two grouts exposed to a Ca/K OH contact solution (pH = 12.3). This choice of contact solution was made to simulate the pore-water of the grout as it is controlled by portland cement. Tracer concentrations in the initial solutions varied by a factor of about 200. These experiments were allowed to age for about 550 days and were then resampled (5 mL samples filered through 0.22 μm syringe filters), the pH measured, and 1 or 2mL aliquots of 1M $KHCO_3$ were added. This was repeated several times to determine the impact of elevated HCO_3^- on tracer concentrations in the contact solution in the presence of the solids. This set of

experiments is referred to as the "aged" experiments. The experiments with the lowest U concentrations were also sampled for analysis of Ca, K, Si, Al, Fe, Mg, Na, P and U.

A second set of batch experiments was set up to determine in more detail how actinide concentrations change in contact with the two grouts, the individual component materials and simulated pore water, as the HCO_3^- content increases. In all cases the contact solution was the Ca/K OH solution. In the case of U these experiments consisted of 8.0 g of solid and 200 mL of contact solution. Uranium was added (1 mL of 10,000 mg/L NIST Standard) as U(VI) nitrate in HNO_3. Smaller experiment volumes were used for other actinides but the same solid to liquid ratio were used. One mL aliquots of 1 M $KHCO_3$ were added at each sampling interval, after having taken and filtered a 5 mL sample and measured the pH. At least 48 hours were allowed to pass between samplings. pH was measured at the time of each sampling. These are referred to as the "new" experiments. Simulated pore water experiments were set up to assess the effect of $KHCO_3$ addition with no solids present. These consisted of the contact solution with tracer added as above. Otherwise they were treated as one of the experiments, with addition of $KHCO_3$ and filtration during sampling. Another set of solutions was made in the same way but aliquots of 1 molal HNO_3 were added to adjust the pH. These served as references against which experiments that did contain solids could be compared.

Column Experiments

Approach.

The four column experiments were conducted to assess of changing U concentrations, pH and other chemical parameters, over time, as a simulated West Valley groundwater flowed through the grouts. These data, parameterized in terms of pore-volumes, can be extrapolated to long times, based on groundwater modeling estimates of the number of pore-volumes per year expected to flow through the system. In this way the chemistry of U in the grouts can be described in terms of time. Two of the columns, one of each formulation, contained uranium and two did not. These control columns were used primarily as replicates for pH and to make sure that no U was found in leachate from the grout itself.

Materials.

Two grout formulations were prepared based on formulae provided by West Valley. For Grout 21, the composition was: 7.6% cement, 32.6% fly ash, 10% zeolite, 12.5% slag, and 37.2% water. For Grout 26, it was 8.9% cement, 42.2 % fly ash, 12.0% apatite, 13.0% slag, and 23.9% water. As instructed, the criteria for the mixture is based on a slump test and the quantity of water may be reduced to meet the slump test criterion of a circle of 10 to 12 inches diameter after 30 seconds. Based on an earlier determination, each batch for the column experiments was made to a mass of 200 g.

For the materials receiving uranium, 3 mL of a NIST uranium standard were pipetted into the grout as it was being mixed, after most of the water had been added. This standard contained 10,000 mg/L in 10% nitric acid. For the column materials that did not contain uranium, 3 mL of 10% nitric acid were added. The grout was allowed to cure for 54 days in sealed containers and was then lightly crushed so that it passed through a # 20 (<0.84mm) sieve. The material was stored under high purity nitrogen for future use.

Flow-through column experiments.

Four flow-through column experiments were conducted; the two grout formulations, G-21 and G-26, containing U at 0.15 mg/g and the two grouts containing no U. The column barrels had internal dimensions of 3.2 cm in diameter and 6.2 cm in height. End caps and grid plates added a small amount of dead space that contains fluid but not any grout. The grouts were added with water present in the columns to allow it to settle readily. The volume of water displaced and the mass of grout used were measured. The plexiglass columns were sealed with o-rings and plastic grids from filter assemblies. A Gilson Minipuls 2 peristaltic pump was used with 1.85 mm inside diameter pump tubing. Figure 1 is a photograph of the experimental set up.

Figure 1. Experimental set-up for the grout columns during the tritium pulse test using a fraction collector.

In Figure 1 the four one liter reservoir bottles partially obscure the peristaltic pump. The two columns containing U are shown with the influent tubes entering the bottom of the columns and the effluent tubes leading into 1 liter Tevlar sampling bags (SKC catalog # 232-01) that were evacuated prior to use. These bags have a valve on them that allows the sample to be sealed just before being removed from the effluent tube. The figure also shows the fraction collector that was used during the tritium pulse experiment. When the bags were changed, the weight of each filled bag was taken and an aliquot (about 15 mL) removed and analyzed for pH. For those samples used for other analysis, a sub-sample was withdrawn for HPLC or UV-Vis spectroscopy (in which the sample must not be acidified), then 1 mL of 20% HNO_3 was pipetted into the bag. The bag was manipulated to stir the contents and then poured out into polyethylene bottles. The acidified effluent was used for ICP analysis. Not all samples were analyzed. Initially every fifth sample was analyzed for U, Ca, Si, Al, Mg, Fe, Na, and K. From Interval 45 on, every other sample was analyzed for U. Initial analysis was done by ICP, then samples were

reanalyzed by Kinetic Phosphorescence Analysis (KPA) (Model KPA-11, ChemChek Instruments, Inc.) to obtain much lower detection limits. One mL samples were diluted

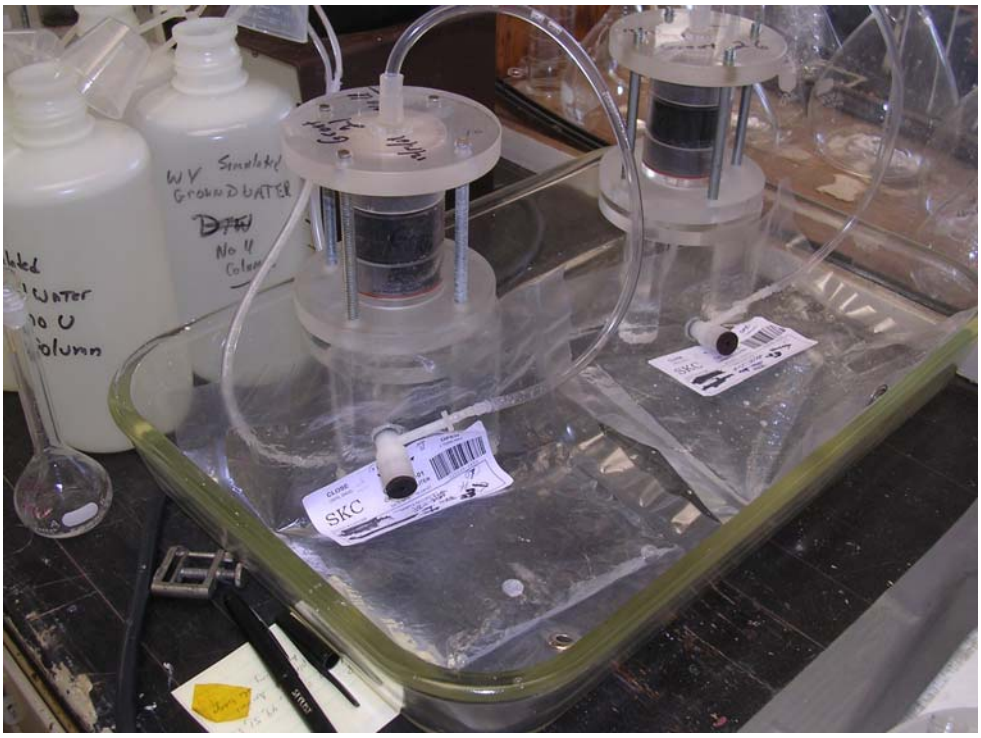

Figure 2. Grout columns showing the Tevlar collection bags.

with deionized water to eliminate interferences from other elements in the samples. Standards were run periodically as were instrument response check samples and blanks of effluent from columns that do not contain uranium. The detection limit of this method is 1 ug/L. For both the ICP and KPA methods standards traceable to NIST were used.

Pore Volume Determination.

To determine the pore volume of each U bearing column, a ^{3}H (tritium) slug test was conducted. A solution of simulated West Valley groundwater was made, containing 0.2 μCi of tritiated water in 50 mL (grout 21) and 60 mL (Grout 26). The inlet tube, leading to the peristaltic pump, was placed into the tracer solution which was allowed to run for 4-8 hours. The tube was then placed back into the regular groundwater reservoir. From the start of the tracer flow, effluent from the column was taken with a fraction collector.

For Grout 21 samples were taken every 10 minutes until interval 51. Samples were then taken every 30 minutes over about 14 hours. For Grout 26, samples were initially taken every 20 minutes and then changed to 30 minutes after interval 23. The volume of each fraction was determined by weight. One mL aliquots of samples were pipetted into scintillation vials containing 14 mL of Ultima Gold scintillation cocktail. These were counted for 10 minutes on a Wallac Model 1400 DSA liquid scintillation counter. A sample of the starting tracer solution was counted as a reference. Data from the tritium slug tests are shown in Figure 3. These tests were run after the columns had been flowing for 120 and 151 days for Grouts 21 and 26 respectively. Parameters for the two columns containing U are given in Table 2.

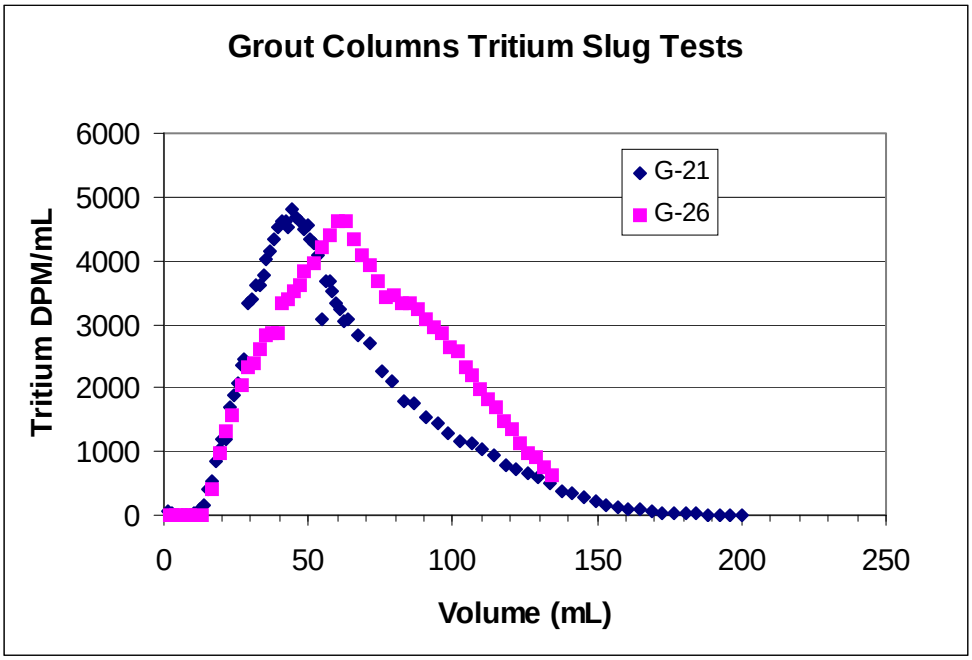

Figure 3. Results of tritium slug tests to determine porosity of columns.

Table 2. Parameters for Columns

Column	Column Volume (mL)	Flow Rate (mL/hr)	Grout Mass (g)	Pore Volume (mL)	Duration (days)	Total Volume (mL)	Number Of Pore Volumes
Grout 21 uranium	49.9	9.96*	46.08	23	152	27,098	1178
Grout 26 uranium	49.9	9.29*	50.96	27.8	152	25,643	922

* taken at the mid-point of the experiment at interval 44.

Analytical Methods

Sampling

For all batch experiments samples were taken with 5 mL plastic syringes and the liquid was passed through a Whatman syringe filter (SFCA membrane, 0.22 μm pores). Aliquots of 2 to 20 mL were collected as needed.

pH and Oxidation Reduction Potential (ORP) Measurements

For stable elements measurements of pH were made with a Cole-Parmer, Ross type pH combination electrode and a Corning model 313 pH meter. NIST tracable standards from LabChem Inc were obtained at pH values of 7, 10, 12 and 13. Because this meter could not be calibrated beyond pH 10, high pH standards were measured and a correction calculated. This turned out to be linear from pH 7 to 13 and was therefore applied to the sample measurements. The ORP was measured on the same meter using a Corning platinum Redox electrode. Measurements were calibrated with an excess of hydroquinone added to pH standards. There is an effect of pH on ORP and the use of the pH standards plus hydroquinone allowed a correction for this effect. For experiments containing radionuclides, pH was measured at the time of sampling with an Orion pH meter and a gel type probe. The meter was calibrated with NIST traceable pH 7 and 10 or 12 standards.

ICP-OES

Uranium and other elements of interest were analyzed by Inductively Coupled (ICP) Plasma Optical Emission Spectroscopy (Varian, Liberty 100). Commercial NIST traceable multi-element standards from Specs CertiPrep were used for most elements. For U, a single element standard from NIST also was obtained.

Radionuclide Analysis

Gamma-ray emitting tracers were analyzed on intrinsic germanium gamma-ray spectrometers run by Canberra spectroscopy software. After filtration, 5 mL samples were pipetted into plastic vials and counted. Counting times varied, depending on activity, from several minutes to 1000 minutes. When possible, samples were counted in pairs, with the reference and the related sample counted one after the other, this is especially so for short lived radionuclides where decay must be accounted for.

For pure beta-emitting samples, liquid scintillation analysis was done. After filtration, 1 or 2 mL samples were pipetted into scintillation vials containing 18 mL of Packard Ultima-Gold scintillation fluid. The vials were weighed before and after the samples were added. These samples were counted on a Wallac model 1414 WinSpectral Guardian liquid scintillation counter, for times ranging from 5 to 60 minutes. Count rates were normalized to the weight of the sample aliquot. Similarly, some of the alpha-emitting samples were counted in this way. This was only possible in cases where isotopic purity and long decay times minimized concerns with daughter isotopes growing into the sample. This counting system can distinguish between alpha and beta emitters.

X-ray absorption near edge spectroscopy

To determine the oxidation state of uranium in association with the grout, aged and unaged samples of grout containing U were analyzed by x-ray absorption near edge structure (XANES) at beamline X-15B at the National Synchrotron Light Source. A small quantity of grout was placed in a polyethylene sample cell with 6 μm thick polypropylene film on each side. Incident energy was scanned through the M_V edge of U

from 3500 to 3620 eV. A germanium x-ray detector was used with count times of 4 seconds per pixel. The sample chamber was filled with helium to reduce absorption of emitted x-rays by air at the low energies used. Two calcite standards were also run, one containing U(IV) and the other U(VI).

X-ray Microprobe and Microdiffraction

Microbeam x-ray techniques were used at beamline X-26A at the National Synchrotron Light Source at Brookhaven National Laboratory. The incident energy was tuned to 17.2 keV and the spot size was 5 x 8 μm. X-ray fluorescence (XRF) and x-ray diffraction (XRD) were performed simultaneously with the beam focused on selected locations of the samples. These methods provide identification of the mineral phases and associated elemental composition. For XRF, count times were 100 seconds using a 9-element Ge detector. For XRD, we used a Bruker SMART 1500 CCD area detector with count times of 120 seconds. Samples of the precipitate from the U control experiments were pipetted into a small cup and rinsed several times with distilled water. A drop of water and particles was placed on Kapton tape, the water was removed and another piece of tape sealed the sample. For the crystals taken from the aged experiments, a small group of material was scraped from the side of the experiment container and placed on Kapton tape.

Single Crystal X-ray Diffraction

Crystals of the new mineral growing in the batch experiments were collected from three of the U containing batch experiments. They were rinsed with distilled water and individual crystals were mounted on a glass fiber. Measurements were made on a Bruker P4 with a SMART1000 CCD detector. Radiation type was Mo (lambda = 0.71073Å). Monochrometer was a graphite single crystal cut along (111). Beam size was collimated to 0.8mm. Sample to detector distance was 5.016cm calibrated using a natrolite crystal from Horseshoe Dam, AZ. Data were collected using -0.3° phi and omega rotations to obtain a hemisphere of reflections out to 0.75Å in reciprocal space. Initial unit cell determinations were made in the Bruker program SMART. These unit cell parameters where further refined along with data integration in the program SAINT. Absorption

corrections were performed in the program SADABS. Structure solution was performed by direct methods and refined by least squares in the SHELXL-97 suite of software. Difference Fourier maps were searched until all significant residual electron density was accounted for. This work was done at the Geosciences Department at SUNY Stony Brook, thanks to Aaron Celestian and Prof. John Parise.

Geochemical Modeling

The solid and solution uranium species were modeled using Geochemist's Workbench (GWB) (Rockware, Golden, CO), a PC-based aqueous geochemical simulation program. The Lawrence Livermore National Laboratory thermodynamic database was used to provide values for stability constants of soluble species and solubility products for mineral species (Delaney and Lundsen, 1989). This database was customized by the addition of reactions for U species from the most recent literature (NEA, 2005).

RESULTS

The first results presented set the chemical environment of the grout system. These results include both batch and column experiments and are generally based on the uranium experiments because its low specific activity allowed us to perform other analyses on these materials. Included is a discussion of oxidation/reduction potential measurements as well as analysis of some solid materials by x-ray methods that help define behavior of the system. Following this, results are arranged by element, with U presented first, followed by the other actinides, other radionuclides, and then the RCRA and other elements. For the actinides both the isotherms and the desorption/solubility results are combined, while only isotherm experiments were generated for other elements.

Chemical Setting of the Grout System

Evolution of pH

pH in Batch Tests. The pH of water in contact with the two grouts was measured at various times in the RCRA element kinetics experiments. Solution pH was strongly controlled by the grout and there was no change in pH caused by the presence of the different contaminants. Figure 4 is a composite of pH values taken from the metal kinetics uptake experiments at different times. The pH rose within a day or two to around 12.6 followed by a slight decline over time. Initially, Grout 21 had a lower pH than did Grout 26, but by only a few tenths of a unit. This is likely due to the presence of the zeolite that reacts with alkaline media. After about 100 days, there is no difference between the two grouts. At that time the scatter increased among samples and may indicate that carbonation is beginning to take place. At this alkalinity CO_2 is readily dissolved into the solution, reacting with Ca to form calcium carbonate and reducing the pH very slightly.

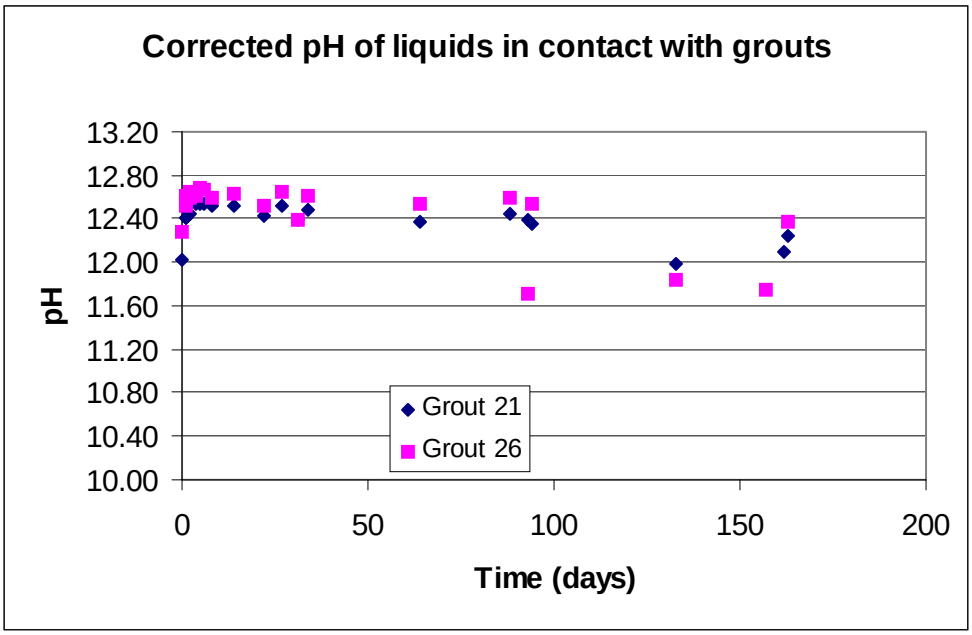

Figure 4. Corrected pH values of water in contact with the two grouts.

Figure 5 shows the solution pH, after 54 days, from the Cr experiment in which the individual grout components were examined. Most values are around 12.6 but those for the zeolite tend to be closer to 11, illustrating that zeolite does react with the alkaline medium and is indeed the reason that the grout containing zeolite has a lower pH. From this, it is apparent that a relatively small compositional fraction of the grout can alter the pH of the system fairly significantly. However, in the grout this effect is quite small because of the reserve alkalinity retained in the cement and slag solids. Another point taken from these data is that contact with relatively large quantities of contaminants (e.g. 200 ppm of Cr) does not alter the pH.

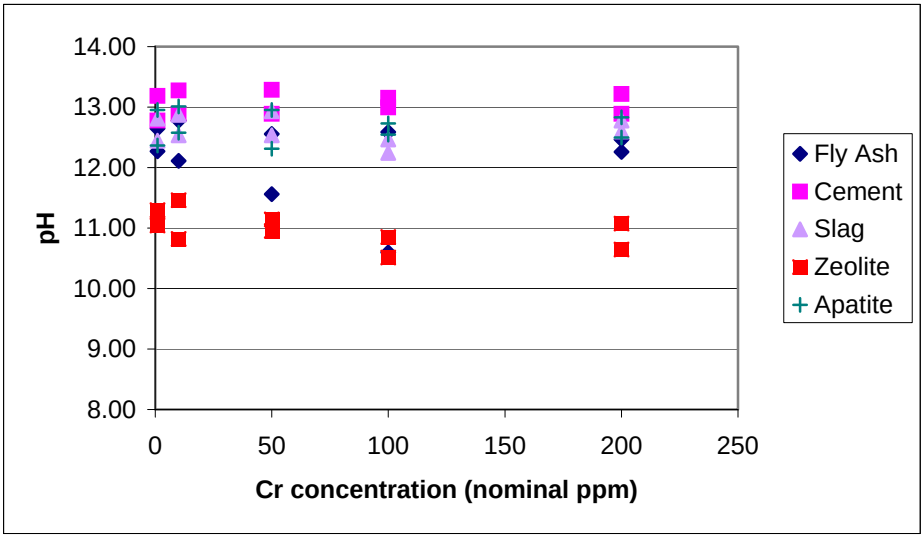

Figure 5. pH of samples of the grout components in contact with different concentrations of Cr, after 54 days.

pH in Column Tests. In all of the columns the initial pH was around 12, with the first samples from the two grout 21 columns being 11.83 and 11.93 while the initial effluent of the two grout 26 columns were 12.00 and 12.08. The pH of all columns fell slowly to about 8.2 after 150 days. Toward the end of the experiments, the pH of the two columns containing U tended to become more scatted than those without U. It seems unlikely that this is the results of the presence of the U tracer. Results for the uranium containing columns are shown in Figure 6 and for those without uranium in Figure 7.

As discussed by Berner (1992), in carbonate rich groundwater, portland cement will maintain porewater pH in excess of 12 for about 1100 pore volumes and by 7500 pore volumes the pH would be about 11. The tank backfill grout behaves very differently, as one would expect, since it contains materials other than portland cement. In our experiments, by 1000 pore volumes, the pH was about 8.4. Our batch experiments showed that zeolite and fly ash reacted to substantially reduce pH of the contact solution and as a result even the initial pH of leachate from the grout columns was less than would be expected for cement alone.

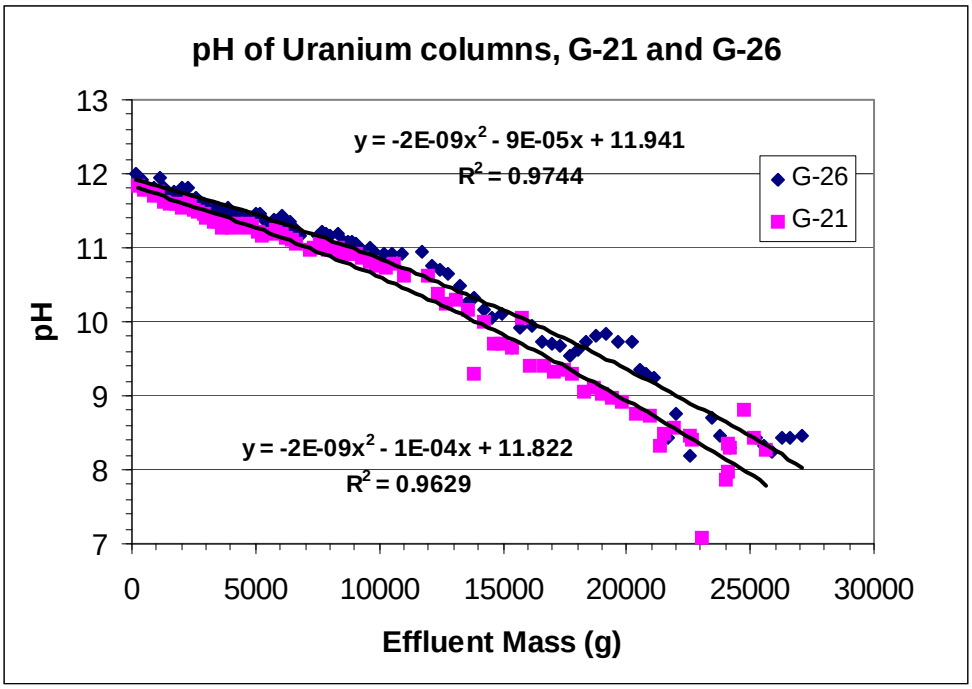

Figure 6. Evolution of pH from the two grouts containing uranium over a period of 152 days or about 1100 pore volumes. Polynomial trend lines are fit to each data set.

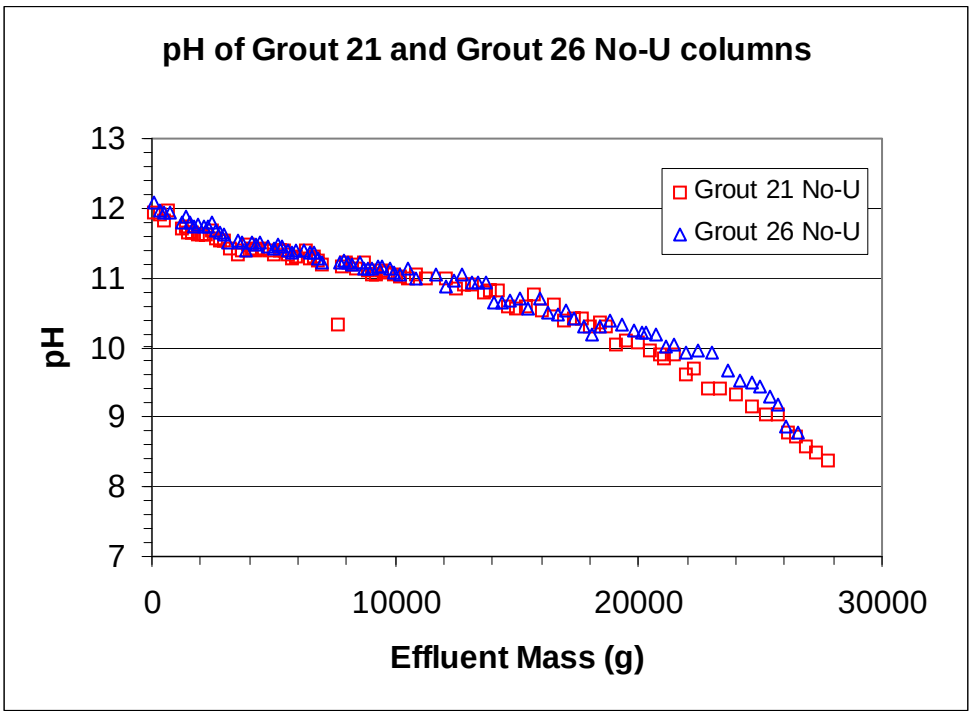

Figure 7. Evolution of pH from the two grouts that did not contain uranium, over a period of 154 days.

The behavior of the static (batch) experiments was quite different than that of the flow-through (column) experiments. Initial pH in the static system was slightly higher and was maintained at much higher levels over 150 days than in the dynamic systems. The static experiments started at pH 12.5 and over 150 days decreased to about 12.1. Over longer times the pH of static experiments decreased more, often to around 10 after 500 days. In contrast, over a 150 day period, the pH of the flow-through systems all decreased to around 8.2. Two major differences exert control over pH. The first is that in the flow-through tests, each gram of grout was exposed to about 20 times more water than in static tests. In the grout 21 column, each gram of solid was exposed to 588 g of water and in the grout 26 column it was 503 g of water. In the static tests each gram of solid was exposed to only 25 g of water. The second factor is that during the flow-through tests significant quantities of reactive elements (e.g. Ca, OH) were removed from the system with the outflowing liquid. Both types of experiments involved exposure to carbonate/bicarbonate that resulted in formation of $CaCO_3$ minerals, but the methods of carbonate introduction were different. In the static experiments CO_2 was drawn from the air. This was limited by well sealed containers but some CO_2 did access the experiments over long times. In the column experiments, a simulated West Valley ground water was used and this contained bicarbonate. In a sense, one could view these experiments as end-members in a set of scenarios for the grout, that range from static (mostly closed system) to a flow-through (open) system.

Evolution of ORP

Values of ORP were determined at one hour and 11 days, as the grout component materials reacted with the alkaline contact solution and with deionized water. These results are given in Table 3 along with pH measurements taken at one hour for the DIW samples. In the distilled water, the ORP was slightly negative for the cement and blast furnace slag. After one hour, the ORP values of fly ash and zeolite samples were not substantially different than water, but after 11 days they were reduced. The slag samples had the lowest ORP at –162mV. In the alkaline contact solution, after one hour, all samples were negative, ranging from -4 to –43 mV. These values all decreased by 11 days. Again, blast furnace slag values were the lowest averaging -112 mV. The lower

ORP values in the contact solution is typical and is an effect of the elevated pH of the contact solution.

Table 3. ORP and pH of Grout Components in Replicate

	Solution	**ORP (mV)** 1 hour	**pH** 1 hour	**ORP (mV)** 11 days
Cement	DIW	-15, -22	12.66, 12.66	-36, -45
	Contact	-22, -27		-59, -60
Apatite	DIW	48, 73	8.08, 7.89	92, 77
	Contact	-42, -43		-60, -60
Blast Furnace slag	DIW	-9, -7	10.89, 10.82	-163, -162
	Contact	-27, -35		-82, -141
Fly Ash	DIW	221, 225	6.50, 6.68	158, 149
	Contact	-14, -17		-48, -49
Zeolite	DIW	213, 215	8.72, 8.69	56, 90
	Contact	-4, -10		-23, -21

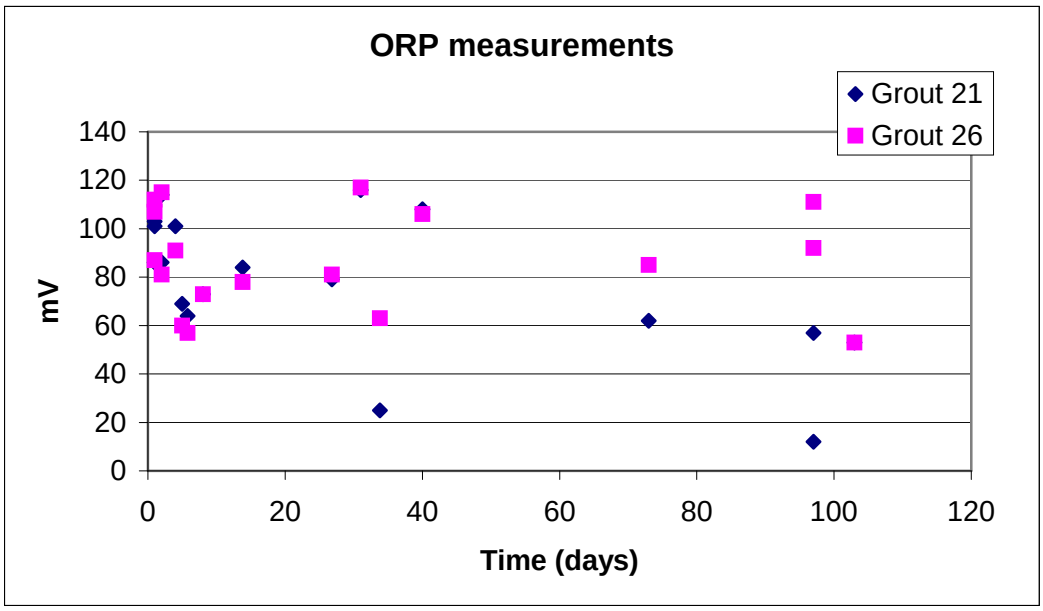

Figure 8. The measured ORP of solutions on contact with grouts from the various metals kinetics experiments.

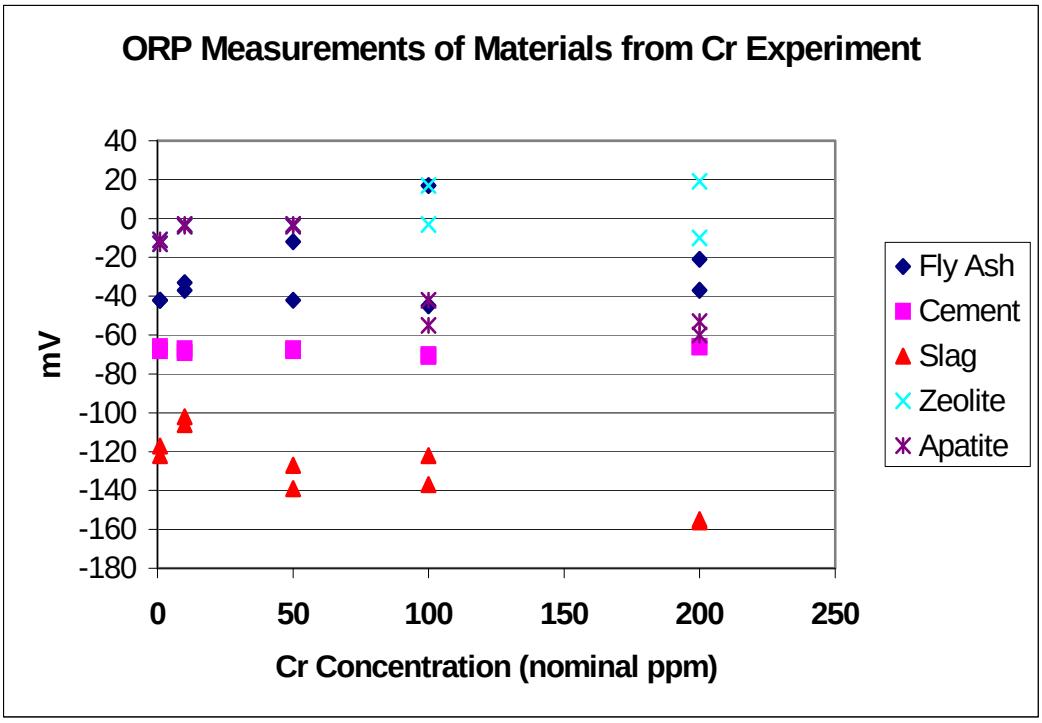

Figure 9. ORP measurements for solutions of the Cr sorption experiments, after 54 days.

Evolution of ORP from the grouts themselves is shown in Figure 8. These values initially rose to as much as 115mV and then rapidly declined to as low as 60 mV. By 100 days the ORP averaged about 70 mV, with scatter of ± 50 mV. Figure 9 shows ORP measurements conducted on the materials experiments for Cr uptake. These experiments are the same as shown in Figure 5 for pH. These results are similar to in Table 3 for the grout materials (no contaminants added) at 11 days. Again the slag had the lowest values while the fly ash and zeolite had the highest. The Cr contaminant is the highest concentration in the waste and is an oxidizer, nevertheless, Figure 9 indicates that there is no deleterious effect, with respect to ORP, from the addition of the contaminant ion. Comparing the ORP values from the component experiments with those measured for the grouts, at similar times, it is apparent that the ORPs for the grouts are consistently higher.

X-ray Absorption Spectroscopy of Oxidation State of Cr and U in Solids

The mechanism for retention of Cr in grouts such as these would be expected to be reduction of the Cr from the Cr^{+6} form to the much less soluble Cr^{+3} form. The slag would be expected to provide the reducing capacity. Instead we see much more retention on the cement phase and only limited activity by the slag. To investigate this behavior a set of the solids from these experiments, and a contact solution for reference, were analyzed by X-ray Absorption Near Edge Structure (XANES) at Beamline X23A2 at the National Synchrotron Light Source at Brookhaven National Laboratory. This technique was used to determine the oxidation state of Cr in the samples. Figure 10 shows a set of XANES scans of Cr. The sharp peak at 5995 keV is a pre-edge feature of Cr^{+6} that is diagnostic for Cr^{+6} because Cr^{+3} has essentially no feature in the pre-edge region. The height of this peak, from a normalized spectrum, can be used to determine the percentage of Cr^{+6} in the sample. As detailed in Figure 11, the contact solution is entirely Cr^{+6} and so too is the Cr sorbed on the cement and grout 26. This is a surprise since one generally considers the reduction of Cr^{+6} to Cr^{+3} as a necessary step in immobilizing Cr. We suspect that the chromate ion is substituting for sulfate as the cement reacts and

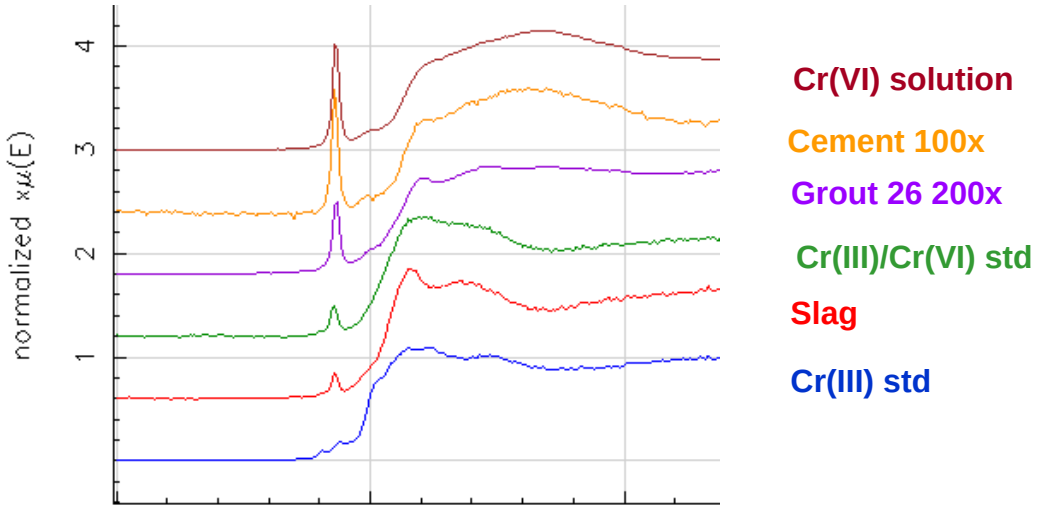

Figure 10. XANES spectra of Cr on various materials from the grout system.

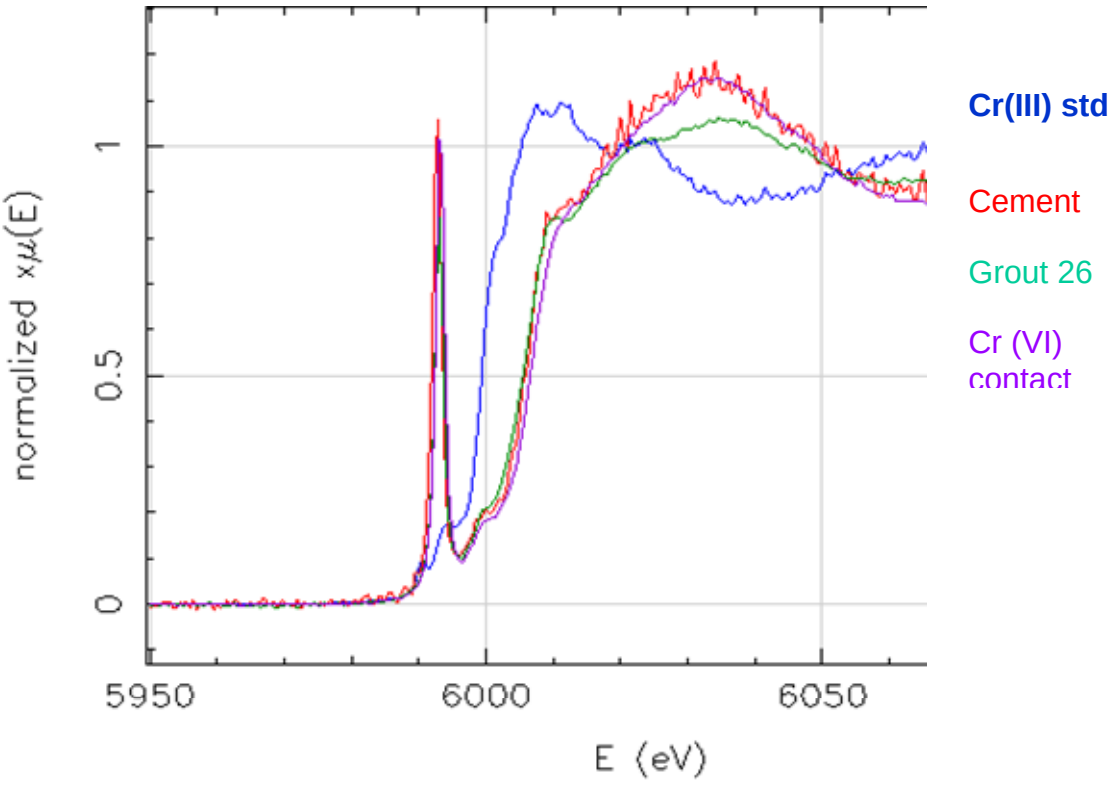

Figure 11. XANES spectrum of Cr from cement, slag and the contact solution showing that the Cr is in the Cr(VI) form. A spectrum from a Cr(III) standard is shown for reference.

forms ettringite, a calcium silicate sulfate, which is important in the early setting process of cement. How stable it is in the long-term is unclear.

The slag does effectively reduce the Cr(VI) as shown in Figure 12. The slag was in contact with the Cr(VI) solution, but only a small percentage of the Cr on the slag remains in the VI form, affirming the materials ability to reduce Cr. However, the effect on Cr reduction is lost in the grout.

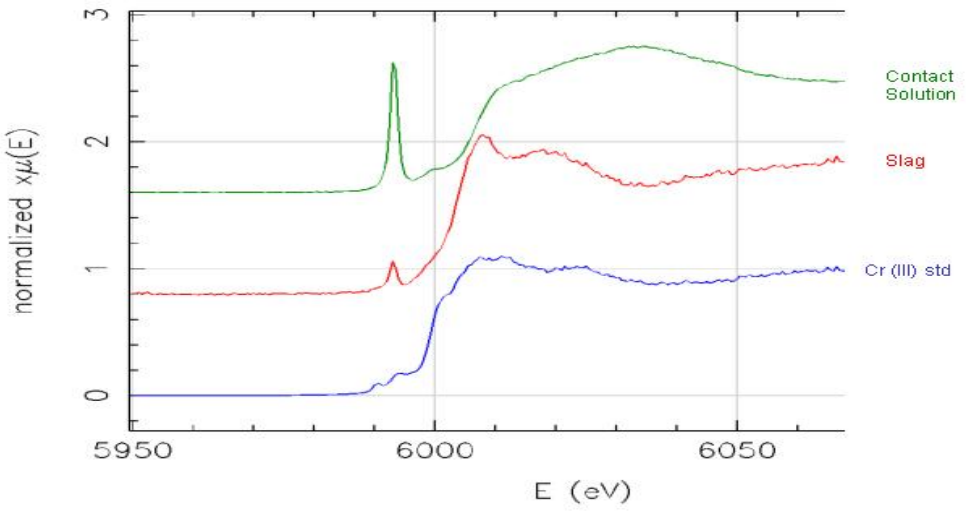

Figure 12. Cr XANES spectra showing that the slag does reduce most of the Cr that it has sorbed from the Cr (VI) contact solution

XANES of U in grouts

X-ray Absorption Near Edge Spectroscopy (XANES) analysis was performed at the National Synchrotron light Source in order to determine the oxidation state of U in the two grouts. A sample of each of the grouts from the aged experiments was taken on April 2005, from the U 100 experiments (batch experiments containing a nominal 100 mg/L of U) (see Table 7 on page 42). These samples had aged for almost two years, as grout contained in contact solution. Some of the solids were removed from the experiment, placed in a sample holder, and sealed with two layers of polypropylene film (6 μm thick). A sample of a newly produced grout was also run. This material had been

made for the column experiments and was about 150 days old, but it had been sealed in a jar in a dessicator that was filled with high purity nitrogen. It had not been in any solution. Two calcite standards were run that contain U, one in the U(IV) form and the other in the U(VI) form. Note the position of the U(IV) peak in the standard Figure 13. Edge positions of the two aged grouts were compared to those of the standards. As shown in Figure 13, the energies of the grout U edges correspond to that of the U(VI) standard. Uranium in the aged grouts is in the oxidized form. The peak for the new grout is slightly to the left of the U(VI) standard but not as far as the U(IV) standard. This indicates that U is probably present as a mixture of (IV) and (VI) in the grout as it forms, but over time it oxidizes.

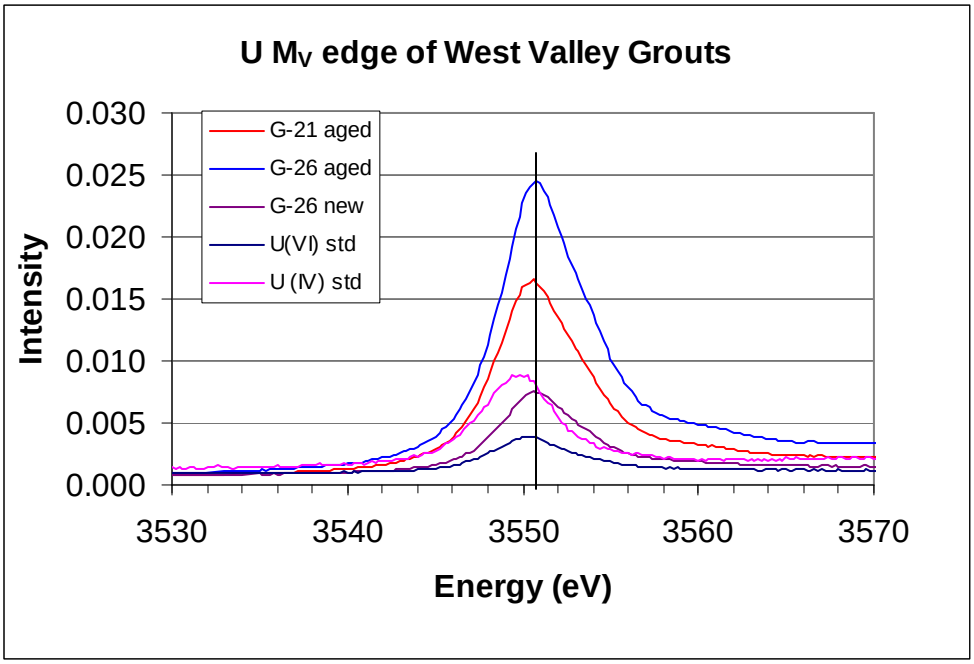

Figure 13. XANES scans of the U M_V edge for several grout samples and U(IV) and U(VI) standards.

The redox data tend to provide a similar picture of conditions that initially are weakly reducing but soon become oxidized sufficiently that U and Cr are present in their oxidized form. The slag does provide some reduction capacity, but much of that capacity is lost on production of the grout. This is not too surprising given the reactions that take

place in the grout as it sets. Any reactive reduced Fe (presumably particles of iron metal) will be exposed to very high concentrations of OH^- in the porewater and its surface will be coated with an iron hydroxide and other cementitious minerals that will be much less reactive than the reduced iron.

Evolution of Water Chemistry

Batch Experiments

A set of experiments, the "aged" experiments, had been set up for determination of isotherms in 2003. These solutions were sampled for ICP analysis to determine steady state concentrations that would evolve over time. Four specimens of each of the grouts were analyzed and one each of the component materials. These were determined from experiments in which the grouts contacted water (2g grout and 40 g water (some water having been removed earlier for sampling)) for over 550 days. Results are shown in Table 4.

Table 4. Concentrations (mg/L) in Solution in Contact with Grouts And Component Materials After 550 days

	pH	Ca	Si	Al	Na	K	Fe
Grout 21	11.3	44	4.0	0.8	27	48	< 0.05
Grout 26	11.3	41	3.8	0.8	13	64	< 0.05
Zeolite	8.6	45	11	1.0	120	31	< 0.05
Cement	12.5	550	< 0.01	0.1	28	480	< 0.05
BF slag	12.1	180	0.1	1.4	29	320	< 0.05
Fly Ash	8.8	21	< 0.01	1.2	8.3	270	< 0.05
Apatite	11.5	6.3	0.8	5.2	1.6	250	< 0.05
Contact Solution	12.5	640	0	0	0	330	0

Column experiments

Other elements were analyzed in the column effluents and concentrations are given in Tables 5 and 6 for the grouts containing uranium. These concentrations are important in describing the overall chemistry of the grouts as they age and can be used in geochemical

thermodynamic modeling of the system to estimate the stable phases and likely aqueous phases of the various contaminants of interest. Some trace elements are especially important. For example the presence of a few ppm of Si can slowly alter the stable U bearing solid phase from an oxyhydroxide to a silicate. Calcium, sodium, and potassium are likely the dominant elements in the grout. In the first intervals from both columns these elements are substantially elevated but rapidly decline to more steady state concentrations. Sodium and potassium do this in a few intervals but calcium concentrations decreased slower, reaching steady state by interval 65 or about 700 pore volumes, as shown in Figure 14. Silicon concentrations, shown in Figure 15, increased for the first 200 pore volumes but seemed to attain steady state between 9 and 12 mg/L. Grout 21 tended to leach slightly more Si than grout 26. This is likely an effect of more Si present because of the zeolite component. Releases of Al were highest initially but were never more than 3.6 mg/L. In both columns Al reached steady state concentrations of approximately 0.1 - 0.25 mg/L. Concentrations of Mg in the effluent was also low, with concentrations around 1 mg/L. Figure 16 shows Mg concentrations increased linearly to 500 – 600 pore volumes, and then declined. No Fe was observed in the leachate.

The relationship between pH and solution concentrations of Ca, Si and Al may be important in defining secondary phases that develop over time. Figure 17 shows that Ca concentrations dropped steeply as pH decreased from 12 to 11. Figure 18 shows that the concentration of Al was highest at high pH and decreased with pH to steady state concentrations between 0.1 and 0.2 mg/L. Si concentrations increased sharply as pH declined from 12 to around 11, as shown in Figure 19. From that point it remained consistent at 12 mg/L.

Table 5. Elemental Concentrations in Effluent from the Uranium Column for Grout 26 (G-26U)

sample	pH	Sum effluent g	Pore volumes	Al mg/L	Si mg/L	Fe mg/L	Mg mg/L	Na mg/L	Ca mg/L	K mg/L	U µg/L
1	12	192	7	2.17	9.4	0	0.05	218.0	171.0	146.00	--
5	11.81	1323	48	2.48	5.4	0	0.06	62.9	229.0	4.42	--
10	11.8	2246	81	1.92	7.1	0	0.09	68.1	189.0	3.70	--
15	11.53	3297	119	1.53	9.0	0	0.14	70.6	173.0	3.70	--
20	11.47	4261	153	1.23	10.9	0	0.24	72.9	154.0	3.09	--
25	11.38	5373	193	0.95	11.3	0	0.26	78.2	138.0	2.70	0.0
30	11.36	6422	231	0.64	11.2	0	0.44	79.2	129.0	1.04	0.0
32	11.16	6784	244								16.4
35	11.22	7670	276	0.53	12.8	0	0.46	76.5	121.0	1.50	30.0
40	11.07	8722	314	0.53	12.3	0	0.51	76.2	115.0	1.40	30.0
43	10.98	9262	333								92.0
45	10.95	9814	353	0.47	12.3	0	0.55	72.8	110.0	1.50	30.0
47	10.93	10519	378	0.38	12.5	0	0.61	76.0	108.0	1.40	25.8
49		11233	404	0.38	12.8	0	0.62	76.8	107.0	1.20	26.9
51	10.75	12114	436	0.29	11.3	0	0.69	70.0	104.0	0.88	41.9
53	10.64	12815	461	0.27	11.1	0	0.73	71.9	96.6	0.56	28.6
55	10.24	13517	486								20.6
57	10.15	14249	513	0.25	11.6	0	0.91	80.5	90.8	0.60	25.0
59	10.1	14929	537								20.8
61	9.93	15673	564								30.3
63	9.73	16571	596								28.8
65	9.68	17294	622	0.24	11.7	0	0.75	76.8	81.7	1.19	27.0
66	9.54	17673	636								31.4
68	9.73	18385	661								27.6
70	9.85	19155	689	0.26	11.2	0	0.69	74.2	83.6	0.97	28.6
72	9.72	20221	727								19.2
74	9.31	20756	747	0.25	11.3	0	0.72	77.5	83.0	0.72	20.3
76	8.44	21686	780								24.7
78	8.18	22542	811	0.22	10.3	0	0.71	75.2	78.4	0.81	14.2
82	8.3	24180	870	0.23	9.7	0	0.69	76.9	81.8	0.42	17.5
84	8.43	25193	906	0.18	9.3	0	0.67	75.0	82.2	0.34	17.0
86	8.25	25914	932								16.1
88	8.43	26641	958	0.19	9.1	0	0.68	75.4	82.8	0.34	13.3

Table 6. Elemental Concentrations in Effluent from the Uranium Column for Grout 21 (G-21U)

		sum	Pore								
sample #	pH	effluent	Volumes	Al	Si	Fe	Mg	Na	Ca	K	U
		(g)		mg/L	mg/L	mg/L	mg/L	mg/L	mg/L	mg/L	µg/L
1	11.83	216	9	3.57	5.0	0	0.04	131.0	212	338.00	
5	11.63	1294	56	1.54	10.3	0	0.11	73.8	180	15.50	
10	11.63	2339	102	1.23	12.8	0	0.16	73.5	165	7.61	
15	11.36	3291	143	1.05	14.5	0.02	0.26	73.0	150	6.06	
20	11.32	4235	184	0.82	14.8	0.03	0.31	76.3	142	4.40	
25	11.22	5085	221	0.65	13.4	0	0.31	80.0	134	4.00	
30	11.13	6217	270	0.43	10.5	0	0.73	78.2	116	2.30	0.0
32	11.06	6607	287								15.7
35	11.05	7561	329	0.39	13.7	0	0.76	77.4	111	2.10	14.5
40	10.91	8694	378	0.31	13.4	0	0.83	75.7	105	1.90	33.0
43	10.87	9277	403								19.6
45	10.77	9870	429	0.32	12.9	0	0.92	76.5	98.7	1.90	18.0
47	10.79	10628	462	0.22	13.4	0	0.93	73.5	101	0.96	20.7
49		11390	495	0.22	13.0	0	1.05	74.0	92.8	1.30	29.0
51	10.37	12337	536	0.18	11.4	0	1.12	63.7	93.2	1.04	36.2
53	10.31	13092	569	0.17	12.1	0	1.13	68.8	88.1	1.04	42.0
55	9.31	13850	602								49.3
57	9.71	14637	636								57.8
59	9.66	15342	667								36.9
61	9.41	16082	699								69.0
63	9.32	17050	741								51.2
65	9.3	17829	775	0.11	13.4	0	1.17	79.2	78.6	0.96	
66	9.06	18236	793								51.1
70	8.91	19827	862	0.09	12.0	0	1.04	75.9	79.14	0.67	47.0
72	8.73	20970	912								35.1
74	8.48	21544	937	0.12	12.3	0	1.06	79.2	82.6	0.91	31.5
76	8.47	22540	980								28.6
78	7.07	23052	1002	0.08	11.4	0	1.02	77.6	84	0.56	30.3
80	7.86	24021	1044								31.9
84		24181	1051								34.1
85		24166	1051	0.13	14.2	0	0.76	79.2	96.8	0.83	12.9
88	8.42	25116	1092	0.11	10.9	0	0.83	79.7	79.8	0.99	24.6
89	8.26	25643	1115								

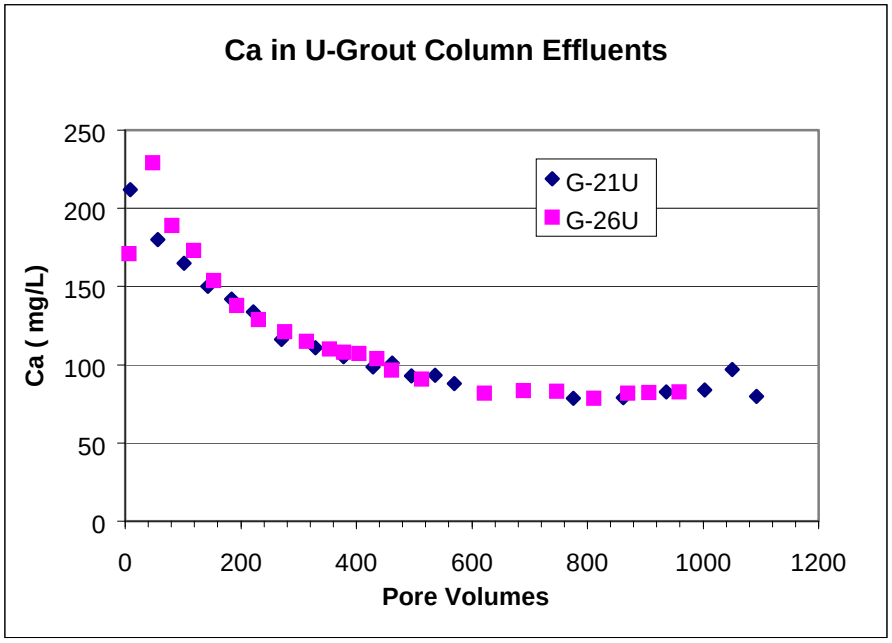

Figure 14. Calcium concentrations in effluent from both U bearing columns.

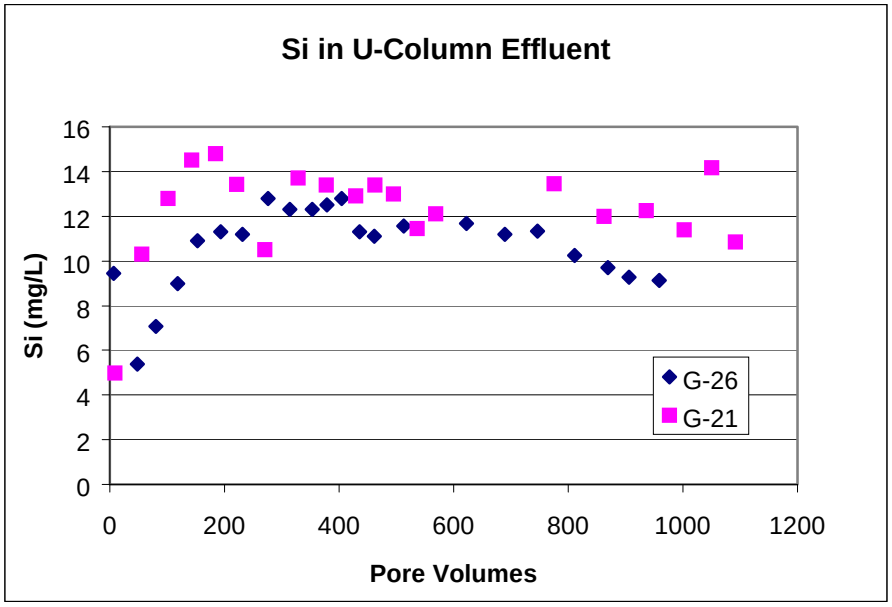

Figure 15. Silicon concentrations in effluent from both U bearing columns.

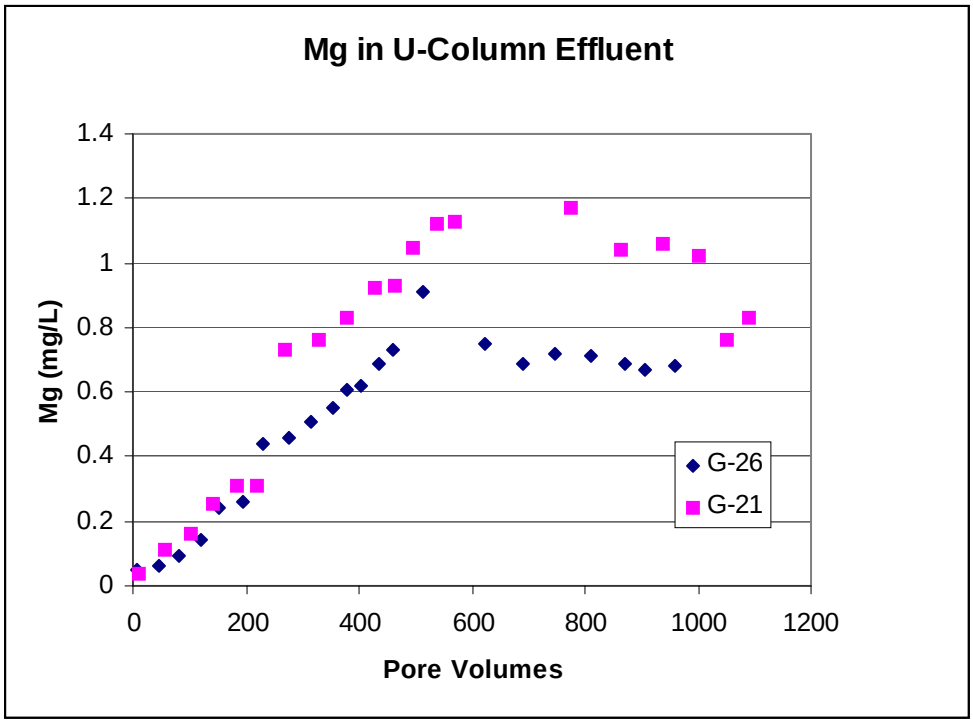

Figure 16. Concentrations of Mg in effluent from both U bearing columns.

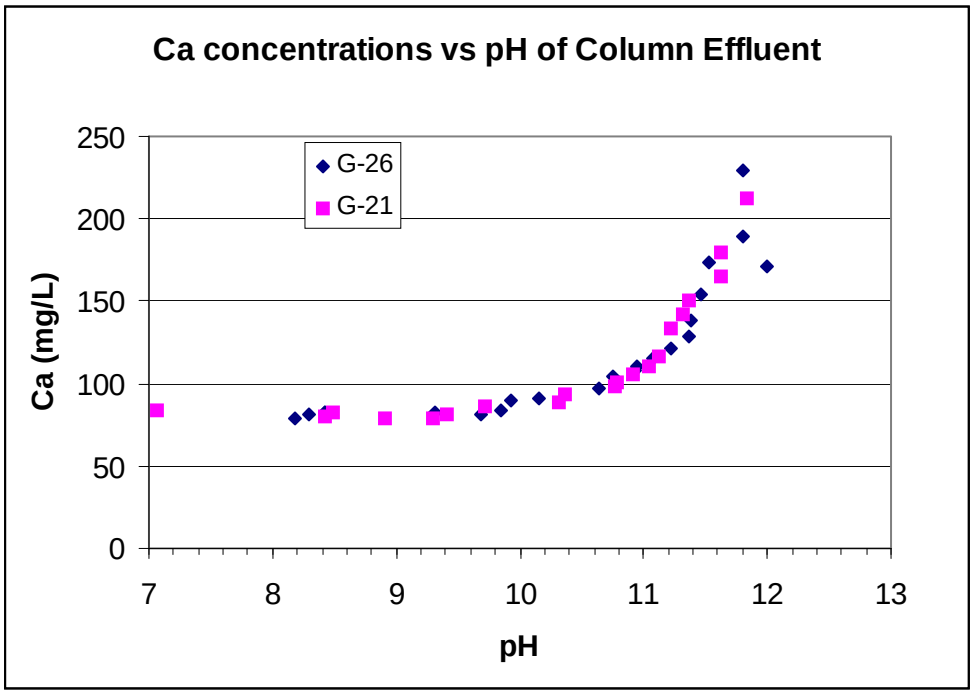

Figure 17. Relationship between pH and Ca concentrations of column effluent.

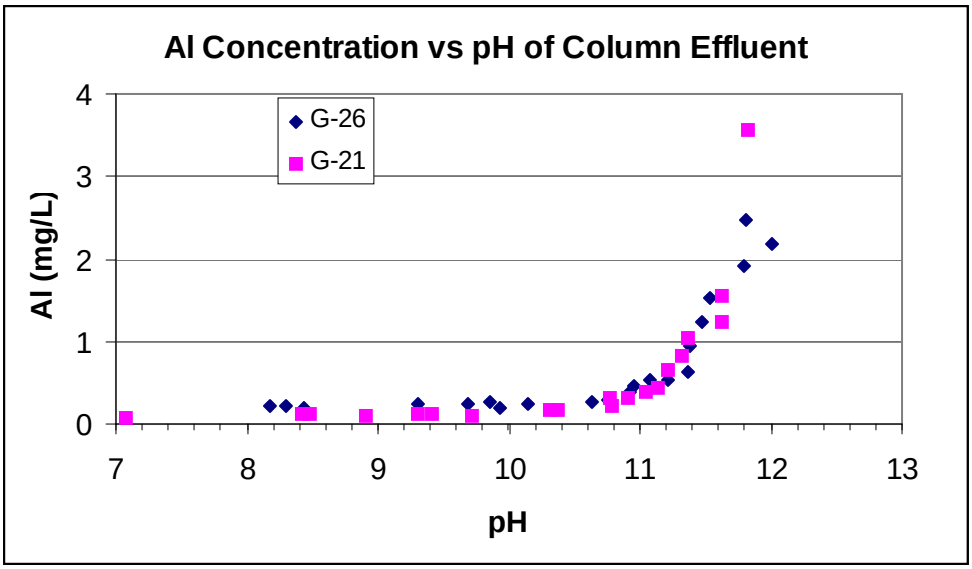

Figure 18. Relationship between Al concentration and pH of column effluent.

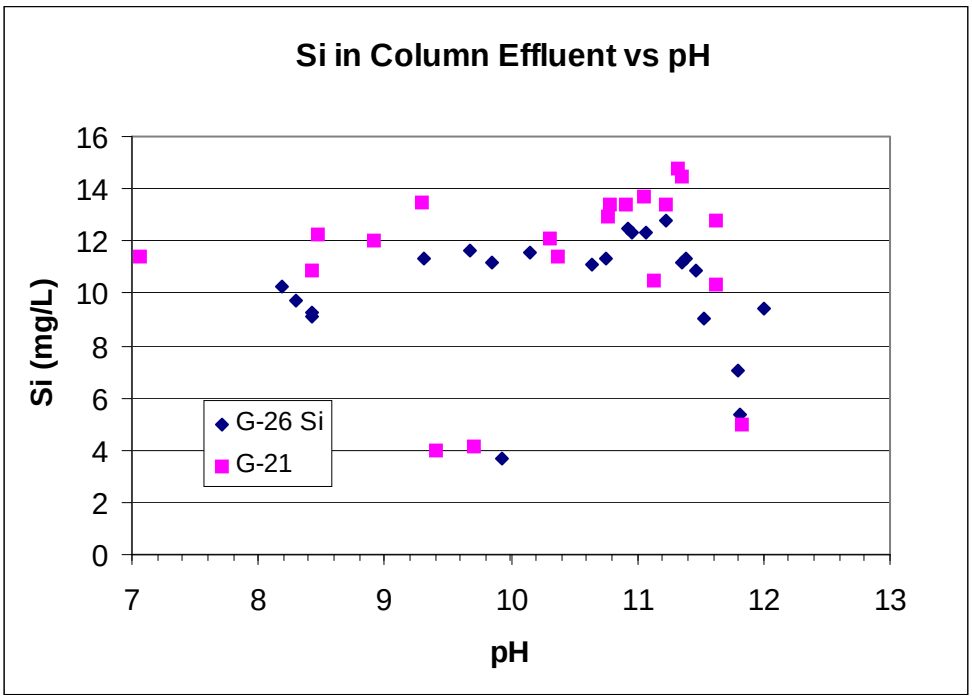

Figure 19. Relationship between Si concentrations and pH in column effluent.

Uranium Results

Background

Solubility of U at alkaline pH. In the absence of carbonate, the solubility of U (VI) attains a minimum concentration under alkaline conditions. Ewart et al. observed that as pH was adjusted, in the presence of portland cement and blast furnace slag, U concentrations decreased to 10^{-7} M at pH 10.5 and increased to 10^{-5} M as pH increased to 13 (Ewart et al., 1992) . $UO_2(OH)_2$ in 0.5 M NaCl solution reaches a solution concentration of about 10^{-7} M at pH of 8, maintains that concentration to at least pH 10 and then the U concentration increases to $10^{-5.5}$ M as pH increases (Fanghänel and Neck, 2002). These concentrations are lower than expected for $UO_2(OH)_2$ and indicates the slow formation of $NaUO_2(OH)_3$. Brownsword et al, (1990) measured the solubility of U(VI) compounds in a variety of cement equilibrated waters. Above pH 7 U concentrations in solution, for both sodium and calcium uranate, was about 3×10^{-6} M. There was a slight increase above pH 12, for sodium uranate. Krupka et al. (1985), measured the solubility of U(VI) hydroxide as a function of pH in carbonate free water and compared it to modeled solubility of schoepite. Using both over-saturation and under-saturation experiments, a minimum U concentration of 10^{-6} M was attained at pH of 9, with increasing concentration as pH increased. The model and the experimental data conformed fairly well at pH values above 9. At lower pH values the fit to the data showed significant discrepancy.

Dissolution of various U minerals has been studied as it is controlled by different complexants. For example metaschoepite and metaautunite dissolve more rapidly in HCO_3 solution than becquerelite and chernikovite (Sowder et al., 2001). The dissolution rates of uranophane, and soddyite increase with increasing concentrations of HCO_3 (Perez et al., 2000). The dissolution of U, which is present as silicates in intragranular precipitates, from sediment samples taken from Hanford was studied by Liu et al. (2004). Dissolution kinetics were found to be more important than mass transfer from the intergranular positions.

The carbonate ligand forms three important monomeric complexes with U(VI): UO_2CO_3, $UO_2(CO_3)_2^{2-}$ and $UO_2(CO_3)_3^{4}$. These uranyl carbonates are relatively strong complexes with stability constants (log K) of 9.7, 16.9, and 21.6, respectively (Clark et al., 1995). In addition, polymeric species can form in high ionic strength solutions and/or under conditions of high U concentration (eg, $(UO_2)_2(CO_3)OH_3^-$). These soluble carbonate species may or may not adsorb to a solid surface because of their neutral or negative charge and their adsorption behavior will depend highly on solution pH. The calcium uranyl carbonate complexes ($CaUO_2(CO_3)_2^-$ and $Ca_2UO_2(CO_3)_3$) have recently been observed and are considered some of the most important species in Ca-rich solutions (with stability constants, log K, of 25.4 and 30.6, respectively)(Bernhard et al., 1992; 1996, Kelly et al., 2007).

U interactions with cement. Atkins et al. (1990) examined the interactions of U with C-S-H (calcium, silica hydrate) gel which is the very stable cementitious material formed in setting portland cement. U solution concentrations over 156 days were around 4×10^{-7} M in contact with CSH. Two U bearing phases were identified associated with the CSH: uranophane ($Ca(UO_2)_2(SiO_3)_2(OH)_2 \cdot 5H_2O$) and a hydrated calcium uranyl oxide (tentatively $Ca_2UO_5 \cdot (1.2\text{-}1.7)H_2O$). When the $Ca(OH)_2$ content was high, becquerelite ($CaO \cdot 6UO_3 \cdot 11H_2O$) was also found. Atkins et al. note that at concentrations of U less than about 10^{-8} M, sorption on solids may be dominant over solubility controls.

As discussed earlier, studies of cement (not a grout) pore water composition show that up to about 1000 pore volumes the pore water chemistry is dominated by solid phase $Ca(OH)_2$ which maintains a high pH. After about 1000 pore volumes the pH begins a sharp decrease so that by 6600 pore volumes the pH is 7.4 (Berner, 1992). With carbonate in the groundwater, most Ca (in the cement model, 83%) will be retained in the solid phase as calcite forms. In the model using $CaUO_4$ the U concentration in solution begins to increase at about 500 pore volumes, from very low concentrations, so that at 1000 pore volumes the pH is 11.2 and U concentrations are $10^{-8.5}$ M. By the time pH has dropped to 10.5 the concentration of U increases dramatically to molar levels.

Interactions of U with Calcite. Calcite is an important reaction product of the weathering of cement based materials. In the case of West Valley this is especially so because the groundwater is bicarbonate rich. Consequently, reactions of U mobilized from the grout with newly forming $CaCO_3$ minerals may be very important in the long term fate of U in this system. Uptake of metals by calcite has been characterized as rapid initial adsorption onto surface sites (or exchange for Ca) followed by slow incorporation of the metals into surface precipitates or solid solutions (e.g. Stipp and Hochella, 1991). In experiments in which a single calcite rhomb was exposed to UO_2^{++} in a basic solution (in an open system), a variety of U phases formed on the calcite surface. These were: UO_2^{++} bearing calcite, uranyl tricarbonates, wyarite II, becquerelite, and schoepite (Schindler and Putnis, 2004). Reeder et al, 2000, reported that U (VI) can co-precipitate with calcite and aragonite, giving solid U concentrations of 1,900 and 10,000 mg/kg, respectively. This high level of co-precipitation takes place if the $CaCO_3$ mineral is rapidly precipitated. Meece and Benninger (1993) examined the partitioning of several actinides into calcite and aragonite in seawater. Co-precipitation of U with Ca carbonates was different than that of Am, Pu or Th, because it was affected by the mineral being formed. In calcite, U (VI) incorporation was not favored (K_d less than 1with respect to Ca), while in aragonite, U (VI) is more readily taken up. The implication is that UO_2^{+2} is incorporated into $CaCO_3$ minerals by lattice substitution for Ca. The more open crystal structure of aragonite allows more substitution.

Uranium has been observed in two species in calcite, as indicated by time resolved luminescence spectroscopy and EXAFS (Reeder at al., 2001). One is tris-carbonate like and the other is less well characterized. Elzinga et al (2004) found that U at calcite surfaces was in two forms both of which, though slightly different, were similar to the aqueous $Ca_2UO_2(CO_3)_3$ complex (which has been described by Bernhard et al., 2000) that dominates U solution chemistry around pH 8 and near calcite saturation conditions. The implication is that U(VI) first interacts with calcite surfaces by sorption as a uranium tris-carbonate specie. Interactions of this species with calcite surfaces takes place between Ca and CO_3 ligands on both the surface and the sorbing species, but the presence of U leads to some distortion of the calcite structure (Reeder et al, 2001). However, the

coordination of U in natural calcite is different and indicates that reordering with aging or kinetics of sorption may take place (Kelly et al., 2003). The picture of carbonate mineral interactions with metals is that of a dynamic process at the mineral surface that involves adsorption of uranyl at low concentrations, perhaps as a carbonate complex, and co-precipitation of uranyl with Ca carbonate at greater solution concentrations (Elzinga et al., 2004).

Uranium Isotherms

Uptake of U on the two grouts was determined using a solution of natural uranium as U (VI) in nitric acid from NIST (10 mg/mL). Concentrations in the starting solutions were 0.6, 11.0, 46.0, 98.0, and 201 mg/L. These experiments ran for 61 days. Samples were analyzed by ICP-OES with a detection limit of about 0.2 mg/L, and were calibrated with NIST traceable standards.

All U concentrations in experiment solutions were close to or below the detection limit and there was no trend with starting concentration. Results are shown for the two grouts in Figure 20.

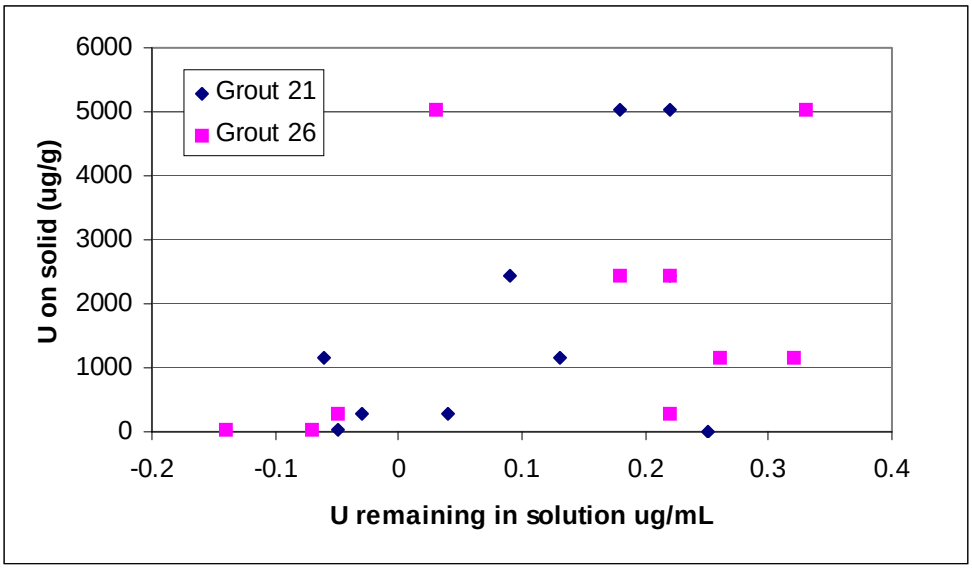

Figure 20. Isotherm plot for the two grouts, showing that concentrations of U in solution are generally at or below ICP detection limits of 0.2 mg/L.

Partitioning of uranium between the solid and liquid phases is primarily controlled by solubility limits. As a result K_d values are reported in Table 7 as "greater than" values determined from U concentrations that are essentially detection limits. At the high pH of the contact solution there are several U oxy-hydroxide phases that can form. The solubility of some of these compounds is low and pH dependant, but others (such as $(UO_2)_3(OH)_7^-$) are quite soluble. Measurements of U(VI) solubility in a cement/ blast furnace slag system was lowest at pH 10.5 with a concentration of 0.04 mg/L. The concentration rose to about 5 mg/L at pH 13 (Ewart et al, 1992). At the pH of our experimental system, 12.4, the U concentration based on Ewart et al, should be about 2 mg/L. In precipitation/dissolution experiments with U under oxidizing, carbonate free conditions, Krupka et al., 1985, found a minimum in solubility at pH 9.5 – 10 at concentrations of 0.24 mg/L but a rapid increase as pH increased. This was interpreted to be the result of anionic U-hydoxide phases growing into solution. At pH 12.4 the U concentration was about 100 mg/L. Our experimental data show significantly lower U concentrations than either of these papers at pH 12.4. The lower solubility may be related to reactions with other components of the grout or reduction of U (VI) to U (IV). Ewart et al, (1992) measured the solubility of U(IV) in the cement/ BFS system at about 0.024 mg/L at pH values ranging from 5 to 13. From this it appears that the various components of the grout may be providing a lower solubility than observed in cement/ BFS systems, although it is unknown if the mechanism is reduction or reactions with other grout components. From these data there is no difference between the two grout formulations.

Table 7 . Estimated K_d Values for U

	Grout 21			Grout 26		
Nominal Conc.	**Start cpm/mL**	**End cpm/mL**	**K_d (mL/g)**	**Start cpm/mL**	**End cpm/mL**	**K_d (mL/g)**
200	201	< 0.2	> 25000	201	< 0.2	> 20000
100	97.5	< 0.2	> 19000	97.5	< 0.2	> 12000
50	46.3	< 0.2	> 8900	46.3	< 0.2	> 4000
10	11.0	< 0.2	>6800	11.0	< 0.2	> 1200
1	0.6	< 0.2	> 36	0.6	< 0.2	> 50

Experiments were conducted to determine the effect of each component of the grout on the solution concentration of U. In all cases the U precipitated, due to the high pH and remained out of solution. There was no dissolution of U caused by any of the components.

U Batch Tests Results

Determine if U, which has been sequestered in contact with the two grouts, returns to solution as the grouts age.

Batch experiments that had aged 550 days. A set of experiments, the "aged" experiments, had been set up for determination of isotherms in 2003. These samples had been retained and were resampled to compare to the more recent, shorter term, new experiments that were described in the Methods Section above. Under the initial highly alkaline chemical conditions of these experiments U rapidly precipitated in the contact solution. After aging, in all but one case, U was below the ICP detection limit of 0.3 mg/L. Results for U are shown in Table 8. Uranium was only observed in a sample in which the pH had declined to 9.3, the lowest of the samples. Concentrations of Ca, Si, Al, Na, K, and Fe for these experiments are given in Table 4. Speciation modeling with

Geochemist's Workbench indicates that under the initial conditions $CaUO_4$ is likely to form. If silica is available in solution, then soddyite $(UO_2)_2SiO_4(H_2O)_2$ can be expected, but it may take some time to form. It is unclear how kinetics control the solid phases, but there is evidence that aging lowers the solubility of some U precipitates as a more crystalline structure develops or a new compound forms incorporating the U (Fanhanel and Neck, 2002).

Table 8. Concentrations of U in "Aged" grout samples

Sample	Initial U (mg/L)	Grout 21		Grout 26	
		pH	U (mg/L)	pH	U (mg/L)
U-50A	46.3	10.80	< 0.3	10.99	< 0.3
U-50B	46.3	10.70	< 0.3	9.30	2.0
U-100A	97.5	11.35	< 0.3	11.10	< 0.3
U-100B	97.5	11.10	< 0.3	10.90	< 0.3
U-200A	201.4	11.30	< 0.3	11.40	< 0.3
U-200B	201.4	11.20	< 0.3	11.42	< 0.3

All samples in the experiment were started in the contact solution. The differences between the contact solution content and the experiment solutions indicate the extent to which the various materials reacted over time. Particularly important may be the reduction in pH in the zeolite and fly ash experiments, since the short-term batch experiments discussed above, show that pH is a major control on U solubility in the grouts. Another potentially important consideration is the availability of Si in the grout solutions and the relatively low concentrations of Ca (see Table 4). These values are used as input to speciation modeling to better understand reactions of U in contact with these materials.

Determine if U sequestered with the aged grouts returns to solution on contact with increasing concentrations of $KHCO_3$.

The long-term batch experiments were analyzed for solution composition after aging, as given in Tables 4 and 8. Following this sampling the pH was incrementally adjusted with $KHCO_3$ and samples of the liquid were filtered and analyzed for U. Results are shown in Figures 21 and 22 for the grout experiments that had the highest U content (201 mg/L).

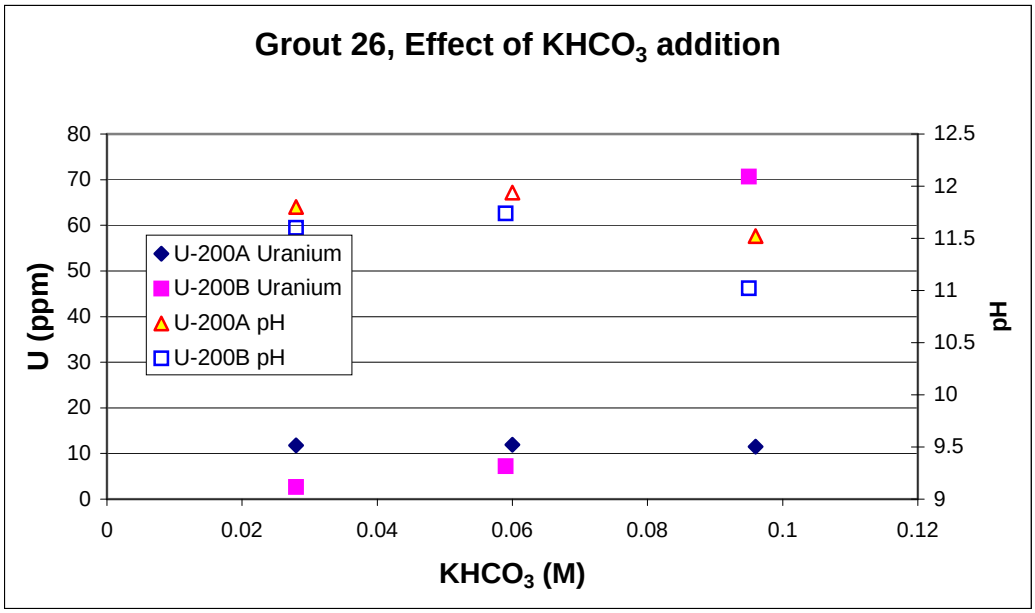

Figure 21. U content and pH of liquid in contact with grout 26 after aging and with addition of $KHCO_3$.

The U content of the liquid in contact with Grout 26 after aging was below ICP detection limits of about 0.3 mg/L for both replicates. On addition of $KHCO_3$ some U was released to solution. With the addition of 0.06 M $KHCO_3$, U concentrations in solution rose to between 7 and 12 mg/L. At higher concentrations of $KHCO_3$ one sample released U to a solution concentration of 70 mg/L, while the other sample was only about 12 mg/L. This difference is likely explained by the slightly higher pH of the latter sample relative to its replicate. Thus a difference of pH between 11.5 and 11.0 results in a very significant change in U solubility under these experimental conditions.

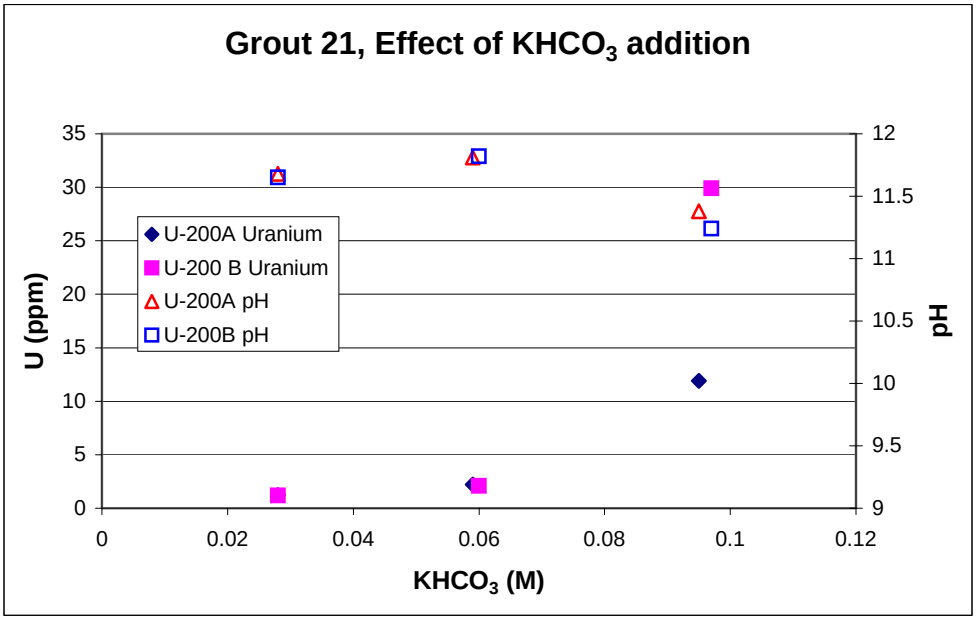

Figure 22. U content and pH of liquid in contact with grout 21, after aging and addition of $KHCO_3$. Solid symbols are uranium concentrations read on the left Y-axis, while the unfilled symbols show the pH for the same two experiments, read on the right Y-axis.

The behavior of Grout 21 is similar. While U concentrations are below detection limits prior to any addition of $KHCO_3$, with addition of 0.06 M the U concentration was 2 mg/L at pH 11.8. The next increment of $KHCO_3$ pushed its concentration to 0.095 M and the U concentrations increased to 12 and 30 mg/L with the pH decreasing to 11.4. These data are consistent with the short-term experiments discussed later. The introduction of $KHCO_3$ results in release of U which initially is low (e.g. at 0.06M $KHCO_3$ the U concentrations range between 1 and 2 mg/L), but then becomes much greater as the pH begins to drop and the carbonate/bicarbonate speciation changes.

Figure 23 allows a comparison of uranium concentrations in solution as a function of the addition of $KHCO_3$ for all aged samples (the 50, 100, and 200 ppm U concentrations) for both grout formulations in the long-term experiments. These data show little difference in U concentrations in solution in contact with the two grout formulations, although grout 26 tends to be somewhat higher. As $KHCO_3$ additions approach about 0.02 M, the uranium in solution began to be detectable. Figure 24 contains the same data set shown as a function of pH. Grout 21 maintained pH primarily between 11 and 12, while grout

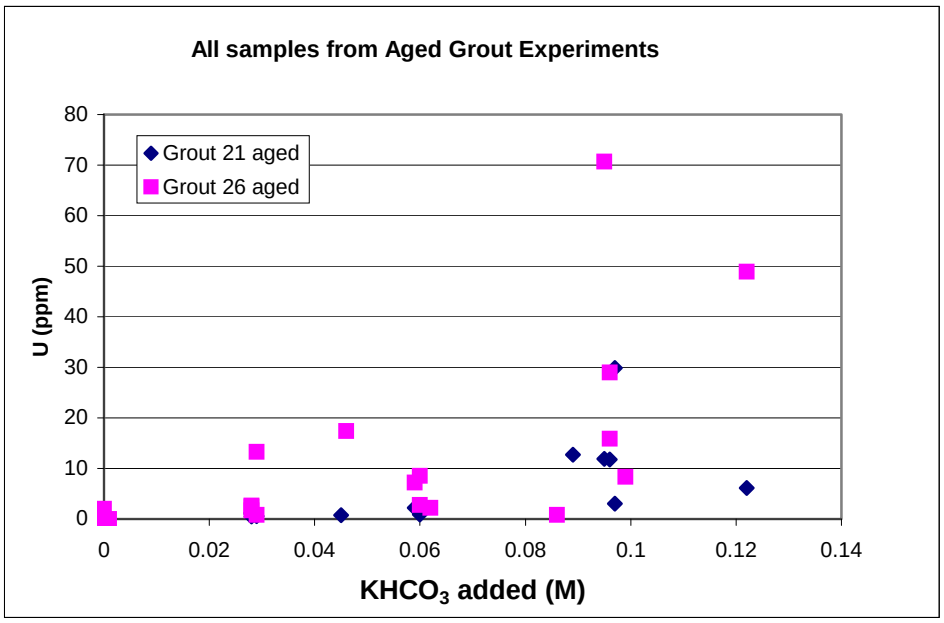

Figure 23. Comparison of U releases from all aged grout samples from the long-term experiments shown as a function of $KHCO_3$ added.

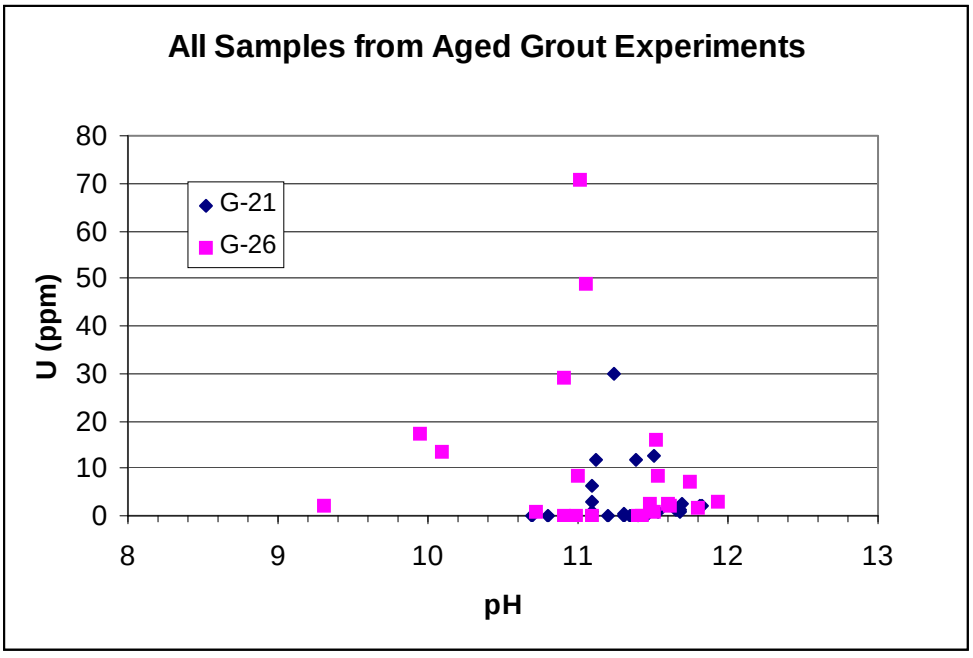

Figure 24. Comparison of U releases from all aged grout samples from the long-term experiments, with and without $KHCO_3$ added, shown as a function of pH.

26 was more varied. For grout 26, solution U reached a maximum of 70 ppm at pH 11and then decreased as pH moved down. We suspect that this is a result of calcium carbonate precipitation that is carrying uranium with it.

Determine the behavior of U that has precipitated in a simulated grout pore water (without grout present), as the pH is lowered or $KHCO_3$ content is increased.

Two experiments were conducted in which U was added to a simulated grout pore water. In one experiment the pH was incrementally lowered and the U concentration followed. In the other, the carbonate/bicarbonate concentration was altered to provide information on the solubility of U under conditions taken to resemble weathering of the grout. These experiments contained no grout. At the initial pH of 12.3, U readily precipitated. Lowering pH,

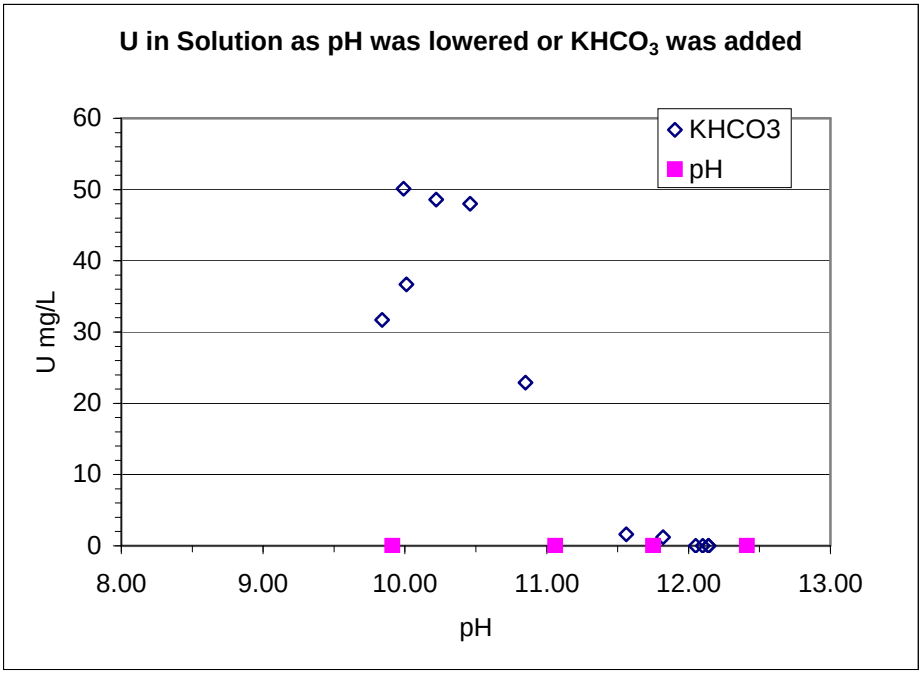

Figure 25. U in solution in the simulated pore water experiments showing the effect of lowered pH and addition of $KHCO_3$.

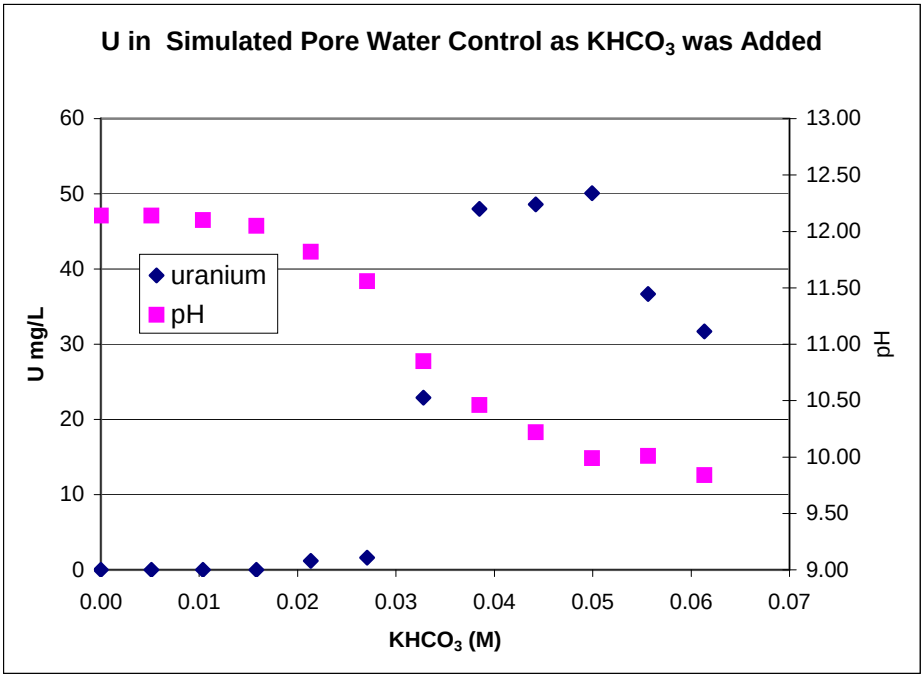

Figure 26. Relationship between addition of $KHCO_3$ and U in the simulated grout pore water for the control experiment, consisting of U added to the Ca/K hydroxide contact solution.

from 12.3 to 9.9 had no apparent effect on U concentration in solution. The concentrations were all below detection limits of about 0.3 mg/L. Results for the $KHCO_3$ experiments are shown in Figures 25 and 26. The addition of $KHCO_3$ resulted in dissolution of the precipitated U after pH went below 12. By pH = 10.5 essentially all of the U had returned to solution (50 mg/L). As additional $KHCO_3$ was added, there was little change in pH, but U concentrations decreased sharply. This is primarily the result of calcite precipitation and is discussed in a later section. The point where CO_3^{-2} and HCO_3^{-1} are equal in concentration in solution takes place at about pH 10.3. This is quite close to the observed point in Figure 26 where U and pH cross. At the point where the concentration of added $KHCO_3$ was 0.02 M, uranium started to dissolve and pH began to decline. By 0.035 M the process was complete and most U had returned to solution.

Determine the behavior of U in simulated grout pore water in contact with the components of the grout: portland cement, blast furnace slag, fly ash, zeolite, and fluorapatite.

The next set of experiments to be discussed are the "new" batch experiments that consist of the Ca/K OH simulated pore water contact solution, the various solids (both grouts and their components), and U(VI). These are fresh materials that had not aged. The behavior of U in contact with the two grouts is shown in Figure 27. At $KHCO_3$ concentrations below 0.02 M, the pH remained consistent at about 11.7, about where it started, and no U was detected in solution.

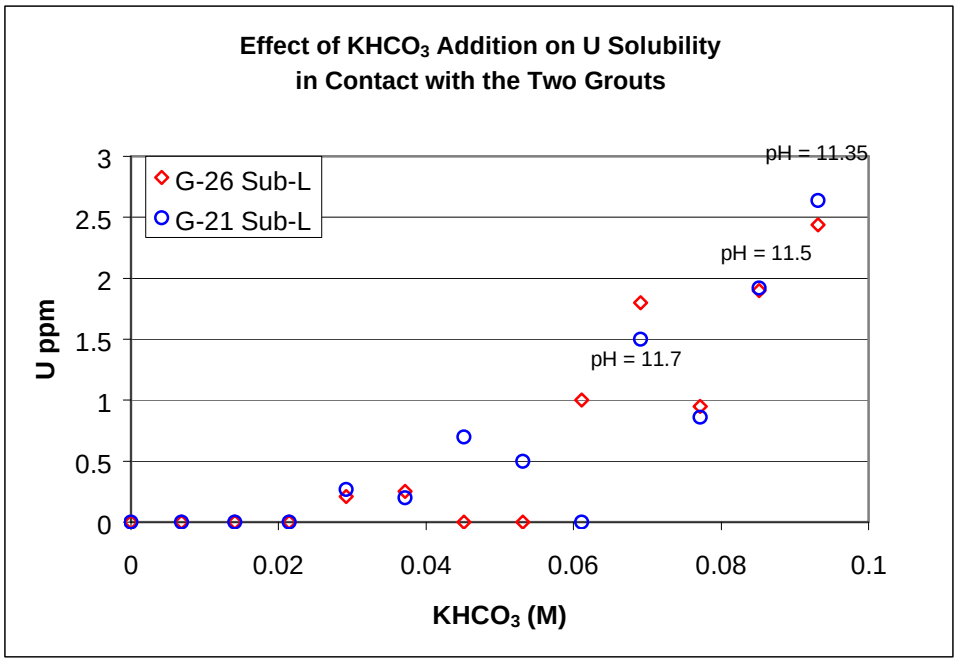

Figure 27. Effect of $KHCO_3$ addition on U concentrations in solutions in contact with grouts.

When the $KHCO_3$ concentration exceeded 0.02 M, U started to dissolve, even though pH remained unchanged. The start of dissolution took place at the same $KHCO_3$ concentration as in the pore water control experiments. U concentrations became greater

than 1 mg/L at $KHCO_3$ concentrations greater than 0.07 M and slightly reduced pH. In contrast, the simulated pore water $KHCO_3$ control experiment, consisting of similar conditions but with no grout present, reacted more rapidly to return U to solution. Both

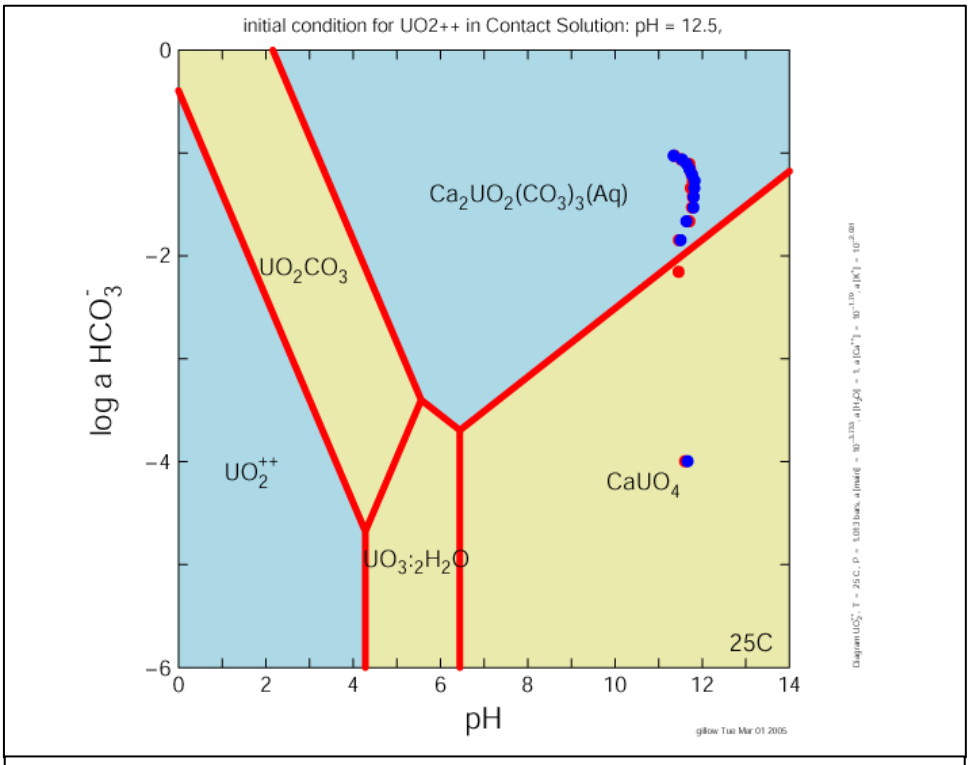

Figure 28. pH - activity diagram for 50 mg/l U (VI) in the presence of calcite. The data points are for the U batch experiments in the presence of Grout 21 (red points) and grout 26 (blue points).

contained the same quantity of U, but the presence of the grout strongly retained U and kept it from returning to solution. In comparison, in the simulated pore water experiment all U was in solution (50 mg/L) at $KHCO_3$ concentration of 0.04 M while in the presence of the grout U was barely detectable by ICP (about 0.5 mg/L). This was not simply an effect of pH buffering by the grout. In the grout samples at pH = 11.35 the concentration of U was 3 mg/L while in the simulated pore water experiment at the same pH, and with much less $KHCO_3$ added, the U concentration was about 35 mg/L. It is likely that the carbonate/bicarbonate react with Ca from the grout to form $CaCO_3$ minerals, lowering the Ca and carbonate content of the solution and lowering the carbonate ligand available to

complex with U. In addition, as mentioned above, $CaCO_3$ formation does carry uranium with it.

Figure 28 shows the stability fields of uranium species as calculated by GWB for a system containing the contact solution (pH = 12.5, Ca= 640 mg/L) and U(VI) at 50 mg/L overlain by data from the batch experiment. It illustrates that at the start of the batch experiment the solid phase (shown in yellow) is predominantly $CaUO_4$, and as $KHCO_3$ is added the conditions migrate to a field were an aqueous phase, $Ca_2UO_2(CO_3)_3$, is dominant. Figure 29 is a similar diagram but includes SiO_2 and Al at 0.00014 M and 0.00003 M respectively, which are the observed concentrations in the aged samples of the grouts. In addition the speciation is determined in the presence of calcite, which will precipitate in this system. In this case the model indicates the system as it has matured. The presence of SiO_2 has allowed the formation of soddyite and haiweeite. The kinetics of formation of these minerals is slow but they may replace U oxides or hydroxide phases

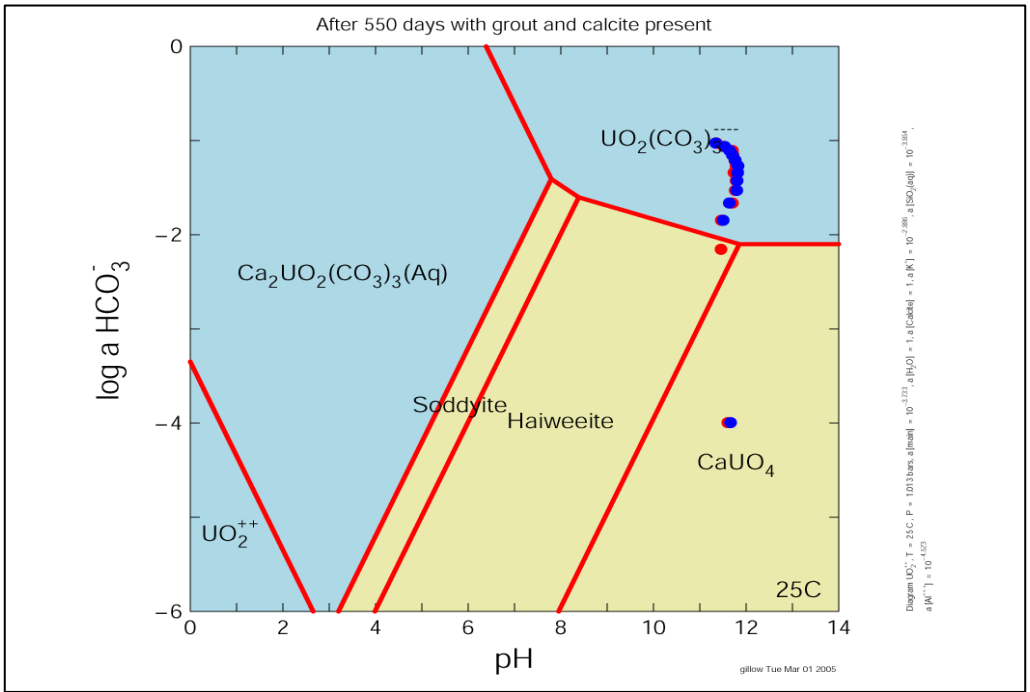

Figure 29. pH –activity diagram for 50 mg U in the presence of calcite but with Al and Si added at low concentrations.

over time [Finch and Murakami, 1999]. In fact U silicates are the most common group of U minerals and they tend to be persistent in nature. An important change takes place in the stability fields with the presence of calcite. This lowers the Ca concentration and shifts the aqueous speciation, at high pH, to $UO_2(CO_3)_3^{-4}$. These diagrams must be viewed with caution because they provides a very simplified concept of the system. Nevertheless, they adequately describe the solid-solution behavior of uranium in the experiments and provide for the possible identification of the uranium species.

Similar experiments with the component materials in the simulated grout pore water provides some insight to behavior of U within the grout. The two materials that maintained high solution pH, portland cement and blast furnace slag, retained most of the U in the solid phase. As $KHCO_3$ was added, the pH changed very little in the presence of these materials. As shown in Figure 30, with addition of $KHCO_3$, U concentrations did not increase in the presence of cement. However with BFS (and the two grouts) there was a slight increase of U to about 3 mg/L as the HCO_3^- increased and pH decreased. From this it appears that above pH 12 U is retained in the solid even as $KHCO_3$ is added. Below 12, addition of $KHCO_3$ does bring U into solution.

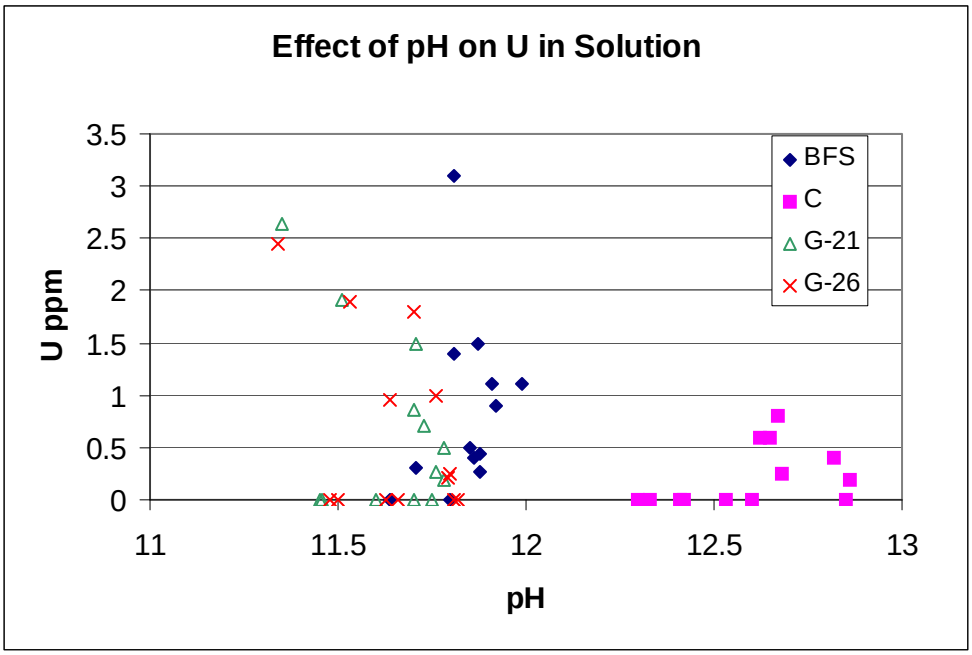

Figure 30. Effect of pH on U in solution in contact with cement, blast furnace slag and the two grouts as $KHCO_3$ was added.

The other materials, fly ash, zeolite, and apatite do not contain reserve alkalinity. They react with OH^- to lower the pH and as a consequence, U concentrations are much higher. In contrast the BFS and cement are a source of OH^- and are able to maintain higher pH. Figure 31 shows how the U concentration in solution reacts to addition of $KHCO_3$ in the presence of fly ash, zeolite, and apatite. With the addition of up to 0.02 M $KHCO_3$ U releases became substantial for apatite and fly ash. At a concentration of 0.033 M of $KHCO_3$ essentially all of the U was in solution in the apatite sample and 80% in the fly ash. Similarly all of the U in the simulated pore water control returned to solution. The zeolite released less U, with a maximum solution concentration of about 22 mg/L. At the point where 0.055 M $KHCO_3$ had been added, all of the samples experienced a decrease in U concentrations, the zeolite less dramatically than the other materials.

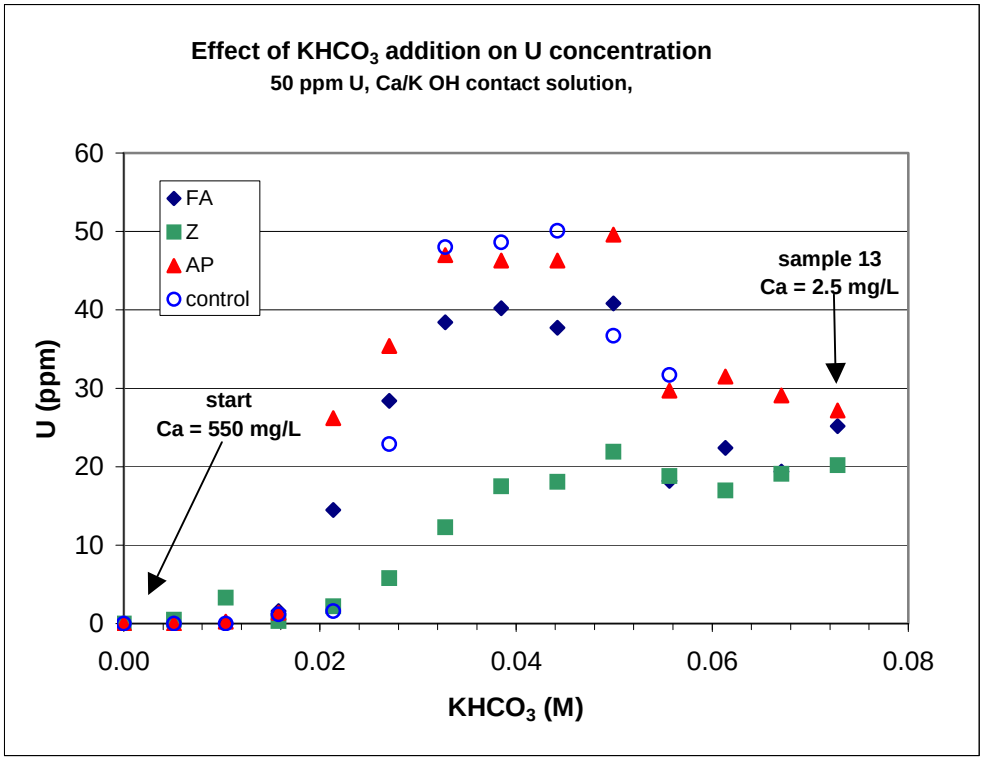

Figure 31. U concentration in solution in the presence of fly ash, zeolite, and apatite. Also shown is a control, consisting of U added to the contact solution.

These same data are shown plotted against pH in Figure 32. Zeolite retained U until about pH 9.4. The other materials and control began to release U by pH 11.0. All U (50 mg/l) was in solution by pH 10.5 for the control and by 9.5 for the apatite. Fly ash also reached a maximum concentration by pH 9.5, but the concentrations were about 40 mg/L. While the zeolite retained U better than fly ash and apatite, the reaction of zeolite with U and $KHCO_3$ is apparently complex, resulting in decreased and then increased pH while the U in solution slowly increased.

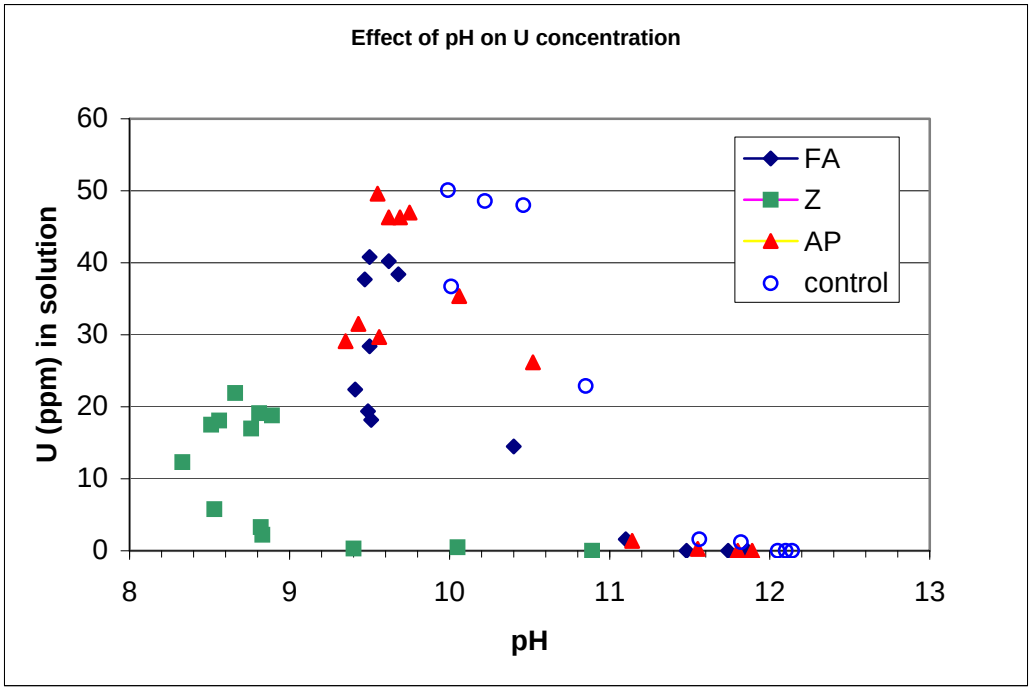

Figure 32. Data from Fig. 31 shown plotted against pH.

For fly ash, apatite and the control, there was a rapid loss of U from solution at pH 9.5, which also corresponds to a $KHCO_3$ concentration of 0.055 M. This precipitate is white, as opposed to the bright yellow of the earlier calcium uranate precipitate. Modeling with Geochemist's Workbench does not indicate a new phase reaching a solubility limit at this point. However, calcite is supersaturated throughout the experiment once $KHCO_3$ was added. X-ray diffraction and x-ray fluorescence analysis, discussed later, show that calcite did precipitate and carried substantial quantities of U with it. Based on a 547 mg/L difference in Ca concentrations from the beginning to the end of the control experiments, we calculate a mass of 198 mg of $CaCO_3$ precipitating. This calcite removed 2.6 mg of U from solution with U concentration of the precipitated calcite being 13.1 mg/g, while the solution concentration was around 0.02 mg/mL (20 ppm, see Figure 32). These concentrations result in a partition coefficient (K_d = [U on solid] / [U in solution]) of 660 mL/g.

From these experiments it is apparent that both of the grouts maintain their ability to retain U in the solid phase even as significant addition of $KHCO_3$ takes place. This is

principally related to maintaining pH above 11.5 but may also be the result of incorporation of U into new minerals, perhaps those forming as the cement reacts over time, such as ettringite. Portland cement and blast furnace slag both provide a similar benefit since they are the components that keep the pH very high. Apatite provides little benefit; in its presence all U was released to solution by pH 9.5. Fly ash did retain about 20 % of the U, but most entered solution as the pH dropped and $KHCO_3$ increased. The zeolite retained U effectively down to pH 9.0. Slowly U in solution increased as additional $KHCO_3$ was added. It appears that the zeolite reacted with the contact solution and the HCO_3^- and only as excess HCO_3^- became available did the pH began to move back up. From Figure 32 it seems that U concentrations, in contact with the zeolite, may have stabilized at about 20 mg/L.

Compare the concentrations of U in "new" and "aged" experiments as $KHCO_3$ is added.

A comparison between uranium released in the new grout experiments and releases from the aged experiments for grout 21 is shown in figure 33. The new experiments are compared to the aged samples that originally contained 50 ppm U in solution, so both started at the same concentration. The new and aged experiments both follow the same trend. Initially U concentrations were below detection limits, but U concentrations increased in solution with addition of $KHCO_3$ to similar concentrations. The implication is that results of short-term experiments compare favorably with those that aged for 550 days or more and, by implication, the short term behavior of U in contact with these materials is indicative of long-term (1-2 years) behavior.

Determine pH, U and other elemental concentrations in column effluent relative to pore volumes flowing through the grout.

Overall, the columns functioned as hoped for. The use of the Tevlar bags provided good exclusion of atmospheric CO_2 as evidenced by no formation of Ca carbonate or any other precipitate. The effluent in all cases was clear and stayed that way in the stored bags. The pH measurements generally were quite consistent and tracked appropriately.

Precipitates were observed in the tubing on both the outlet and the inlet sides of the columns. This developed slowly and, on the inlet side, was assumed to be the result of

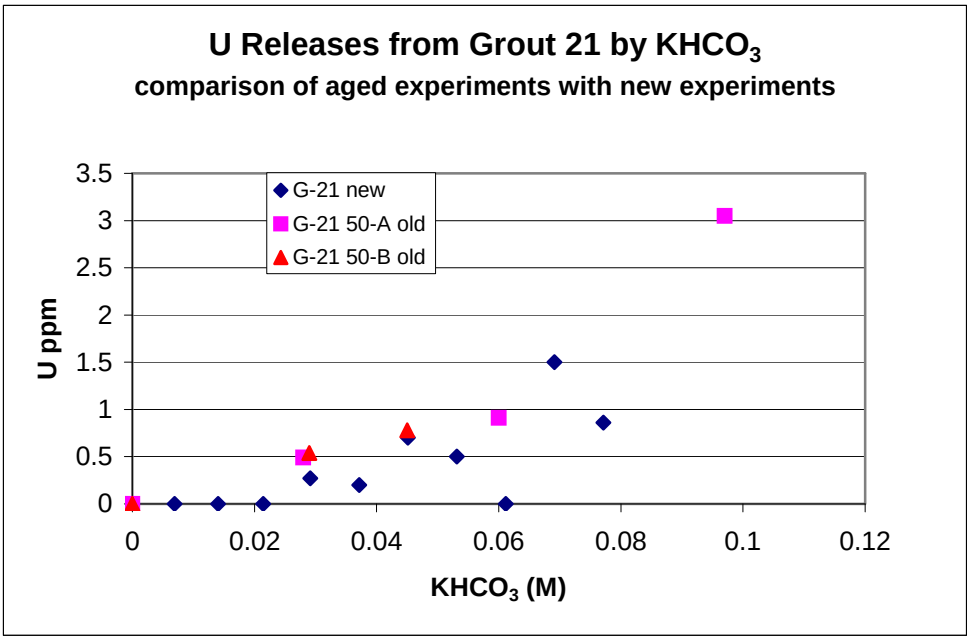

Figure 33. Comparison of new and aged U release experiments for grout 21 showing that results are similar.

back diffusion of alkalinity from the grout. The precipitate effervesced in acid, implying that it was calcium carbonate.

The leaching of uranium from each of the U-bearing columns was determined by KPA analysis. Concentrations of uranium in the leachate are shown in Figure 34 as a function of the number of pore volumes and in Figure 35 as a function of pH. The profile of U concentrations differed somewhat for each grout but in both cases were consistently below 70 µg/L, as shown in Figure 34. For grout 21 the profile of uranium release over time started at about 5000 g of effluent, or 200 pore volumes. U concentrations increased linearly to 70 µg/L at 700 pore volumes and pH of 9.4. From that point U concentrations decreased to the end of the experiment at 1178 pore volumes and pH of 8.4. At this point

U concentrations had declined to a range between 12 and 32 µg/L. Over the length of the experiment 664,500 ng of U were released in a total of 27,100 g of effluent, averaging

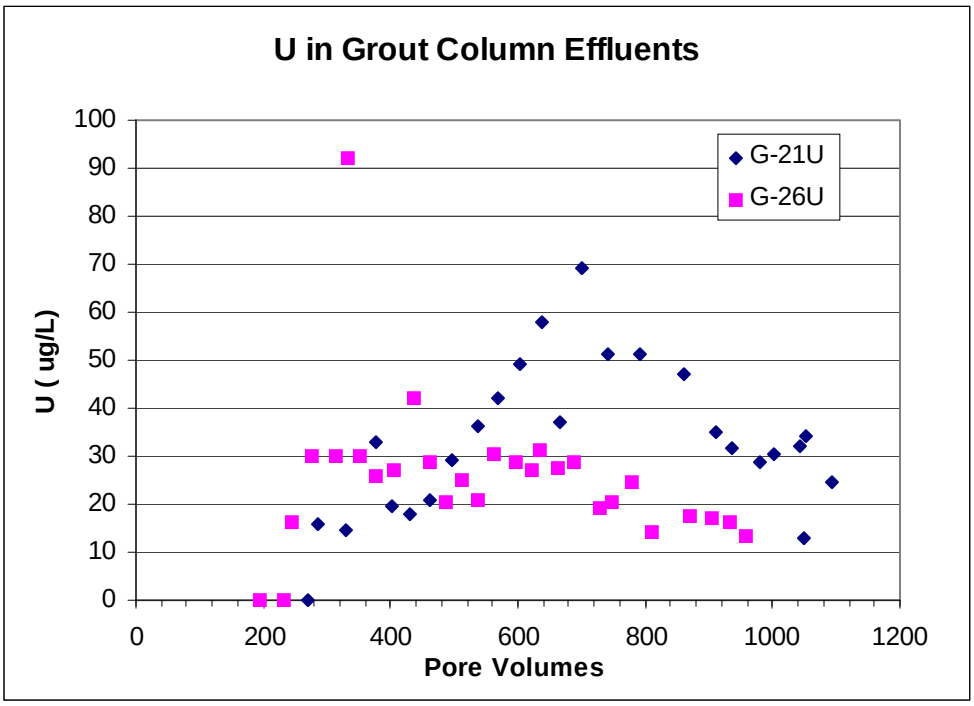

Figure 34. Uranium concentrations in effluent from the two uranium grout columns.

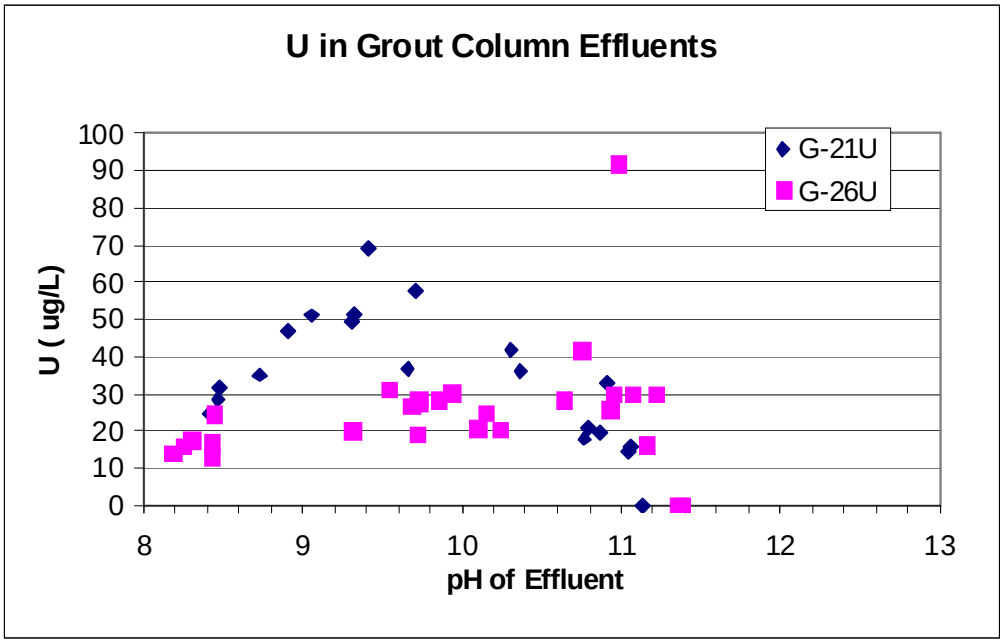

Figure 35. Uranium concentrations from the uranium grout columns plotted as a function of effluent pH.

24.5 ng/g. The column originally contained 6.74 mg of U and 0.66 mg were lost to the effluent over the course of the experiment, resulting in a 9.7 % mass loss of uranium over 1178 pore volumes.

For grout 26 the U release profile was different. As with grout 21, no U was detected in the effluent until about 5000 g or 180 pore volumes had passed through the column. The U concentration increased to between 30 and 40 μg/L where it remained for most of the experiment (one sample reached 92 ppb). By 20,000 g of effluent or 720 pore volumes, the U concentration began to decline. It had decreased to 12 μg/L by the end of the experiment at 922 pore volumes and pH of 8.2. Over the course of the experiment the grout 26 column released 495,800 ng of U, in a mass of 26,600 g of effluent, averaging 18.6 ng/g. The grout 26 column originally contained 7.27 mg of U and 0.495 mg were leached, with a loss of 6.8% uranium over 922 pore volumes. Table 9 summarizes the results of uranium leaching from the columns.

In both cases no uranium was detected (at detection limits of about 1 μg/L) in the effluent until between 180 and 200 pore volumes. At this point the pH was 11.2-11.4. The ending pH and U concentrations were similar for both grouts, but grout 26 provided a lower average concentration of U by 24%. Since U was distributed throughout the material in the column at the start of the experiment and about 200 pore volumes flowed through the systems before U was found in the effluent, it is likely that pH controlled the start of release of U from the grouts. Start of U leaching at pH 11.2 - 11.4 is consistent with results of the batch tests. The U simulated pore water control experiment for pH began to show U in solution around pH 11.5, while the batch experiments with new grouts showed leaching starting at pH 11.8. In the $KHCO_3$ control experiment U began to be seen in solution at pH of 11.6.

Table 9. Uranium leached from Columns

Column	Mass of U in Column (mg)	Mass of U leached (mg)	% U leached
G-21	6.74	0.66	9.7
G-26	7.27	0.50	6.8

There may be several processes controlling U concentrations from the grouts; and they may be different for the two materials. Based on the low fractional releases of 9.7 and 6.8 % mass loss of U, it is unlikely that the decreasing concentrations shown in Figure 34 are the result of uranium depletion of the columns. Further, the $KHCO_3$ simulated pore water control experiments show that U, not in the presence of grouts, would be entirely in solution by pH 10.5 as shown in Figure 26. Consequently, U concentrations must be controlled by interactions with solids in the column; either the grout or a new mineral that formed.

There are several possible interactions with solids that could control aqueous U concentrations. The U concentration of effluent from grout 21 increased linearly as pH declined, with U first being observed in solution at pH 11.4. The uranium concentration in column effluent increased to pH 9.4 and then began a linear decline. It is at this pH that U concentrations in the batch experiments containing fly ash and apatite (and near the pH of the simulated pore water experiment) all rapidly dropped as calcite precipitated. Co-precipitation of U with calcite may be responsible for the decreasing U concentrations in the columns. This process may control the U content in effluent of grout 26 too. However, the calcite precipitation would need to start earlier in the columns history to provide an almost steady state concentration.

Identify newly formed solid phases that influence U concentrations in the batch experiments.

Analysis of solid phase materials provided important information on uranium behavior in these materials. Figures 25, 26, and 31, in the previous sections, show there is a significant loss of U from solution as $KHCO_3$ was added and pH was lowered. This occurred in the simulated pore water experiment at pH 9.5 and in the apatite and fly ash experiments at pH 10. The precipitate that formed in the pore water experiment at this time was sampled and photographed with a Zeiss Axioscope microscope under ultraviolet light (mercury lamp with 330 – 350 nm excitation and > 420 nm emission filters) and white light (tungsten broad-spectrum lamp), and analyzed by microbeam x-ray diffraction mineralogy and x-ray fluorescence for elemental composition. Figures 36 and 37 are photomicrographs of the precipitate under white light and UV light respectively. Almost all of the precipitate were small tabular crystals of similar size. A very few were slightly larger with a different morphology. The photos show both forms.

Figure 36 shows that the larger particle is strongly fluorescent indicating that it contains significant quantities of UO_2^{+2}. In fact, fluorescence was so strong that it can be seen in Figure 18 under white and UV light. The smaller particles are only weakly fluorescent. This is not necessarily an indicator of U concentrations since only some minerals containing UO_2^{+2} are fluorescent. Uranyl (U VI) produces fluorescence in many but not all oxidized minerals (U (IV) minerals do not fluoresce); in general Ca, Ba and Na-Ca phosphates, arsenates, and carbonates are strongly fluorescent (either yellow-green or whitish-green) (Heinrich, 1958).

Figure 36. The same field as in Figure 37 but taken under UV light showing that the small particles are only weakly fluorescent while the less common ones fluorescence intently.

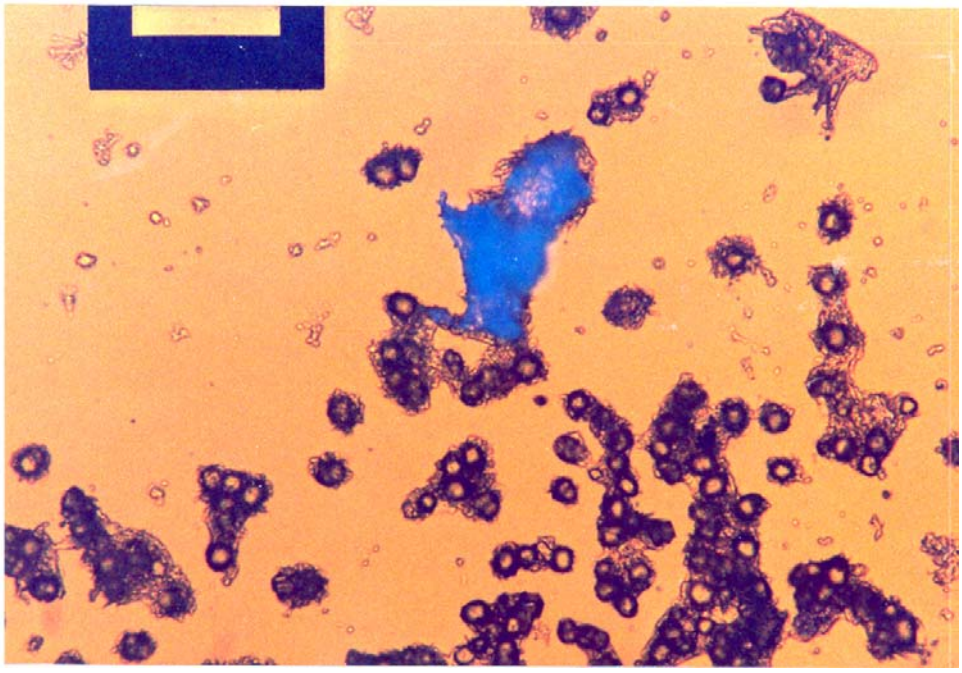

Figure 37. Precipitate from the U simulated pore water experiment showing both forms of the precipitate under white light. The small particles were the dominant phase by far. The larger particle fluoresced so strongly that it was apparent even under white light.

For this precipitate from the U simulated pore water experiment, the XRF results are shown in Figure 38. Uranium and calcium are the dominant elements in the precipitate. Some Sr is present as would be expected in a system containing calcium. In Figure 38, Cu and Zn are background and the other features between 5 and 7.5 keV are due to scattering and escape peaks. The presence of U and Ca in this spectrum could be the result of several minerals such as becquerelite $(Ca(UO_2)_6O_4(OH)_6(H_2O)_8$ or clarkeite $(Na,Ca)(UO_2)(O,OH)(H_2O)n$ (where n = 0 or 1) which contain U, Ca, O, and H. The O and H are not detected by this method. A microbeam x-ray diffraction plot of the precipitate is shown in Figure 39. It shows only peaks for calcite ($CaCO_3$). From these data it is apparent that calcite precipitated from the U control experiment at about pH

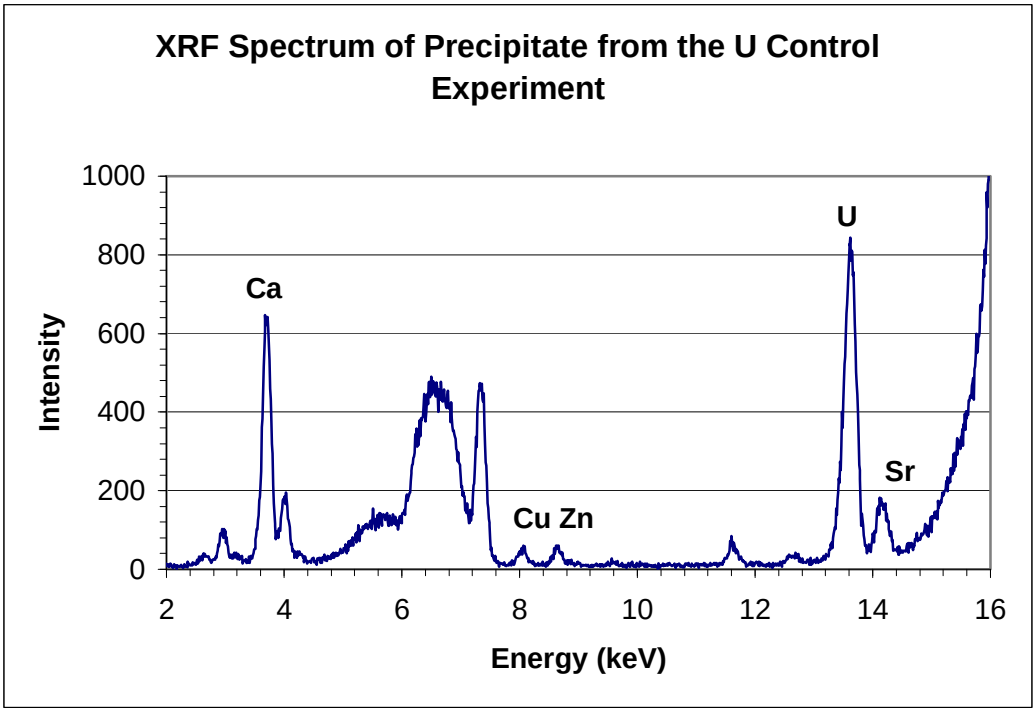

Figure 38. XRF spectrum of the small grained precipitate from the simulated pore water U control experiment.

10 and the calcite took significant quantities of uranium with it. This process also took place in experiments for apatite and fly ash in the contact solution, as the pH was adjusted to about pH 9.5 with addition of $KHCO_3$. Calcite is known to take up significant quantities of U (VI) as discussed earlier.

X-ray diffraction of bulk samples of the "aged" grouts after $KHCO_3$ was added was performed on Beamline X-7a, which is dedicated to high resolution XRD studies, at the NSLS. Dried samples were loaded into glass capillary tubes and placed on the diffractometer and scanned through two-theta. Diffractograms of both grouts contained significant signals for both calcite and aragonite. In addition the grout column experiments showed ample precipitation of calcium carbonates. Calcite is a major weathering product of cementitious materials, and of the grouts, and partitioning of uranium to calcite is an important control on its long-term fate.

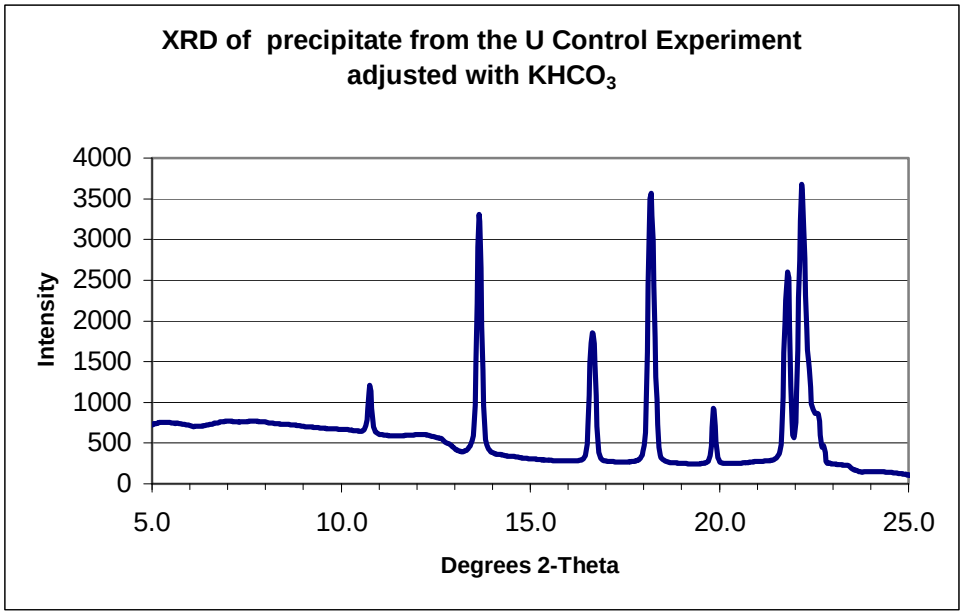

Figure 39. Microbeam X-ray diffractogram of precipitate from the simulated pore water U control experiment showing peaks only for calcite.

Microbeam XRF and XRD were used to examine crystals that grew in the aged grout experiments in which the grout was immersed for 550 or more days. These needle-shaped crystals grew in clusters and individually on the container sides and on the surface

of the grout. Similar looking crystals appeared in experiments with other actinides. Initially it was assumed that this material was $CaCO_3$. As shown in Figure 40, one of these crystals, taken from the grout 21 U experiment contains Ca, as a major element and U, As, Sr, Pb, Se and possibly Ce as minor components. Figure 41 shows a very similar spectrum for grout 26. We suspect that another major component is phosphate but were unable to obtain a signal for it at X-26a which is optimized for detection of elements with energies greater than P. While there are a number of minerals that could contain U and As as trace components, there are few minerals in which U (VI), Ca and As are major components; one is uranospinite $(Ca[(UO_2)(AsO_4)]_2(H_2O)_{10}$. The arsenates are structurally very similar to the phosphates, have very low solubilities, and likely form solid solutions with them (Finch and

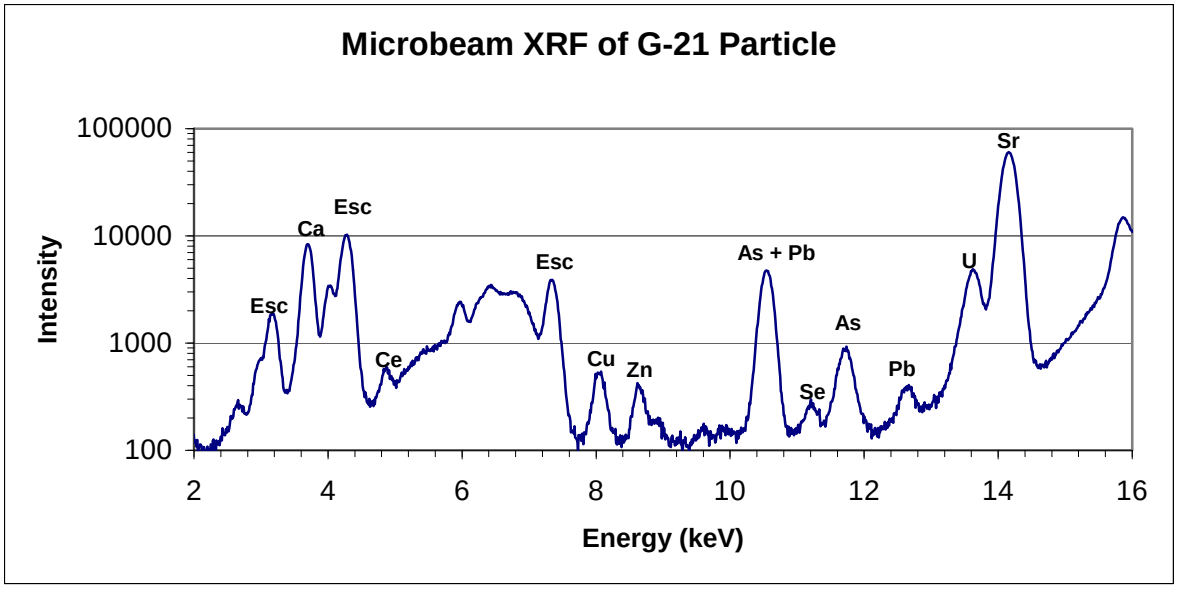

Figure 40. XRF spectrum of crystal taken from an aged Grout 21 U experiment. "Esc" designates escape peaks.

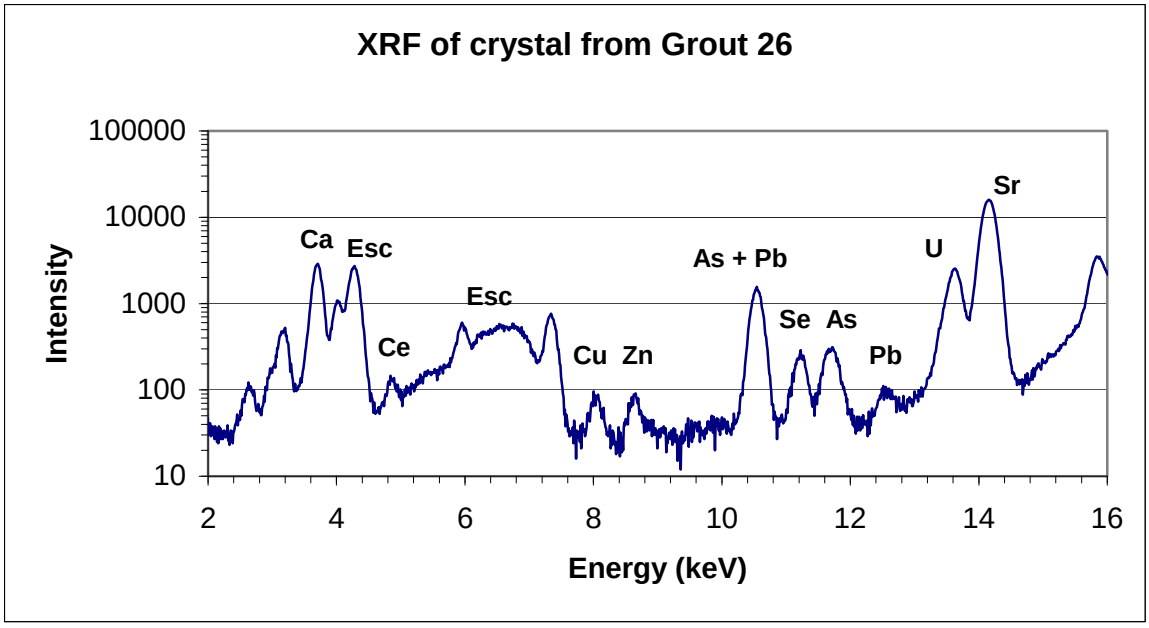

Figure 41. XRF spectrum of crystal taken from an Aged Grout 26 experiment.

Murakami, 1999). These minerals probably control groundwater concentrations of U in some locations (Finch and Murakami, 1999). Micro-beam x-ray diffraction was used on crystals from both G-21 and G-26 uranium experiments but was unable to identify the mineral. Subsequent analysis of three of these crystals from different U experiments was performed on a single crystal diffractometer at the Department of Earth Sciences at Stony Brook University (with thanks to Prof. John Parise and Dr. Aaron Celestion). These detailed analyses provided unit cell parameters for the crystals (a=b=4.9903(7) c=17.0867(34)) and identified all three as calcite. All three samples had essentially the same spacing and there was no indication of changes in the cell parameters with incorporated U. From this it is apparent that calcite as it is forming in these conditions incorporates several additional elements. Most of these are oxyanions. Because of the observation of As and Se in these crystals, samples of effluent from the column experiments were run by ICP for As, Se, V and P. The sample intervals for both grout 21 and 26 were: 5, 25, 45, 65, and 88. None of the elements were observed above detection limits of about 0.1-0.4 mg/L. Calcite also forms in the flow-through systems but it is

unclear if this more rapidly forming material incorporates trace elements as in the batch experiments.

Summary of Uranium in Contact with Grout

Both grouts retain U under their initial pH of about 12 to 11.7. This is so for experiments aged for over 550 days and for those run for only about 2 months. Concentrations of U in solution were below ICP detection limits of 0.3 ppm, under these conditions. In both the aged and new experiments the addition of $KHCO_3$ resulted in similar trends in releases of U. Grout 21 retained U up to additions of about 0.08 M of $KHCO_3$ then U concentrations increased to a maximum of 30.0 mg/L at 0.1 M. Grout 26 was more susceptible to $KHCO_3$ with release of U to 17 mg/L taking place with addition of 0.03 M $KHCO_3$, in one specimen, reaching a maximum of 70 mg/L at 0.1 mM $KHCO_3$. Grout 21 also provided better pH buffering around 11-12 on addition of $KHCO_3$, while Grout 26 was pushed to lower pH values. From these data, Grout 21 provided better retention under ambient groundwater conditions and under high bicarbonate addition. A major factor that is likely to control U releases from the grout is incorporation into secondary phases that form as the grout weathers and interacts with carbonate/bicarbonate bearing waters. The dominant minerals to form are the calcium carbonates; calcite, aragonite and vaterite. These were observed in grout experiments to which $KHCO_3$ had been added. Precipitation of calcite in new experiments lead to removal of U at the rate of 13.1 mg/g of $CaCO_3$ giving a K_d of 660 mL/g. Calcite also was observed as small needle-like crystals in essentially all of the aged grout experiments and contained trace concentrations of U, As, Pb, Se and Sr. It is likely that this material is controlling solution concentrations of U and As in contact with the grouts.

The columns provided data over a pH range of 12 to 8.3. This change in pH required approximately 1000 pore volumes of simulated ground water. The leaching profiles of U, Ca, Mg, Na, K, Fe, Si and Al were determined. In both columns U did not appear in the leachate until after 200 pore volumes. From that point the columns behaved differently. Uranium from Grout 21 increased linearly to a maximum of 70 μg/L at 700

pore volumes and then decreased steadily to between 10 and 25 μg/L. Uranium from grout 26 reached a maximum concentration of 42 μg/L at 440 pore volumes and then slowly declined to 13 μg/L. Precipitates of $CaCO_3$ were observed in the tubing from the columns and this implies that $CaCO_3$ and perhaps other authigenic minerals control U concentrations over extended pore volumes. Over the course of the experiment the Grout 21column leached 9.7% of its U, while the Grout 26 column leached 6.8%.

References for U

Atkins M., J. Cowrie, F.P. Glasser, T. Jappy, A. Kindness, and C. Pointer, 1990, Assessment of the Performance of Cement-Based Composite Material for Radioactive Waste Immobilization, Scientific Basis for Nuclear Waste Management XIII, Oversby and Brown (ed), Mat. Res. Soc. Symp. Proc. Vol. 176, pp 117-127.

Bernhhard, G., G. Geipel, T. Reich, V. Brendler, S. Amaryi, and H. Neitsche, 2001, Uranyl (VI) carbonate complex formation. Validation of the $Ca_2UO_2(CO_3)_3$ (aq) species, Radiochimica Acta, 89, 511-518.

Bernhard, G., G. Geipel, V. Brendler, and H. Nitsche, 1996, Speciation of uranium in seepage waters of a mine tailing pile studied by time-resolved laser-induced fluorescence spectroscopy (TRLFS), Radiochimica Acta 74, 87-91.

Brownsword, M., A.B. Buchan, F.T. Ewart, R. McCrohon, G.J. Ormerod, J.L. Smith, and H.P. Thomason, 1990, The Solubility and Sorption of Uranium (VI) in a Cementitious Repository, Scientific Basis for Nuclear Waste Management XIII, Oversby and Brown (ed), Mat. Res. Soc. Symp. Proc. Vol. 176, p 577-582.

Berner, U. R., 1992, Evolution of Pore Water Chemistry, Waste Management, Vol. 12, pp. 201-219.

Clark, D.E., D.L. Hobart, and M.P. Neu, 1995. Actinide carbonate complexes and their importance in actinide environmental chemistry. Chemical Reviews, 95, 25-48.

Delany J. M. and Lundeen S. R. (1989) The LLNL thermochemical database. Lawrence Livermore National Laboratory Report UCRL-21658.

Elzinga, E., C. Tait, R. Reeder, K. Rector, R. Donohue, and D. Morris, 2004, Spectroscopic Investigation of U(VI) sorption at the calcite-water interface, Geochimica et Cosmochimica Acta, 68, 2437-2448.

Ewart F.T., J.L. Smith-Briggs, H.P. Thomason, and S.J. Williams, 1992, The Solubility of Actinides in a Cementitious Near-Field Environment, Waste Management, Vol. 12, pp.241-252.

Fanghänel, Th. and V. Neck, Aquatic Chemistry and Solubility Phenomena of Actinide Oxides/Hydroxides, Pure and Applied Chemistry, 2002, vol. 74, pp. 1895-1907.

Finch, R. and T. Murakami, 1999, Systematics and paragenesis of uranium minerals, pp.91-180, In: Uranium: Mineralogy, Geochemistry, and the Evironment, (P. Burns and R. Finch, editors), Reviews in Mineralogy, Volume 38, Mineralogical Society of America, Washington, D.C.

Heinrich, E. W., 1958, Mineralogy and Geology of Radioactive Raw Materials, New York: McGraw Hill. 654 pp.

Kelly, S., M. Newville, L. Cheng, K. Kemner, S. Sutton, Fenter, P., N. Sturchio, and C. Spotl, 2003, Uranyl incorporation in natural calcite, Environmental Science and Technology, 37, 1284-1287.

Kelly, S., K. Kemner, and S. Brooks, 2007, X-ray Adsorption Spectroscopy Identifies calcium-Uranium- Carbonate Complexes at Environmental Concentrations, Geochimica et Cosmochimica Acta, 71, No. 4 pp. 821-834.

Krupka, K., D. Rai, R. Fulton, and R. Strickert, 1985, Solubility Data for U (VI) Hydroxide and Np (IV) Hydrous Oxide: Application of MCC-3 Methodology, Scientific Basis for Nuclear Waste Management VIII, Jantzen, Stone, and Ewing (ed), Mat. Res. Soc. Symp. Proc. Vol. 44, pp 117-127.

Liu, C., J. Zachara, O. Qafoku, J. McKinley, S. Heald, and Z Wang, 2004, Dissolution of uranyl microprecipitates in subsurface sediments at Hanford Site, USA, Geochimica et Cosmochimica Acta, 68:4519-4537.

Meece D. and L. Benninger, 1993, The coprecipitation of Pu and other radionuclides with $CaCO_3$, Geochimica et Cosmochimica Acta, 57, 1447-1458.

Perez, I., I. Casas, M. Martin, and J. Bruno, 2000, The thermodynamics and kinetics of uranophane dissolution in bicarbonate test solution, Geochimica et Cosmochimica Acta, 64:603-608.

Reeder R., M. Nuggent, C. Tait, D. Morris, S. Heald, W. Hess, and A. Lanzirotti, 2001, Co-precipitation of uranium (VI) with calcie: XAFS, micro-XAS, and luminescence characterization, Geochimica et Cosmochimica Acta, 65, 3491-3503.

Schindler and Putnis, *Crystal Growth of Schoepite on the (104) Surface of Calcite*, Canadian Mineralogist, 2004, p.1667-1681.

Sowder, A.G., Clark, S.B. and R. Fjeld, 2001, The impact of mineralogy in the U(VI)-Ca-PO_4 system n the environmental availability of uranium, Journal Radioanylitical and Nuclear Chemistry, 248:517-524.

Stipp, S. and M. Hochella, 1991, Structure and bonding environments at the calcite surface observed with X-ray photoelectron spectroscopy (XPS) and low-energy diffraction (LEED), Geochimica et Cosmochimica Acta, 55, 1723-1736.

Plutonium Results

Summary of Environmental Plutonium Chemistry

The chemical identity, solid-solution behavior, and long-term fate of plutonium in the natural environment is poorly understood; the majority of fundamental studies of its chemistry have been performed under conditions relevant to nuclear weapons production; generally acidic and at high concentrations (markedly different chemical conditions than that encountered in grouts). The following is a brief survey of the environmental chemistry of Pu.

Near Surface Environments: Plutonium most commonly occurs in soils and wastes as mobile non-aqueous-phase organic- and inorganic-complexes or insoluble-oxides and hydrolysis products of Pu(IV). In oxic soils, at pe values between 5-11 and at pH ~4-9, Pu can exist in the +3, +4, +5, or +6 oxidation state; generally the +5 oxidation state (PuO_2^+) predominates in more oxidizing waters with low concentration of DOC (Rai et al., 1980; Choppin, 1991). Here Pu(V) is stable especially at < 10^{-6}M Pu because disproportionation reactions (radiolytically induced redox reactions in which Pu(V) is transformed to Pu(IV) and Pu(VI)), are minimized. The effective charge of the $Pu(V)O_2^+$ is lowest of all of the oxidation states of Pu, therefore, the overall tendency to form complexes is low. Even so, Pu (V, VI) carbonate species can be very stable in groundwaters with carbonate concentrations ~10^{-3} M (Runde, 2000). However, in soil solutions that contain natural organic matter (NOM), Pu(V) tends to reduce to Pu(IV) (Reed, 1998, Andre and Choppin, 2000). The aqueous Pu(IV) that is not complexed with NOM will most likely be present as the $Pu(OH)_4(aq)$ species (Runde et al., 2002). This species has a tendency to polymerize and form an amorphous hydroxide ($Pu(OH)_4(am)$) with very low solubility (log K_{sp}= -58.7; Rai, 1984). The amorphous Pu hydroxide can form a stable colloid (>25 nm) and has been implicated in transport of Pu in near-surface environments (Penrose et al., 1990). Other colloidal forms of Pu in oxic environments include adsorbed species on Fe oxides (Lu et al., 1999) and organic macromolecular (10-15 kDa) complexes possibly consisting of extracellular polymeric substances (Santschi et al., 2002). The sorption of Pu(V) onto Fe oxides increases with increasing pH and the affinity of Pu for Fe oxides is as follows: hematite (α-Fe_2O_3) > ferrihydrite

($Fe_{10}O_{15}\cdot 9H_2O$) > goethite (α-FeOOH) (Triay et al., 1997). Duff (2001) showed by XANES that Pu(V) adsorbed to Mn(IV) oxides from Yucca Mountain was present as Pu(VI) possibly due to the oxidizing properties of the Mn oxide surface. The least reactive phase in aerobic environments may be the PuO_2(s); however a phase with higher oxygen content (PuO_{2+x}) was recently discovered (Haschke et al., 2000). This phase may not be stable under all conditions in the environment, with the suggestion that Pu(V) may be released to solution and ultimately disproportionating to Pu(IV) and Pu(VI) with hydrolysis of Pu(IV) and complexation of Pu(VI) (Haschke and Oversby, 2002). Ultimately , the retention of Pu by organic matter under oxidizing conditions may strongly limit the aqueous transport in aerobic environments. However, Pu(IV) in association with solid phases in soil may be mobilized due to i) production of ligands with a high affinity for Pu, ii) oxidation of Pu(IV) to more soluble +5 and +6 oxidation states, and iii) production of carbonate species such as $PuO_2(CO_3)^0$, $PuO_2(CO_3)_2^{2-}$, $PuO_2(CO_3)_3^{4-}$, or $PuO_2CO_3^-$. Immobilization may occur due to i) degradation of Pu-complexes with release of Pu as particle- or surface-reactive species, or ii) sequestration with mineral or other sorptive surfaces. Figure 42 shows the expected Pu speciation for the system Pu-O_2-CO_2-H_2O at 25°C.

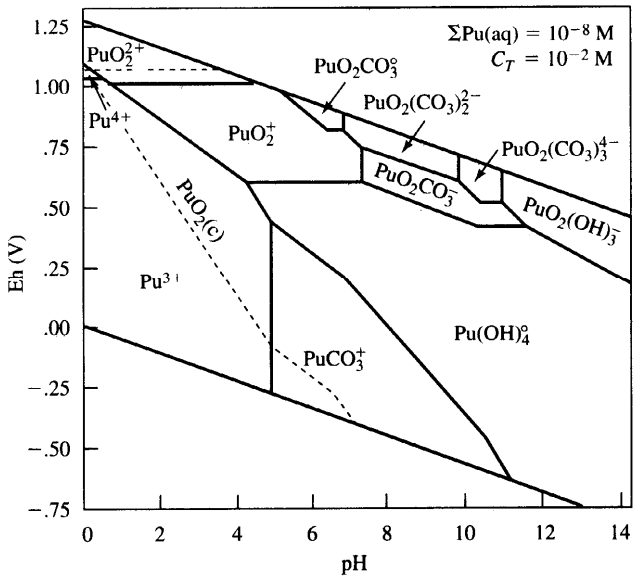

Figure 42. Eh-pH diagram for Pu in the presence of carbonate (C_T=10^{-2} M)(adapted from Langmuir, 1997).

Subsurface Environments: Plutonium in reducing anoxic environments will predominantly be in the +4 oxidation state as an adsorbed species on iron-oxide minerals, in association with colloidal iron species, or as a Pu(IV) organic (possibly a colloid). Litaor and Ibrahim (1996) found that the majority (65%) of Pu was associated with organic matter and 20% with iron oxides in Pit 1 at Rocky Flats. Lu et al. (1998) showed that the majority of Pu in Rocky Flats soil of particle size <25mm resided with the iron oxides and that citrate/dithionate extraction reduced Fe(III) and released occluded Pu into solution. Studies of Pu adsorption to soil from the Snake River Plain of the Idaho National Engineering and Environmental Laboratory revealed that surface complexation with iron oxide minerals and precipitation of hydrolysis products governed Pu immobilization (Mincher et al., 2003). The similarity in reduction potentials for hydrous PuO_2 and α-FeOOH suggests that the establishment of reducing conditions capable of solubilizing crystalline iron oxide phases might reduce Pu (IV) oxyhydroxides. Plutonium (III) is least likely to form complexes and therefore is least surface reactive and is more likely to be soluble relative to Pu (IV).

Still other solid phases may form from reactions between Pu and grout components, not only the cementitious materials, but also the additives used in the grout. Another process that may exert control on Pu concentrations is adsorption onto solids within the grout. These may be additives such as the fluorapatite or zeolite that comprise 12 and 10 % respectively of the grouts, or they may be minerals, typically Ca-Al-Si materials, that form in the grout system as the cement sets. In addition, over time $CaCO_3$ minerals, such as calcite and aragonite, will form as a rind on the grout and as a fracture filling mineral. Based on an estimate by Curti (1999) Pu will be incorporated into these secondary minerals, to a moderate extent with K_d's between 20 and 200, as they precipitate.

Details for Pu experiments

The tracer used was in the form of $Pu(NO_3)_4$ and, based on the nominal 10 μCi tracer obtained from Isotope Products Laboratory, the concentrations in the isotherm experiment solutions were 2750, 1375, 410, 275, and 100 pCi/mL. A blank and a spike were prepared from a grout sample that contained no radionuclides, to determine background count rates and assess if there were any quenching issues. As described in the Methods Section, later experiments were conducted with no solids present, consisting of simulated grout pore water with ^{239}Pu tracer added and periodic additions of $KHCO_3$. An acidic reference gave count rates of 256 cpm/mL or 103 pCi/mL (7.0×10^{-9} M). Another control was made in the same way but aliquots of 1 molal HNO_3 were added to lower the pH of those samples with high pH. These samples also were counted by liquid scintillation with 2 mL of sample in 17 mL of Ultima-Gold cocktail with a Wallac Model 1414 counter and 60 minute count times. This instrument can distinguish between beta and alpha emissions. We used the total alpha count rate which includes daughters that may be present. Concentrations were determined using specific activities reported in the tracer documentation from Isotope Product Laboratories, in conjunction with dilution factors and reference samples. The isotopic content of the tracer is given in Table 10.

Table 10. Pu isotopes in tracer

Isotope	% alpha activity
Pu-239	92.0
Pu-238	0.36
Pu-240	7.07
Pu-241	N/A
Pu-242	0.00
Am-241	0.55

Detection limits for Pu are calculated to be about 0.45 pCi/mL which is equivalent to 3 x 10^{-11} mol/L (Currie, 1968). Table 11 presents the activities and molarities of the tracers in the starting solutions of the "old" isotherm experiments and kinetics experiments used in this study.

Table 11. activity and molarity of Pu in experiments

	Pu tracer	
	nCi/L	mol/L
1	2700	4.4×10^{-8}
2	1170	1.91×10^{-8}
3	220	3.59×10^{-9}
Kinetics	103	1.68×10^{-9}

Plutonium Isotherm Results

Count rates of the samples were all very low, ranging from 0.18 to 0.74 cpm/mL. While acceptable peaks were observed for reference solutions, no alpha peaks were observed in the LSC spectra for samples. The blank, containing liquid of similar chemistry to the samples, gave a count rate of 2.29 cpm/mL which was subtracted from samples and references. Results are shown in Figure 43. The residual low count rates in the samples were treated as if they were actual Pu counts (although they may not be) and were used to

calculate K_d values given in Table 12. Ewart et al. (1992) found the solubility of Pu (as $Pu(OH)_4$) was constant from pH 9 to 13, at 7 x 10^{-11} M. The count rate shown in Figure 43 probably represents a detection limit of our experiment.

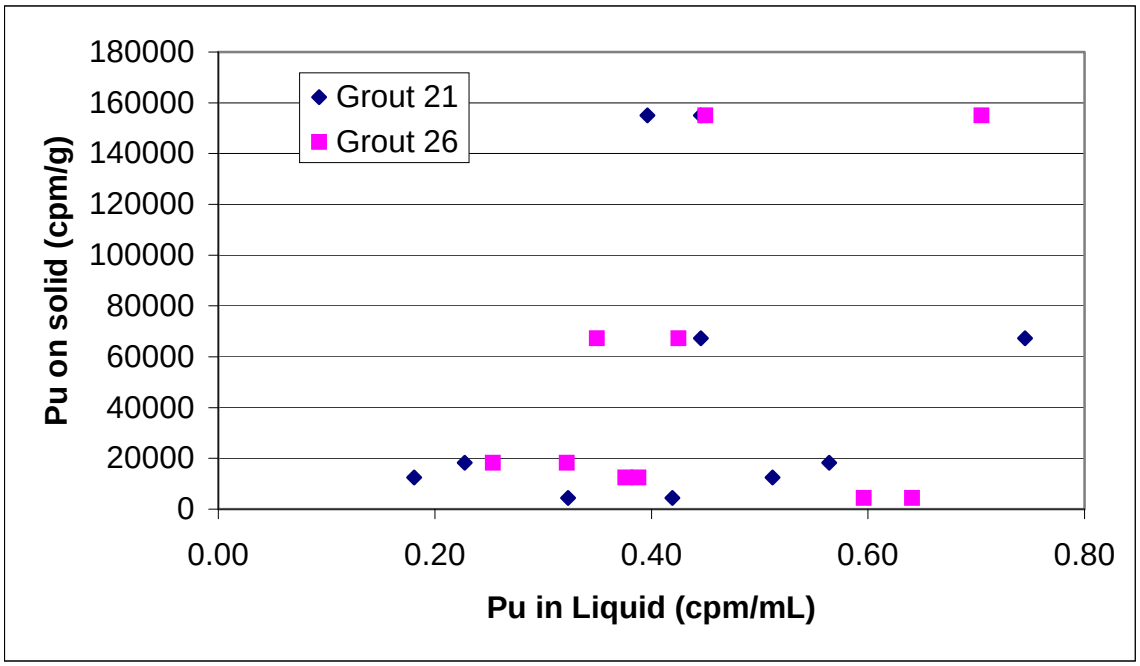

Figure 43. Pu grout isotherms showing the very low count rate for Pu in the aqueous phase.

Table 12. Estimated K_d Values for Pu

	Grout 21			Grout 26		
Nominal Activity	Start CPM	End CPM	K_d (mL/g)	Start CPM	End CPM	K_d (mL/g)
1	175	0.4	12,000	175	0.6	7,000
3	502	0.4	47,000	502	0.3	33,000
4	733	0.4	56,000	733	0.4	64,000
15	2690	0.6	121,000	2690	0.4	175,000
30	6200	0.4	370,000	6200	0.6	282,000

Plutonium Batch Experiment Results

Determine if Pu, which has been sequestered in contact with the two grouts, returns to solution as the grouts age.

Results of resampling aged grout experiments are shown in Table 13 for ^{239}Pu (aged 502 days). Solutions from the three highest tracer concentration sample sets from the isotherm experiments were taken. Averaged results (n = 4 for each set) and starting solution activities are given in Table 13.

Table 13. ^{239}Pu (nCi/L) in Solution in Aged Grout Experiments

Pu (nCi/L)		
Start	**59 days**	**502 days**
2700	< 0.45	< 0.45
1170	< 0.45	< 0.45
220	< 0.45	< 0.45

Results are all below the detection limit of 0.45 nCi/L (3 x 10^{-11} mol/L). After aging, the count rates were very similar to those observed in our earlier short term experiments with these same samples. No differences were observed between the two grout formulations for either tracer.

As the grout experiments aged they attained a range of pH values; they varied from 10.10 to 10.78. These differences are primarily due to some incursion of CO_2 and resultant carbonation of the samples, providing an effect similar to weathering in the environment. Each of these groups is a composite of samples that started with different concentrations of tracer, as mentioned above. Independent of the starting concentrations, all of these count rates are similar, essentially below detection limits. In summary, while the pH of these samples was slightly lowered by aging, overall there was no release of Pu to solution.

Determine if Pu, sequestered with the aged grouts, returns to solution on contact with increasing concentrations of $KHCO_3$.

The effect of $KHCO_3$ addition to the solution in contact with each grout was determined beyond a HCO_3^- concentration equivalent to that of the West Valley groundwater. This is based on the assumption that in an open system, CO_2 ingress will persist. In addition, precipitation of calcite can be inhibited by a number of factors, allowing carbonate/bicarbonate concentrations to become elevated significantly beyond that expected. Figure 44 shows how Pu content and pH were

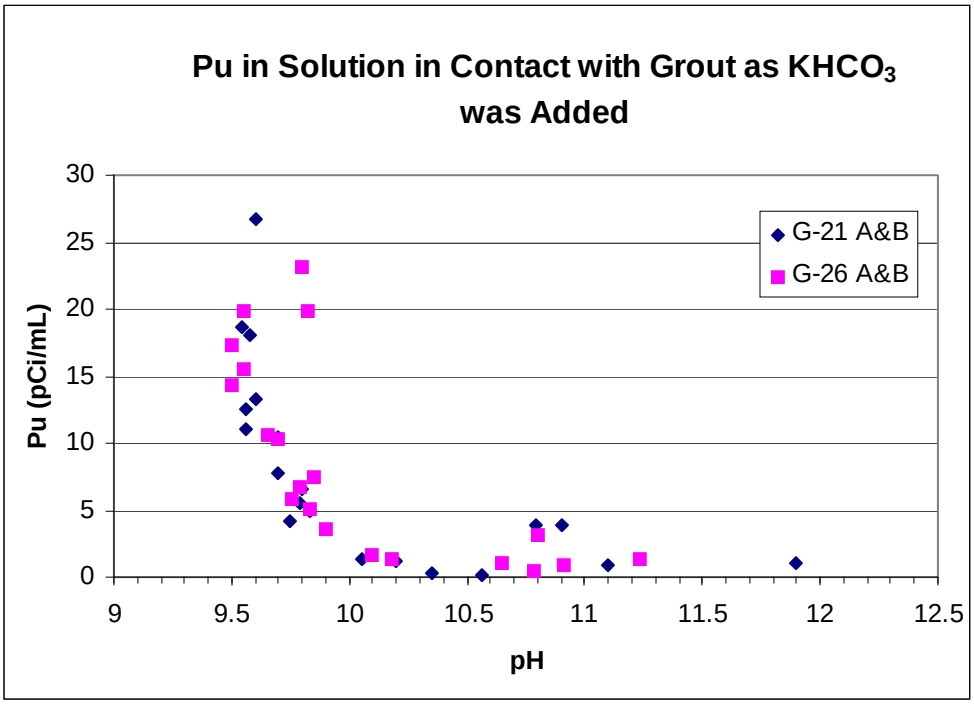

Figure 44. Pu concentrations in solution as a function of pH as $KHCO_3$ was added. These are aged grout experiments that subsequently received additions of $KHCO_3$.

changed by addition of $KHCO_3$ for each of the grouts. These experiments had aged 502 days before the start of additions and the starting pH of grouts 21 and 26 were 11.9 and 11.2 respectively. For this experiment we used the four samples containing the most activity (two for each grout formulation). The original activity at the start of these experiments was 2700 pCi/mL. The concentration of $KHCO_3$ was increased to 0.29 M

(as added) over the course of 10 additions and sampling intervals. This concentration is significantly greater than one would expect in the natural system but additions of $KHCO_3$ were continued to follow the increasing Pu activity in solution. Figure 45 shows that as pH was decreased (and $KHCO_3$ content increased) Pu was released to solution. The maximum concentration in solution was about 0.9% of the total activity in the experiment.

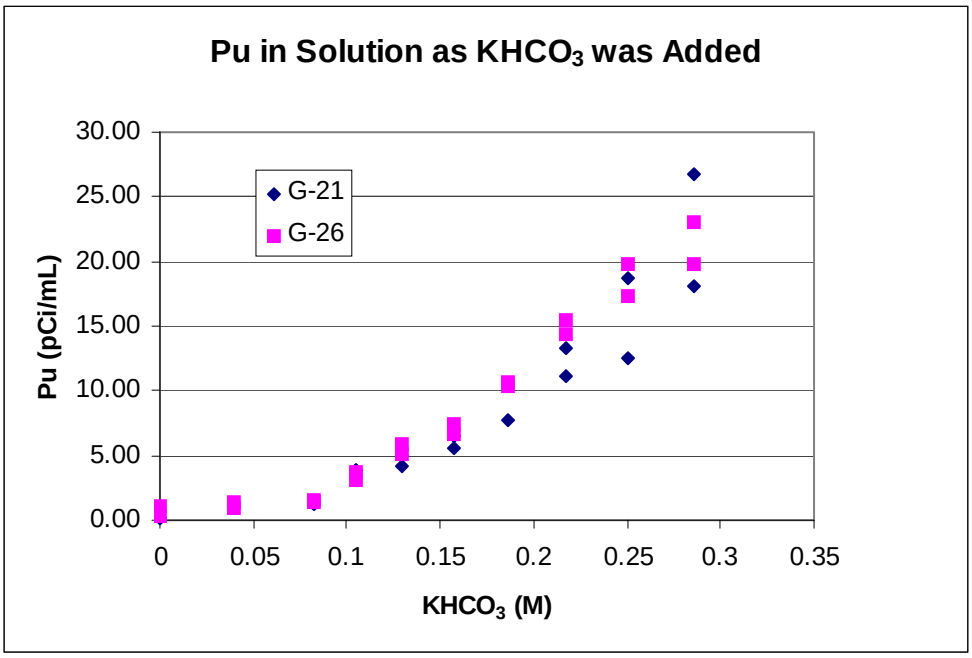

Figure 45. The release of Pu to solution from the grouts increased with increasing $KHCO_3$ additions.

As shown in Figure 45, Pu remained at or near detection limits up to a $KHCO_3$ addition of 0.08 M; then it increased linearly.

Determine the behavior of Pu that has precipitated in a simulated grout pore water (without grout present), as the pH is lowered or $KHCO_3$ content is increased.

Figure 46 shows the aqueous concentrations of Pu in simulated pore water control experiments in which pH or $KHCO_3$ were altered. In both experiments, Pu in the alkaline contact solution was undetectable under the initial condition of pH 12.3. In these two parallel experiments, aliquots of 1M $KHCO_3$ were added to one bottle of simulated pore

water and 1M HNO_3 and NaOH were added to another to adjust pH. As $KHCO_3$ content increased, the Pu concentration increased so that at pH 10 it was 5 pCi/mL. The pH experiment started at pH = 12.3 and was lowered with HNO_3. Pu first was observed in solution starting at pH 11.3 and increased exponentially to around pH 8, reaching a maximum of 7 pCi/mL.

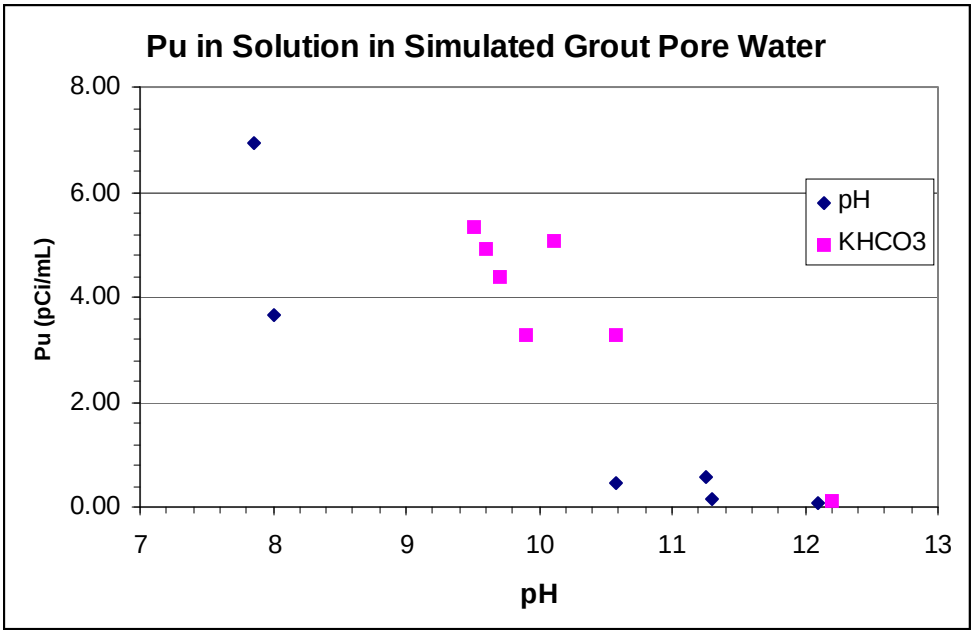

Figure 46. Pu in solution as a function of pH in simulated grout pore water experiments, as influenced by changing pH and $KHCO_3$ content.

The aged grout experiments are plotted with the results of the simulated pore water experiments as a function of pH in Figure 47 and of $KHCO_3$ in Figure 48. Both the pH and $KHCO_3$ pore water experiments resulted in some dissolution of precipitated Pu. In the pH experiments, releases were lower than those receiving $KHCO_3$, with or without grout present. Releases in the $KHCO_3$ experiment seem to parallel those containing grout although the last two points (Figure 47 around pH 9.5) were trending lower. Evidently complexation of Pu with carbonate strongly dominates the system even with the grout present. Calcium carbonates precipitated in the $KHCO_3$ experiment on addition of $KHCO_3$ and were present in the grout experiments as well, as a long-term product.

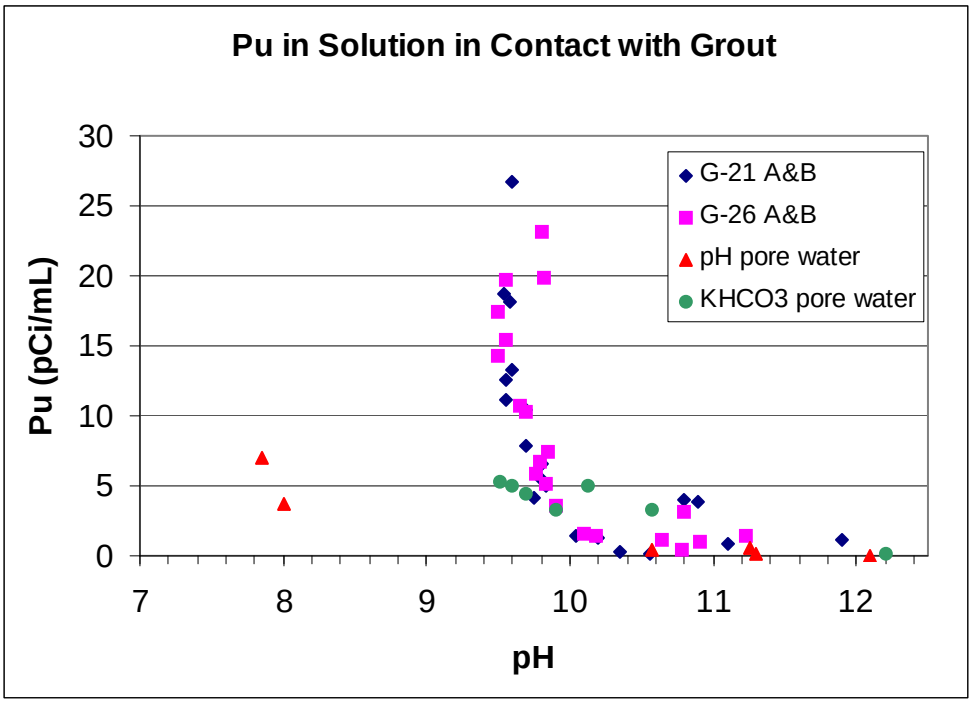

Figure 47. Results of the pH and $KHCO_3$ pore water experiments compared to the grout experiments that were adjusted with $KHCO_3$.

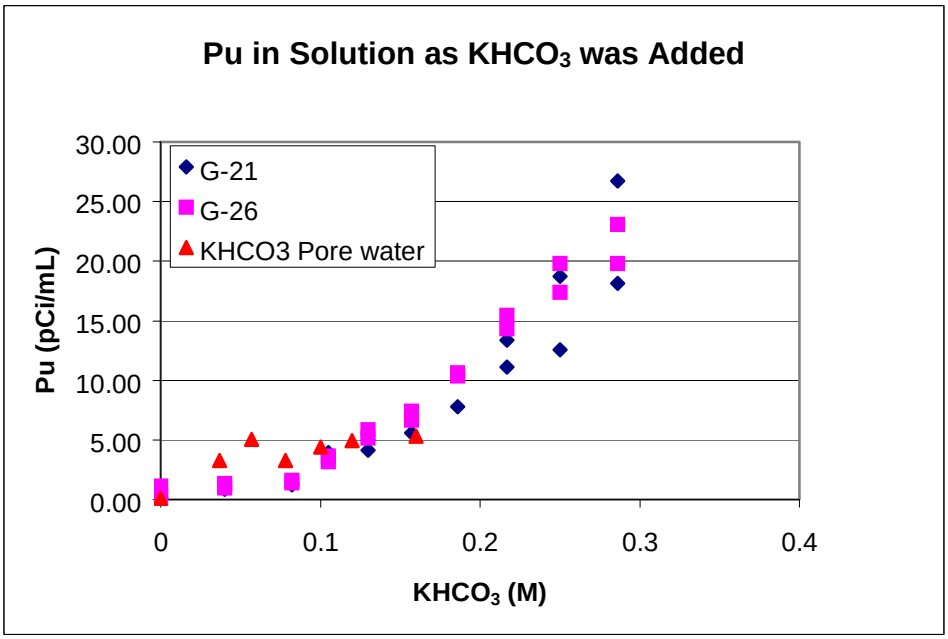

Figure 48. Release of Pu to solution as a function of $KHCO_3$ addition from the grout experiments and from the $KHCO_3$ pore water experiment.

Additional precipitation in the grout experiments, as $KHCO_3$ was added, may have been minimized by the lower availability of Ca since it had been removed from solution by long-term reactions. As a consequence more carbonate/bicarbonate remained in solution to react with Pu forming a soluble complex. The data from the grout experiments seem to follow rather closely the solubility data presented by Kim et al., (1983) for Pu (IV) as a function of pH with carbonate concentration of 3×10^{-3} M. In that work Pu solution concentrations reached a minimum of 2×10^{-9} M between pH 10 and 11.4 and then began to increase as pH increased. Our concentrations are lower, the Pu concentrations at high pH are at detection limits which we calculate to be 3×10^{-11} M.

We performed a simulation of the Pu(IV) speciation in the experiment by using PHREEQCi, a computer program for geochemical speciation calculations (Parkhurst and Appelo, 1999). The thermodynamic constants for various Pu(IV) hydroxide species were obtained from Lemire (2001) and the Pu carbonate species from other sources (Clark et al., 1995; Runde et al., 2002). Figure 49 shows the Pu(IV) speciation in the absence of bicarbonate, and with 0.01 M bicarbonate added. The speciation calculations show that the addition of 10 mM bicarbonate results in the formation of the $Pu(CO_3)_3^{-2}$ species at high pH and represents 50% of the aqueous speciation at pH ~10.8, and the rest consists of the $Pu(OH)_4$ species. In the absence of added bicarbonate, and in the system that is open to the air, the $Pu(OH)_4$ species dominates at pH 9.25 and higher. The addition of bicarbonate has the effect of shifting the pH at which the soluble Pu carbonate species dominates, from 9.25 to 10.8, thus resulting in soluble Pu species at high pH. The $Pu(OH)_4$ species is modeled as a soluble species, but this species is very prone to polymerization and eventual crystallization and is typically colloidal or even insoluble. The modeling does not take into consideration kinetic phenomena, such as the rate of dissolution of $Pu(OH)_4$ by the carbonate ligand, nor does it consider adsorption of Pu to

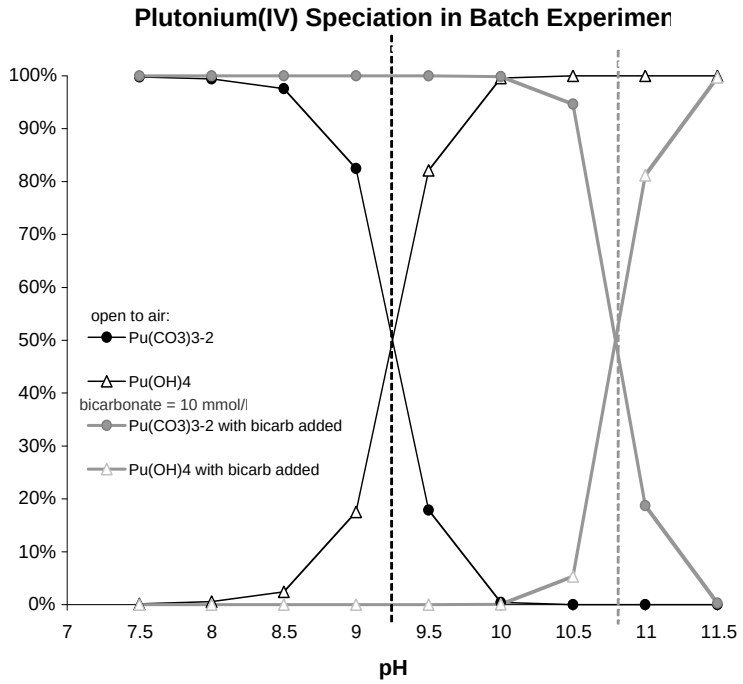

Figure 49 Speciation of Pu (IV) in the absence and presence of added bicarbonate.

solid phases and changes in equilibria between aqueous and adsorbed species in response to the addition of complexing ligands.

Determine the behavior of Pu in simulated grout pore water in contact with the components of the grout: portland cement, blast furnace slag, fly ash, zeolite, and fluorapatite.

Interactions of Pu with individual components of the grout, as they are influenced by pH changes resulting from addition of $KHCO_3$, are shown in Figure 50. Figure 51 shows the same data as a function of $KHCO_3$ addition. For each of the blast furnace slag, fly ash, and cement, only the first sampling provided counts above the detection limit. These samples had high pH values (around 12). In contrast, the simulated porewater experiment had no detectable counts at this pH. That some small quantity of Pu can be observed in the solution may be more related to colloid formation, perhaps as alumino-

silicates, than to truly soluble species. As $KHCO_3$ was added the Pu concentration dropped to below detection limits. The opposite was the case for apatite and zeolite. For these materials, as $KHCO_3$ was added, Pu returned to solution with a maximum concentration of 2.2 pCi/mL. The initial concentration was 103 pCi/mL; so about 2 % returned to solution. Pu in contact with both zeolite and apatite is only slightly lower than in the $KHCO_3$ simulated pore water experiment, indicating that these materials provide little benefit relative to Pu leaching.

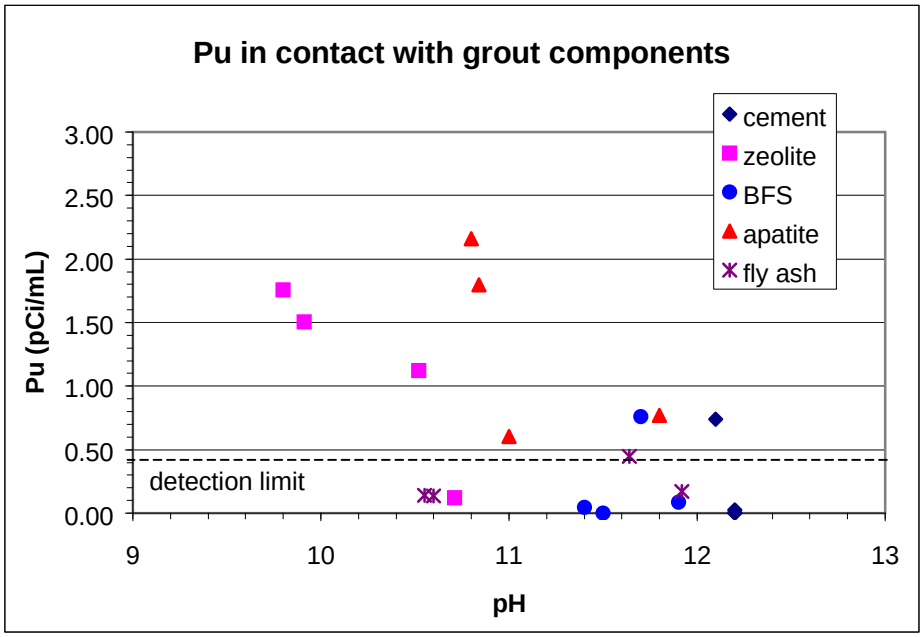

Figure 50. Pu in solution in contact with individual grout components as they are influenced by $KHCO_3$ additions.

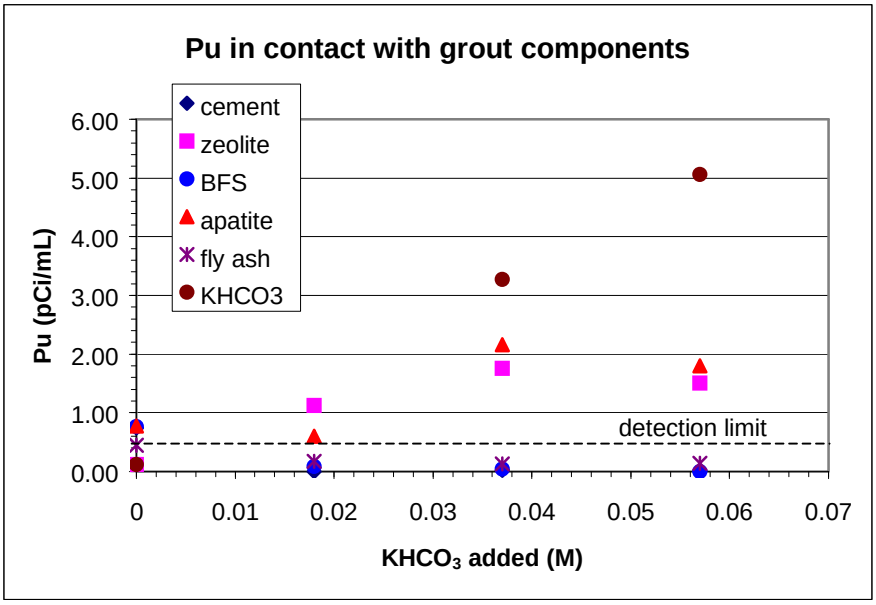

Figure 51. Pu concentrations in solutions in contact with the various grout components as $KHCO_3$ was added. Note the $KHCO_3$ simulated pore water data are substantially higher than the component experiments.

Determine the release mechanisms of Pu from grout over long-times and estimate their leaching relative to pore volumes flowing through the grout.

Plutonium concentrations in grout leachate are the result of both pH and carbonate competing in reactions with Pu. The dramatic increase in concentration seen in the grout/HCO_3 experiments shown in Fig 47 is not expected to take place in the field because the quantity of HCO_3 added to these experiments exceeds anything expected in the real system. This was done to follow the Pu chemistry in order to determine Pu oxidation state based on geochemical modeling. This is discussed elsewhere, but is based on differences in solubility and formation constants of the carbonates of Pu(V) and Pu(VI).

As discussed in the uranium report the results of column experiments show that pH of the grouts is lowered from around 12 to 8 over the course of approximately 1000 pore

volumes. This takes place with simulated West Valley groundwater flowing through the columns as shown in Figure 52.

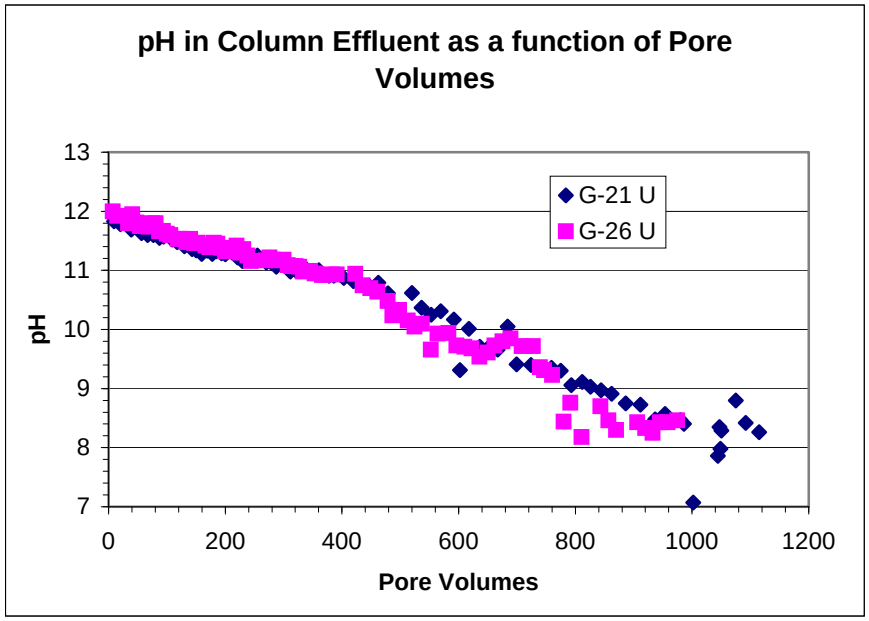

Figure 52. pH evolution of grout effluent from column experiments.

Calcite precipitates in this system and as a result keeps Ca and carbonate at relatively low concentrations in the effluent. The first three samplings of the aged grout (in contact with the Pu tracer for 502 days) experiments should be reasonably representative of this condition. The average concentration of Pu in these samples for grout 21 was 0.83 pCi/mL and for grout 26 it was 1.13 pCi/mL. The overall average is 0.98 pCi/mL (standard deviation = 0.46, n = 12). The $KHCO_3$ concentration (as added) ranged from 0 to 0.082 M and the pH ranged from 11.9 to 10.1.

From Figure 52, about 600 pore volumes are required to bring the pH down to 10. During this period, based on the average Pu concentration observed in the grout batch experiments, we estimate a concentration of 1 pCi/mL in effluent from the grout. The small addition of $KHCO_3$ to the system increased Pu to this level from below detection limits. In the column effluent, Ca became constant at about 80 mg/L. Calcite was precipitating, implying that carbonate was the limiting factor. If calcite precipitation

maintains carbonate at sufficiently low concentrations, there may be very little available to complex Pu and the concentration of Pu in solution would then be maintained at very low concentrations. Under these conditions we expect Pu concentrations to be controlled by $Pu(OH)_4$ solubility. However, a slight increase in carbonate/bicarbonate concentration could mobilize Pu giving a concentration of about 1 pCi/mL.

References for Pu

Andre, C., Choppin, G. R. (2000). Reduction of Pu(V) by humic acid. Radiochim. Acta 88, 613.

Clark, D.L., D.E. Hobart, and M.P. Neu. 1995. Actinide carbonate complexes and their importance in actinide environmental chemistry. Chem. Rev. 95: 25-48.

Choppin, G.R. (1991). Redox speciation of plutonium in natural waters. *J. Radioanal. Nucl. Chem., 147: 109-116.*

Currie, L.A. (1968). Limits for qualitative detection and quantitative determination: applications to radiochemistry. Anal. Chem. 43(3): 586-593.

Curti, E., 1999, Coprecipitation of radionuclides with calcite: estimation of partition coefficients based on a review of laboratory investigations and geochemical data, Applied Geochemistry, Vol. 14, pp. 433-445.

Duff, M. (2001). Speciation and Transformations of Sorbed Pu on Geologic Materials: Wet Chemical and Spectroscopic Observations. In Plutonium in the Environment, Kudo, A. (Ed.), Elsevier: New York. pp. 139-157.

Haschke, J.M., T.H. Allen, and L.A. Morales (2000). Reaction of plutonium dioxide with water: formation and properties of PuO2+x. *Science* 187: 285-287.

Haschke, J.M., and V.M. Oversby (2002). Plutonium chemistry: a synthesis of experimental data and a quantitative model for plutonium oxide solubility. *J. Nucl. Mat.* 305: 187-201.

Kim, J.I., Ch. Lierse, and F. Baumgartner, 1983, Complexation of the Plutonium (IV) Ion in Carbonate-Bicarbonate Solutions, pp.317 – 334, In: Plutonium Chemistry ACS Symposium Series 216, W.T. Carnall and G. R. Choppin, (ed), American Chemical Society.

Langmuir, D. (1997). Aqueous Environmental Geochemistry. Prentice Hall: Upper Saddle River, NJ. 600 pp.

Lemire, R.J. (ed). (2001). Chemical Thermodynamics of Neptunium and Plutonium. New York: Elsevier. 870 pp.

Liatoar, I.M. and S.A. Ibrahim (1996). Plutonium association with selected solid phases in soils of Rocky Flats, Colorado, using sequential extraction technique. *J. Environ. Qual*. 25: 1144-1152.

Lu, N., C.R. Cotter, H.D. Kitten, J. Bentley, and I.R. Triay (1999). Reversibility of sorption of plutonium-239 onto hematite and goethite colloids. *Radiochim. Acta*, 83:167-173.

Mincher, B.J., Fox, R.V., Craig Cooper, D., and Groenewold, G.S. 2003. Neptunium and plutonium sorption to Snake River Plain, Idaho soil. *Radiochim. Acta* 91: 397-401.

Parkhurst, D.L., and C.A.J. Appelo. (1999). User's Guide to PHREEQC (Version 2)-A Computer Program for Speciation, Batch-Reaction, One-Dimensional Transport, and Inverse Geochemical Calculations. Denver, Colorado: United States Department of the Interior Report 99-4259.

Penrose, W.R., W.L. Polzer, E.H. Essington, D.M. Nelson, and K.A. Orlandini (1990). Mobility of plutonium and americium through a shallow aquifer in a semiarid region. *Environ. Sci. Technol.* 24: 228-234.

Rai, D., R.J. Serne, and J.L. Swanson (1980). Solution species of plutonium in the environment. *J. Environ. Qual*. 9:417-420.

Rai, D. (1984). Solubility product of Pu(IV) hydrous oxide and equilibrium constants of Pu(IV)/Pu(V), Pu(IV)/Pu(VI), and Pu(V)/Pu(VI) couples. *Radiochim. Acta* 35: 97-106.

Reed, D.T., D.G. Wygmans, S.B. Aase, and J.E. Banaszak (1998). Reduction of Np(VI) and Pu(VI) by organic chelating agents. *Radiochim. Acta* 82: 109-114.

Runde, W. (2000). The Chemical Interactions of Actinides in the Environment. In Challenges in Plutonium Science Volume II. LA-UR-00-4100. Los Alamos, NM: Los Alamos National Laboratory. pp. 392-411.

Runde, W., S.D. Conradson, D.W. Efurd, N. Lu, C.E. VanPelt, and C.D. Tait (2002). Solubility and sorption of redox-sensitive radionuclides (Np, Pu) in J-13 water from the Yucca Mountain site: comparison between experiment and theory. *Appl. Geochem*. 17: 837-853.

Santschi, P.H., Roberts, K., and Guo, L. (2002a). The organic nature of colloidal actinides transported in surface water environments. *Environ. Sci. Technol*., 36, 3711-3719.

Triay, I.R., A. Meijer, J.L. Conca, K.S. Kung, R.S Rundberg, E.A. Strietelmeier, and C.D. Tait (1997). Summary and synthesis report on radionuclide retardation for the Yucca Mountain site characterization project. Yucca Mountain Site Characterization Program LA-13262-MS, Las Vegas, NV.

Neptunium Results

Background

Neptunium, which we take to be present as Np(V), may be incorporated into a variety of solid phases. At high pH and with no carbonate present one would expect Np_2O_5 and NpO_2OH (Kaszuba and Runde, 1999). The solubility of NpO_2OH has been shown to decrease significantly on aging (Neck et al., 1992). In two types of groundwater from Yucca mountain (total carbonate was 2.8 and 11.4 mM respectively), experiments on Np solubility showed that the Np solids controlling solubility were $Na_{0.6}NpO_2(CO_3)_{0.8} \cdot 2.5$ H2O and $NaNpO_2CO_3 \cdot 2H_2O$ (Nitsche et al., 1992). At pH 8.5, these solids resulted in solution concentrations of 4.4×10^{-5} and 7×10^{-6} mol/L in the low and high carbonate groundwaters respectively. When carbonate is an important component, $MNpO_2CO_3 \cdot H_2O$ or $M_3NpO_2(CO_3)_2$ are expected to be the dominant solid phases, where M is K or Na (Kaszuba and Runde, 1999). However, under high pH conditions (10 or above) Na or K concentrations would need to be in excess of 0.5 M to stabilize the presence of these solids. In the grout system, column effluents contain several hundred mg/L of K in the first day but rapidly the K content drops to only a few mg/L. Sodium is more consistent and remains around 80 mg/L. If Np is first exposed to the grout as it is setting, then the K-bearing varieties of Np carbonate may form, otherwise the high Na concentration makes it likely that the Na form would be present.

Precipitation of Np carbonate solids is well known. As mentioned earlier one form is $MNpO_2(CO_3)$ where M can be one of the alkali metals. However there are differences in the crystal system that the Np carbonate assumes, depending on the ion size of the metal, with some forming hexagonal carbonates and others forming orthorhombic carbonates (Volkov et al., 1979). The solubilities of these solids are 10^{-4} to 10^{-7} mol/L. The speciation and molecular structure of Np in solutions in contact with these solids was determined by EXAFS (Clark et al., 1996).

Still other solid phases may form from reactions between Np and grout components, not only the cementitious materials, but also the additives used in the grout. Another process

that may exert some control on Np concentrations is adsorption onto solids within the grout, which is likely to be dominant at very low Np concentrations. These may be additives such as the fluorapatite or zeolite that comprise 12 and 10 % respectively of the grouts, or they may be minerals, typically Ca-Al-Si materials, that form in the grout system as the cement sets. In addition, over time $CaCO_3$ minerals, such as calcite and aragonite, will form as a rind on the grout and as a fracture filling mineral. Neptunium may be incorporated into these secondary minerals, to a greater or lesser extent, as they precipitate. In studies of sorption of Np onto materials from Yucca Mountain, significant sorption was observed on secondary minerals formed in fractures, such as calcite, Fe oxide and Mn oxide (Triay et al, 1996). Brady et al (1999) found that Np did not sorb on dolomite at pH values below about 6. As the pH increased so did sorption of Np so that by pH 10 the K_d was about 180 mL/g.

Solubility of Np(V) hydroxide is sensitive to both pH and ionic strength (Itagaki et al., 1992). In the presence of Np(V) hydroxide, a minimum in Np solution concentration is found at pH 11 to 11.5. At ionic strength (I) of 0.8 M the minimum Np concentration is 1.3×10^{-7} M while at 0.05 M it is 3×10^{-6} M. At pH 8.5 the I= 0.05 M solution contains 1×10^{-4} M Np. Itagaki et al (1992) give the concentration of total Np in solution as:

$$[Np(V)]_{tot} = (K_{sp} / [OH^-]) (1 + \beta_1[OH^-] + \beta_2[OH^-]^2)$$

where for I = 0.5 M, $\log K_{sp} = -8.9$, $\log \beta_1 = 3.31$ and $\log \beta_2 = 5.74$. Kaszuba and Runde (1999) predict a minimum of Np in solution at pH 12.5. The solution chemistry in neutral to alkaline pH values is dominated by $NpO_2CO_3^-$. Above pH 10 other multi-carbonate Np species become important, as well as several mixed hydroxo-cabonato species which begin to appear around pH 11or 12.

Details for Np Experiments

Uptake of neptunium was studied using ^{237}Np, as Np $(NO_3)_4$, with a specific activity of 705 μCi/g. Samples were counted on HPGe planar gamma detectors using Canberra electronics and software. The photopeak at 86.5 keV (12.6 % abundance) was used to distinguish ^{237}Np from its daughters. Energy was calibrated with a multitracer standard, and an aliquot of the ^{237}Np tracer. This peak was close to a background peak and for low

count rate samples the peak fitting program was unable to discern the two. However, a simple manual approach to sum the peak and subtract background counts was effective. In addition, there is a low intensity peak for $^{212/214}$Pb at 86.8 keV that was quantified in a 2000 minute background count. This was subtracted from the Np counts. Concentrations were determined using specific activities reported in the tracer documentation from Isotope Product Laboratories, in conjunction with dilution factors and reference samples. The detection limit for a 1000 minute count is 0.05 cpm for a typical sample geometry, or 0.01 cpm/mL. Based on reference solution counts, and the specific activity of the tracer (1μCi, is 0.00142 g of Np) we calculate that 0.1 cpm/mL is 5.88×10^{-9} g/mL or 2.5×10^{-8} M.

Neptunium Isotherm Results

The grout experiments were run for 8 days. Figure 53 shows that concentrations in the isotherm experiments were extremely low, if not below detection limits, and were not systematic with respect to starting concentration. This implies that sorption is not the mechanism by which Np is removed from solution. Values of K_d for Np are presented in Table 13, with the caveat that they are essentially artifacts of calculations that are controlled by the starting concentrations in the experiment. The measured count rates in the samples at the end of the experiment tend to be quite similar and are likely the result of solubility controls. Count rates of Np remaining in solution were about 0.1 cpm/mL or less. This is 2.5×10^{-8} M. The solubility of $Np(OH)_4$, among the least soluble Np(IV) compounds, is reported to be 3.2×10^{-9} mol/L by Kaszuba and Runde (1999). Assuming Np is present as Np(V), The slightly higher concentrations in our solutions seem reasonable. It is likely that Np precipitates as Np_2O_5 and that its concentration is controlled by that solubility. Ewart et al, 1992, report the solubility of Np in a cement/ blast furnace slag system at 8×10^{-9} M, with no trend between pH values of 9.5 and 13. From these data it appears that there is no difference in retention capabilities of the two grouts.

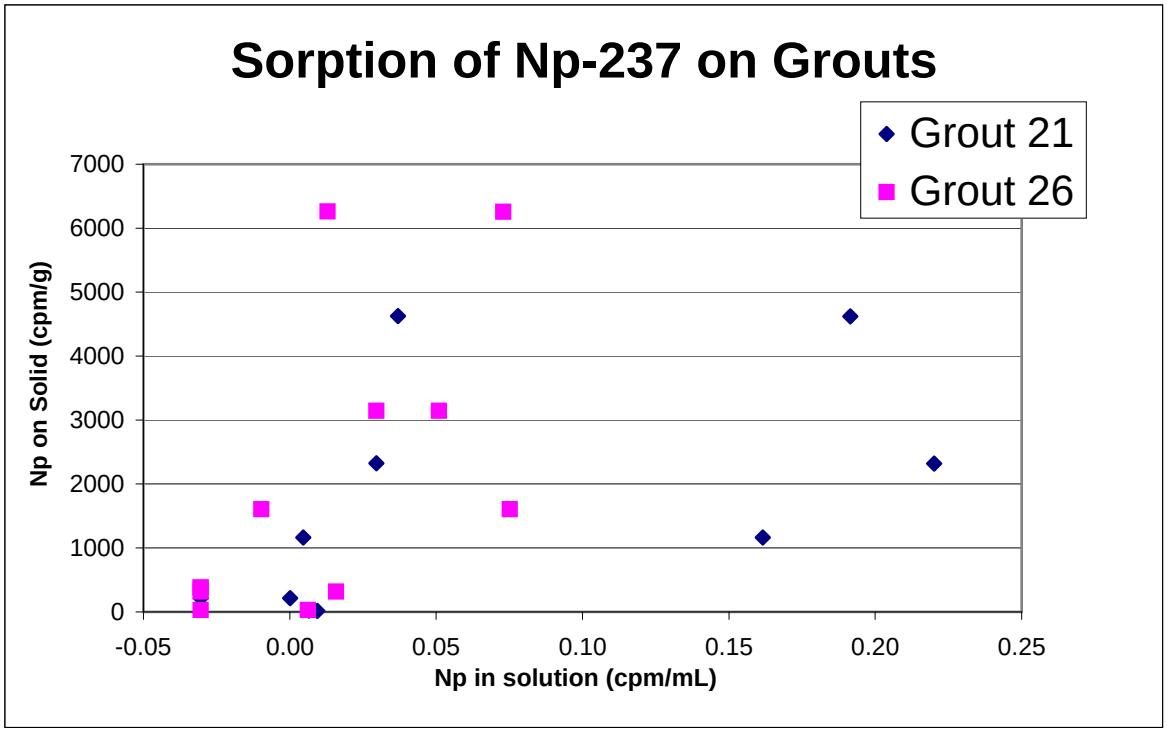

Figure 53. Concentrations of Np in the presence of the grout is controlled not by adsorption, but by solubility, as Np hydroxide forms and precipitates.

Table 13. Estimated K_d Values for Np

	Grout 21			Grout 26		
Nominal Activity	**Start cpm/mL**	**End cpm/mL**	**K_d (mL/g)**	**Start cpm/mL**	**End cpm/mL**	**K_d (mL/g)**
200	185	0.12	75,000	250.4	0.07	100,000
100	92.8	0.13	44,000	125.8	0.07	45,000
50	46.6	0.08	61,000	64.2	0.07	46,000
10	8.68	<0.01	>22,000	2.54	<0.01	> 8,000
1	0.68	<0.01	>1,700	1.26	<0.01	> 3,200

The Np isotherm experiments for the various grout constituents were sampled twice. The first sampling was a preliminary check of activity. The samples were all found to be quite low, and it was taken that the pH of the solution exerted greater control on the Np

distribution than the different solid phases. However, there may be differences in the phase controlling solubility of Np, resulting in subtle differences in concentration in solution. As a result, the higher activity experiments were resampled, filtered and counted for longer times (800 to 1,000 minutes). Subsequently, the pH was measured in the experiment cups. Results are shown in Table 14 and in Figure 54. Sorption of Np in the fly ash samples was poor, with three of the four samples having count rates in excess of 2 cpm/mL. Both cement and blast furnace slag consistently provided count rates that were below detection limits. These materials contribute substantial alkalinity to solution and maintain pH at about 12, a level that keeps Np out of solution. The zeolite material provided slightly less uptake of ^{237}Np than the other samples and the pH was proportionately lower. In a few cases, there were anomalously high measurements of count rates in these solutions. For example, one of the apatite samples had a count rate of 6.28 cpm/mL while the others were all very low. This sample was found to be at pH = 7.9 while all of the others were around 11. From Figure 54, it is apparent that the count rate of ^{237}Np in solution is controlled by pH, no matter the grout component material with which it is in contact. The solution pH of these experiments all started at the same value, but over time the materials reacted with the contact solution causing a decrease in pH, allowing Np to return to solution. As a result, shown in Figure 54, the concentration of Np in solution is proportional to pH.

Table 14. pH and count rate (cpm/mL) of ^{237}Np remaining in solution in contact with grout components

Starting	Cement	Fly Ash	Slag	Zeolite	Apatite
cpm/mL	cpm/mL (pH)	cpm/mL (pH)	cpm/mL (pH)	cpm/mL (pH)	cpm/mL (pH)
97.6	0.004 (12.00)	0.004 (11.31)	0.006 (11.60)	0.065 (9.63)	0.003 (11.69)
103.8	0.007 (12.00)	5.12 (8.03)	0.006 (11.59)	0.125 (9.60)	0.006 (10.97)
209.6	-0.003 (11.90)	2.73 (8.24)	0.011 (11.35)	0.063 (9.72)	-0.007 (11.00)
206.8	-0.001 (11.98)	16.2 (7.82)	-0.001 (11.30)	0.056 (9.65)	6.28 (7.80)

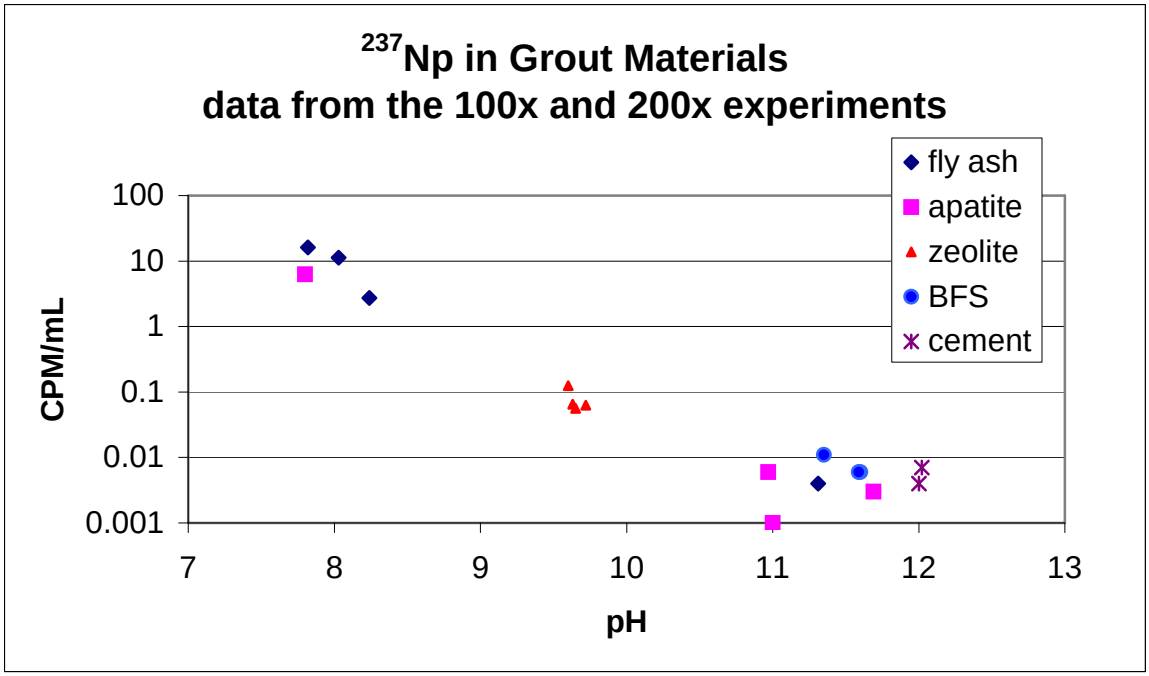

Figure 54. The concentration of ^{237}Np in solution is controlled by pH regardless of the material with which it is in contact.

Neptunium Batch Experiment Results

Determine if Np, which has been sequestered in contact with the two grouts, returns to solution as the grouts age.

Results of resampling aged (550 days) grout experiments are shown in Figure 55. Solutions from the three highest Np concentration sample sets from the isotherm experiments were taken. The original count rates of the starting solutions (prior to contact with any solid) for these samples were 9.4, 18.6, and 37 cpm/mL. After aging, the count rates were very similar to those observed in our earlier short term (8 days) experiments with these same samples. In both cases the count rates were below 0.1 cpm/mL for almost all of the samples. Based on reference solution counts, and the specific activity of the tracer (1μCi is 0.00142 g of Np) we calculate that 0.1 cpm/mL is 5.88×10^{-9} g/mL or 2.5×10^{-8} M.

As the grout experiments aged they attained a range of pH values, from 11.1 to 8.2, possibly due to some incursion of CO_2 and resultant carbonation of the samples, providing an effect similar to weathering in the environment. Table 15 shows

Table 15. Comparison of Np count rates in fresh and aged samples

	8 day sampling cpm/mL	550 day sampling cpm/mL
Grout 21 (n = 7)	0.107	0.063
Grout 26 (n = 7)	0.074	0.099

average count rates for ^{237}Np in solution in contact with the grouts after 8 days and 550 days. The aged sample are consistently lower than the 8 day samples, but the standard deviations are about 50% for these data and there are no significant differences among them. Noteworthy here is the fact that each of these groups is a composite of samples that started with three different concentrations of Np, as mentioned above. Independent of the starting concentrations, all of these count rates are similar. While Figure 55 shows there was a slight increase in count rate as pH decreased, most samples remained below 0.12 cpm/mL or 3×10^{-8} mol/L Np, less than 0.3 % of the starting activity. One sample of grout 26 had a much higher count rate than all of the other samples (0.45 cpm/mL) even though the pH was similar (it was included in the average). In general, grout 21 had slightly higher count rates than grout 26, at any particular pH. In summary, while the pH of some samples was altered by aging, overall there was very little if any change in count rates of Np.

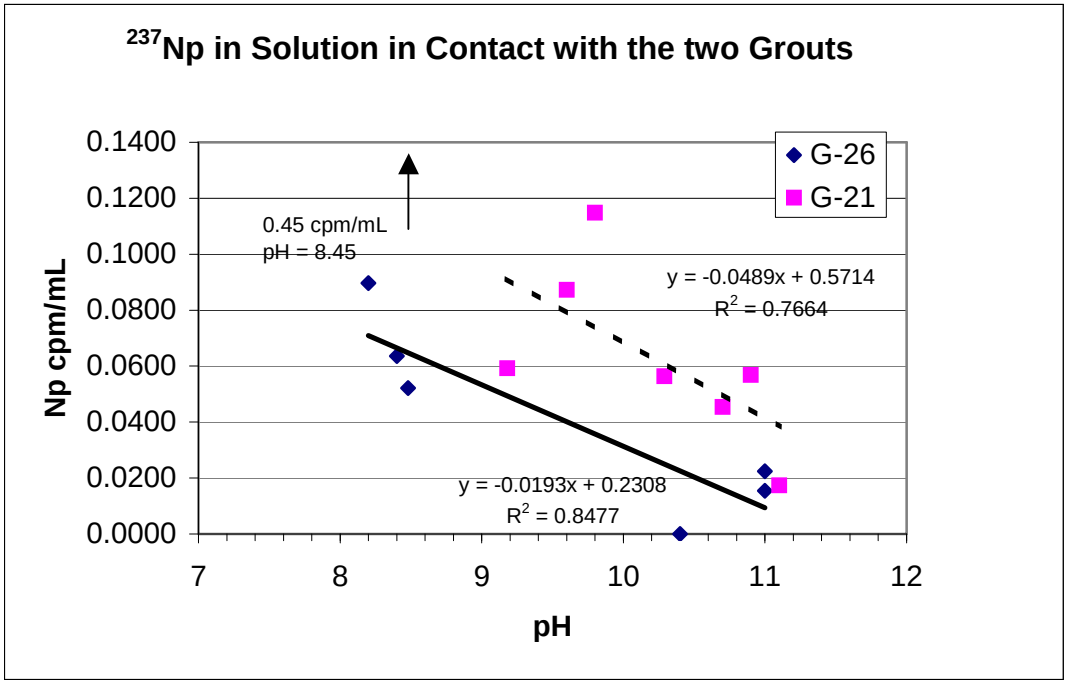

Figure 55. Resampling of aged Np-grout samples showed that decreased pH as a result of carbonation had a small effect on ^{237}Np concentrations in solution.

Determine if Np sequestered with the aged grouts returns to solution on contact with increasing concentrations of $KHCO_3$.

The effect of $KHCO_3$ addition to the solution in contact with each grout was determined beyond a HCO_3^- concentration equivalent to that of the West Valley groundwater. This is based on the assumption that in an open system, CO_2 ingress will persist. The proportion of carbonate/bicarbonate species will change as pH changes but the total quantity will be similar. Figure 56 shows how Np content and pH were changed by

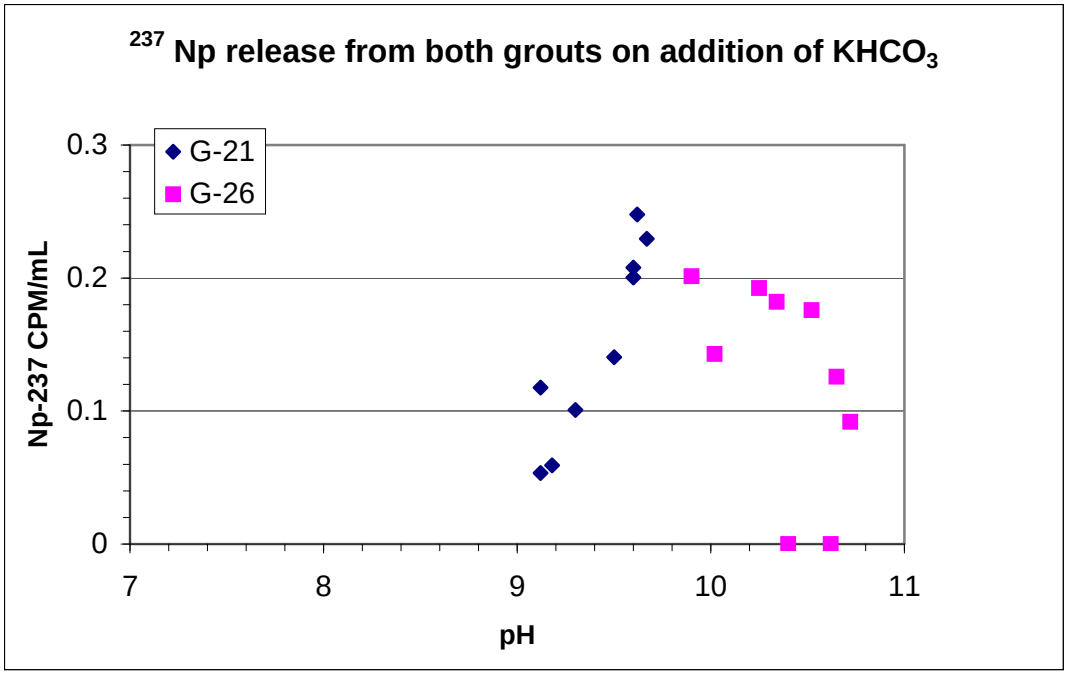

Figure 56. ^{237}Np concentrations in solution as a function of pH as $KHCO_3$ was added. These are aged grout experiments that subsequently received additions of $KHCO_3$.

addition of $KHCO_3$ for each of the grouts. These experiments had aged 558 days before the start of additions. At this point the pH of solutions in contact with grouts 21 and 26 were 9.18 and 10.4 respectively. The original count rate at the start of the experiment was 65 CPM/mL. Changes in pH are not large and are different for each material. The pH of the solution in contact with Grout 21 slowly increased from 9.2 to 9.6 along with a linear increase in ^{237}Np from 0.05 to 0.25 CPM/mL. Grout 26 started at a higher pH, 10.4, and decreased to 9.9 while the ^{237}Np count rate increased to 0.2 cpm/mL from below detection limits. In this case the count rate appears to have leveled off. From this experiment it appears that the two grouts react differently with Np and $KHCO_3$. This may be influenced by differences in the grout formulations, with grout 26 containing fluorapatite and grout 21 containing zeolite. Alternatively, the difference in behavior may simply be the result of differences in the starting pH of the two grouts, with the pH of the $KHCO_3$ solution falling between the two. In either case, with both grouts the addition of $KHCO_3$ resulted in no more than 0.25 cpm/mL in solution. This is consistent with the previously described experiment in which aged grouts, over a range of pH

values, had count rates of generally less than 0.12 cpm/mL. The difference between 0.12 and 0.25, while small, is significant and may represent formation of Np carbonate complexes in the $KHCO_3$ experiments. On aging these complexes may be incorporated into new solid phases that continue to form over time.

Data from the same experiment are shown in Figure 57 plotted as a function of $KHCO_3$ added (calculated as concentration in the experiment assuming no reactions). The two grouts behave similarly. There is an initial increase in ^{237}Np concentration that appears to level off after 0.06 M $KHCO_3$. Addition of $KHCO_3$ does result in a slight elution of ^{237}Np from the grouts but these concentrations are maintained at count rates below 0.25 CPM/mL or 6.2×10^{-7} M (less than 0.04 % of the starting count rate).

Determine the behavior of Np that has precipitated in a simulated grout pore water (without grout present), as the pH is lowered or $KHCO_3$ content is increased.

Figures 58 and 59 show the aqueous concentrations of Np in both the pH and HCO_3 simulated pore water control experiments, on linear and log scales respectively. In both experiments, ^{237}Np in the alkaline contact solution was undetectable under the initial condition of pH = 12.3. In these two parallel experiments, aliquots of 1M $KHCO_3$ were added to one bottle of simulated pore water and 1M HNO_3 and NaOH were added to another to adjust pH. As either pH decreased or $KHCO_3$ content increased, the ^{237}Np concentration increased, with the pH effect being dominant. Even around pH = 12, Np concentrations increased as $KHCO_3$ was added. In contrast, at pH = 12, Np remained at detection limits in the pH experiment. This difference, which was about a factor of 10 at pH 11.95, disappeared around pH 10. Theoretical thermodynamic geochemical modeling with Geochemists Workbench indicates that at high pH, even with addition of substantial quantities of HCO_3 the dominant aqueous species is NpO_2OH. Our results show an increase of soluble Np in the HCO_3 experiment, suggesting that a carbonate complex, which is not accounted for in the model, is increasing Np solubility.

The pH experiment started at pH = 12.3, was brought to pH = 8 with HNO_3 and then was slowly increased by addition of NaOH. Around pH 8.5 the addition of NaOH did not

change the pH but the ^{237}Np content dropped by a factor of 10. From that point to pH = 12.3 the concentration of Np decreased linearly as shown in Figures 58 and 59. Modeling with Geochemists Workbench provides a possible explanation. At higher pH values the Np solution concentration is dominated by the presence of NpO_2OH (aq) in the presence of precipitated Np_2O_5. In the pH control experiment, at pH 8.2 and 1 mM of HCO_3 the Np solution was dominated by $NpO_2CO_3^-$ and no Np was precipitated. At pH 8.6, however, the model indicated that $KNpO_2CO_3$ precipitated and the aqueous speciation was predominantly $NpO_2CO_3^-$ and NpO_2OH. The pH at which this precipitation takes place conforms very well with experimental results. Another possibility, based on observations from similar uranium experiments, is that calcite precipitates and carries the Np with it.

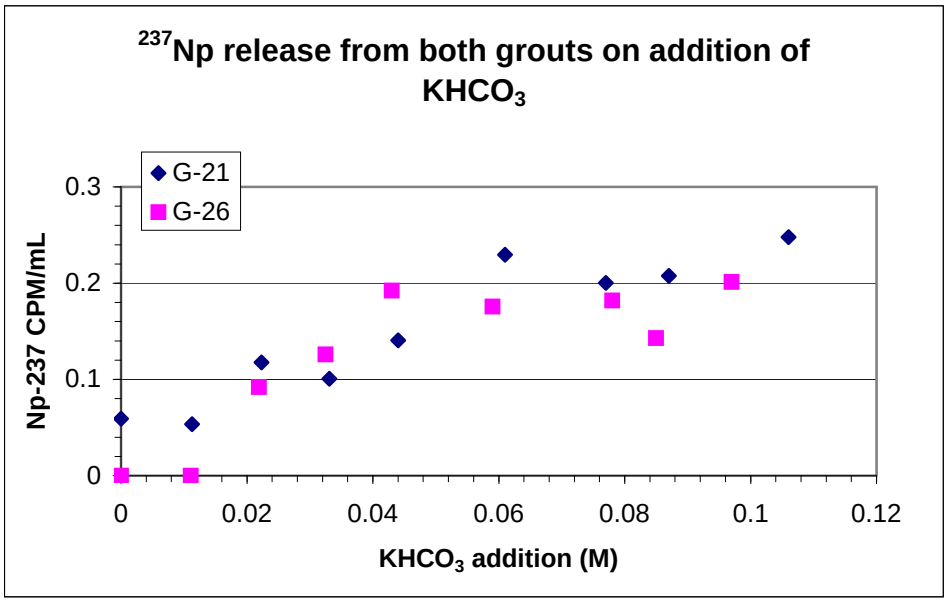

Figure 57. ^{237}Np count rate as a function of the quantity of $KHCO_3$ in solution as it was added.

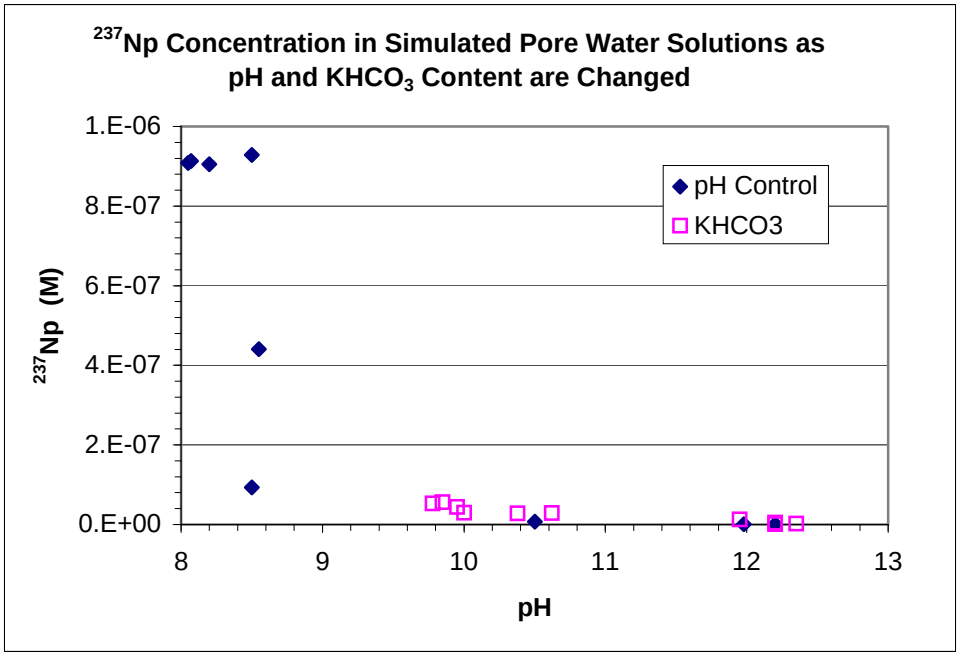

Figure 58. Concentration of Np in solution as a function of pH for both of the simulated pore water experiments; the pH and the HCO_3 experiments.

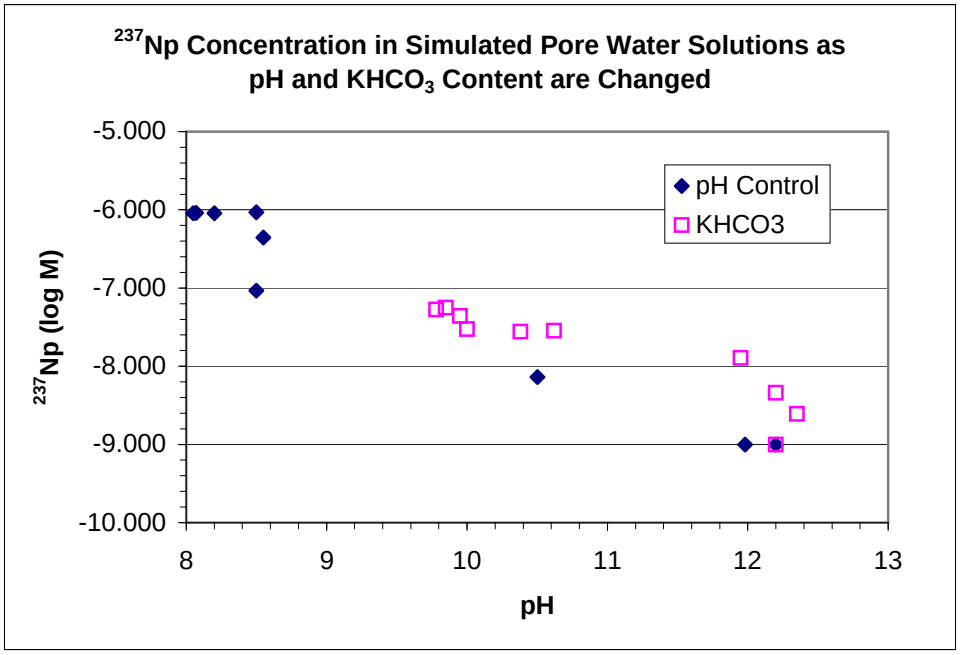

Figure 59. Simulated grout pore water experiments show Np concentrations in the alkaline contact solution in which the pH and $KHCO_3$ content were altered without the presence of grout. Note the log scale for Np concentrations, allowing better assessment of concentrations at low values.

Comparing the aged grout experiments with the results of the simulated grout pore water experiments, as shown in Figure 60, shows that Np concentrations are quite similar above pH 9.5. This implies that in the pH range above 9.5, Np concentrations are controlled by solubility of a Np phase. However, the Np concentrations in solution from the aged grout 26 samples around pH 8.5 are significantly lower than those from the pH control experiments at this pH (as indicated by open circles). This implies that the grout or an associated solid is retaining Np. This may also be true for the aged grout 21, but the pH of these samples did not evolve over time to below 9.2. In summary, from pH = 11 to approximately pH 8.2, releases from grouts are controlled by solubility at concentrations that are about 2.5 x 10^{-8} M, probably by Np_2O_5. Around pH 8.5, Np concentrations are substantially lower than expected based just on pH and may be the result of sorption or may reflect the precipitation of $KNpO_2CO_3$. Releases are only slightly influenced by $KHCO_3$, as shown in Figure 57.

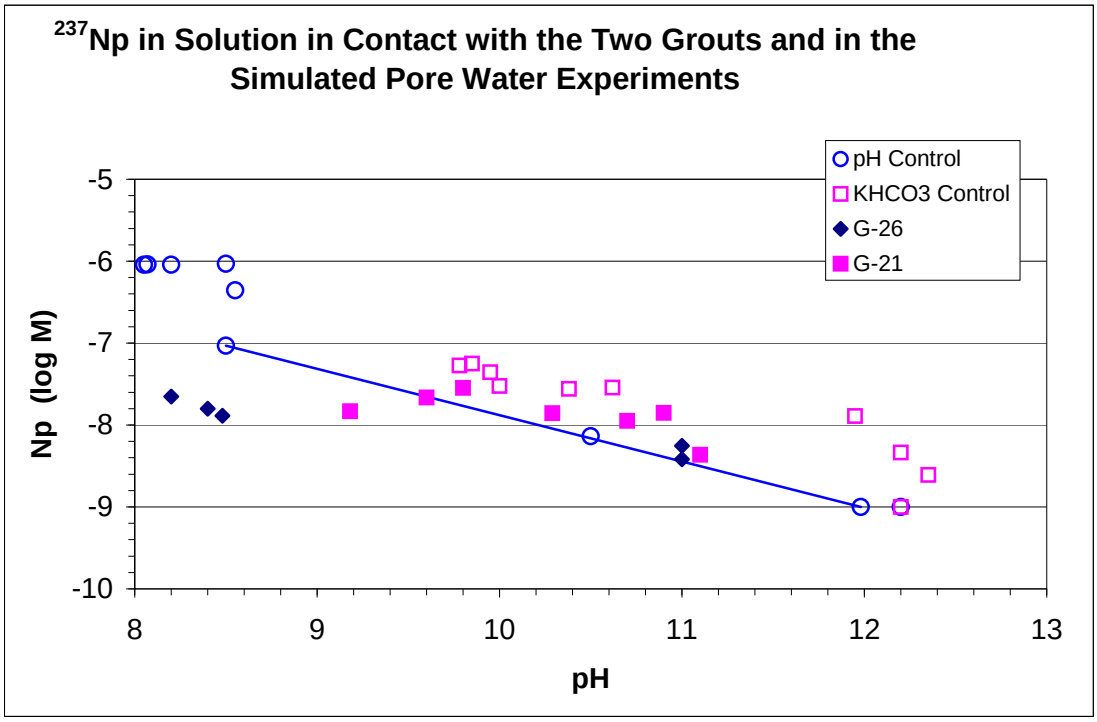

Figure 60. Comparison of aged grout experiments with the simulated pore water control experiments for pH and $KHCO_3$ additions. The line shows the data from the pH control experiment. Note that Np is given in molar concentrations.

Determine the behavior of Np in simulated grout pore water in contact with the components of the grout: portland cement, blast furnace slag, fly ash, zeolite, and fluorapatite.

Interactions of Np with individual components of the grout, as they are affected by pH, are shown in Figure 61. The fly ash, zeolite, and the one sample of the blast furnace slag that is above the detection limit, are all quite close to the regression line for Np solubility in this system as taken from the pH experiments. For most materials solubility is simply pH controlled. However, Np concentrations in water in contact with apatite are about an order of magnitude greater than expected based on pH. The reason may be formation of a soluble complex of Np with a component of the fluorapatite, either fluorine or phosphate. Moore et al, (2003) examined Np concentrations in contact with synthetic hydroxyapatite and found significant control by pH. They calculated a K_d for Np and found it to have a maximum at pH 8.5 of about 70,000, while at pH 11 it had decreased to about 800 mL/g. Fly ash consistently has high Np count rates indicating little uptake.

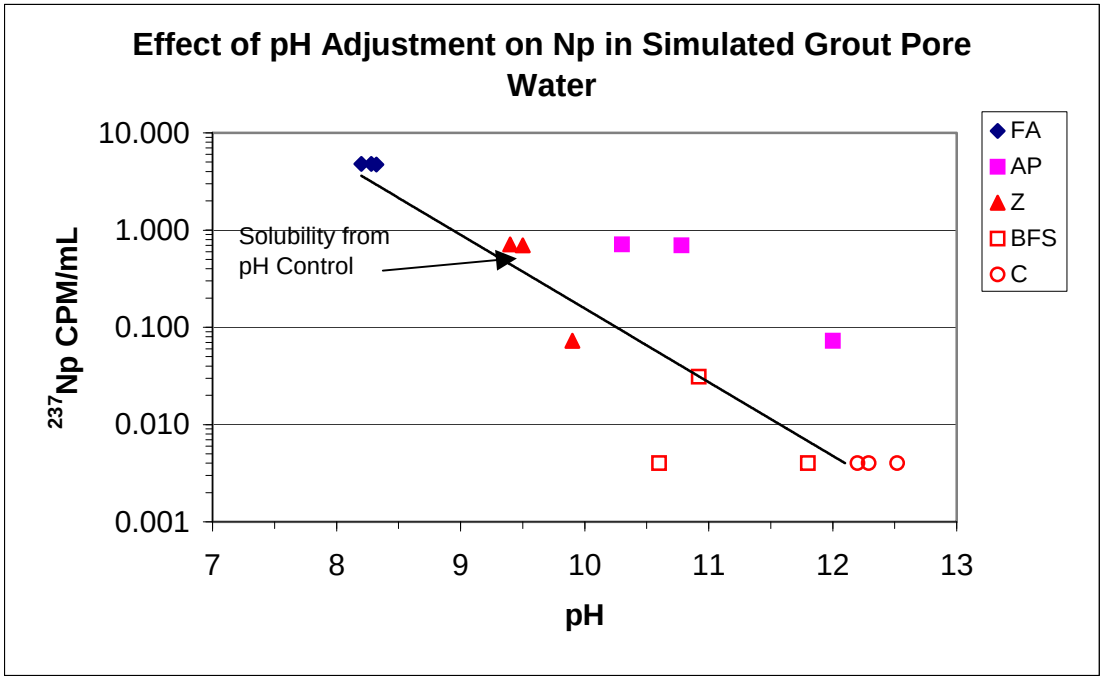

Figure 61. Effect of pH on Np concentration in contact with the component materials, as the pH was adjusted with NaOH and HNO_3. The regression line shown is from the pH control experiment. The detection limit is 0.01 cpm/mL.

Determine the release mechanisms of Np from grout over long-times and estimate leaching of Np relative to pore volumes flowing through the grout.

Data from all experiments are shown on Figure 62, showing Np cpm/mL as a function of pH. Below pH = 11, the concentration of Np in solution was below our detection limits. It then increased slightly, especially in samples that were treated with $KHCO_3$. The solubility of Np, as determined from the simulated pore water pH experiment is shown as the dark line. Except for the four fly ash samples and one apatite, all samples are below about 0.2 cpm/mL. In fact there is a slight downward trend as pH decreases, if one includes all grout samples. This trend is influenced by the Grout 26 samples that had been adjusted with $KHCO_3$, which push concentrations up between pH 10 and 11. Excluding this data set would give a constant concentration of Np in solution from pH 10.8 to 8.2, but may not be realistic if significant carbonation takes place over time.

An important finding of these data is that materials that had aged in the simulated pore water and those that were relatively fresh provided essentially the same data. In addition, the use of the experiments using a simulated grout pore water that were adjusted for pH and bicarbonate/carbonate conformed with the experiments containing solids. That the thermodynamic modeling provided reasonable simulation of the precipitation at pH 8.6 also imparts some level of confidence that these experiments are giving useful information in a thermodynamically sound way, as opposed to being subject to a variety of transient states.

To estimate long-term releases of Np, we made the following assumptions based on the data from these experiments. Above pH 11 Np concentrations are about 0.01 cpm/mL. This concentration is 2.5×10^{-9} M and is conservative. From pH 11 downward, Np concentrations can be described by a linear regression with pH shown in Figure 62 as the dashed line. Using the concentrations derived by the regression (pH below 11) and 0.01 cpm/mL (pH above 11), we have calculated Np concentrations that would evolve over long times based on the pH measured in the effluent of the uranium column experiment (grout 26), discussed elsewhere. The results of this calculation are shown in Figure 63.

The sudden increase in concentration around 330 pore volumes comes from the conservative interpretation of the data plotted in Figure 62 indicating an increase in Npconcentrations around pH = 11. Here we have included the "G-26 adjusted" data set (aged grout experiments with $KHCO_3$ additions), which increases estimated Np concentrations between pH 10 and 11 above the solubility line derived from the pH experiment. Using only data from the aged grout data sets would have provided a slightly lower and smoother distribution of concentrations. In any case, concentrations of Np would stay constant or, as shown in Figure 62, decrease slightly over time. Neptunium concentrations at pH values lower than about 9.5 are substantially lower than those in the pH control experiments. Either sorption or precipitation of a different Np bearing compound controls the aqueous Np concentration. It seems reasonable to suspect that the compound causing the steep decline in Np concentration at pH 8.6 in the control experiment, identified by modeling as $KNpO_2CO_3$, may be influencing the concentration. However, we have no physical evidence for the presence of this compound.

The concentration of Np in solution is not related to how much Np was originally in the experiments. The starting concentrations, being part of an isotherm experiment, varied by a factor of four with concentrations as high as 3.6×10^{-5} M, but all grout bearing experiments resulted in solution concentrations that were about 3×10^{-8} M or less. Estimates of long term releases should be based on the concentration maintained by the grout. From these experiments, the Np concentration is maintained about 3×10^{-8} M even as the grout weathers over time, losing Ca and decreasing in pH.

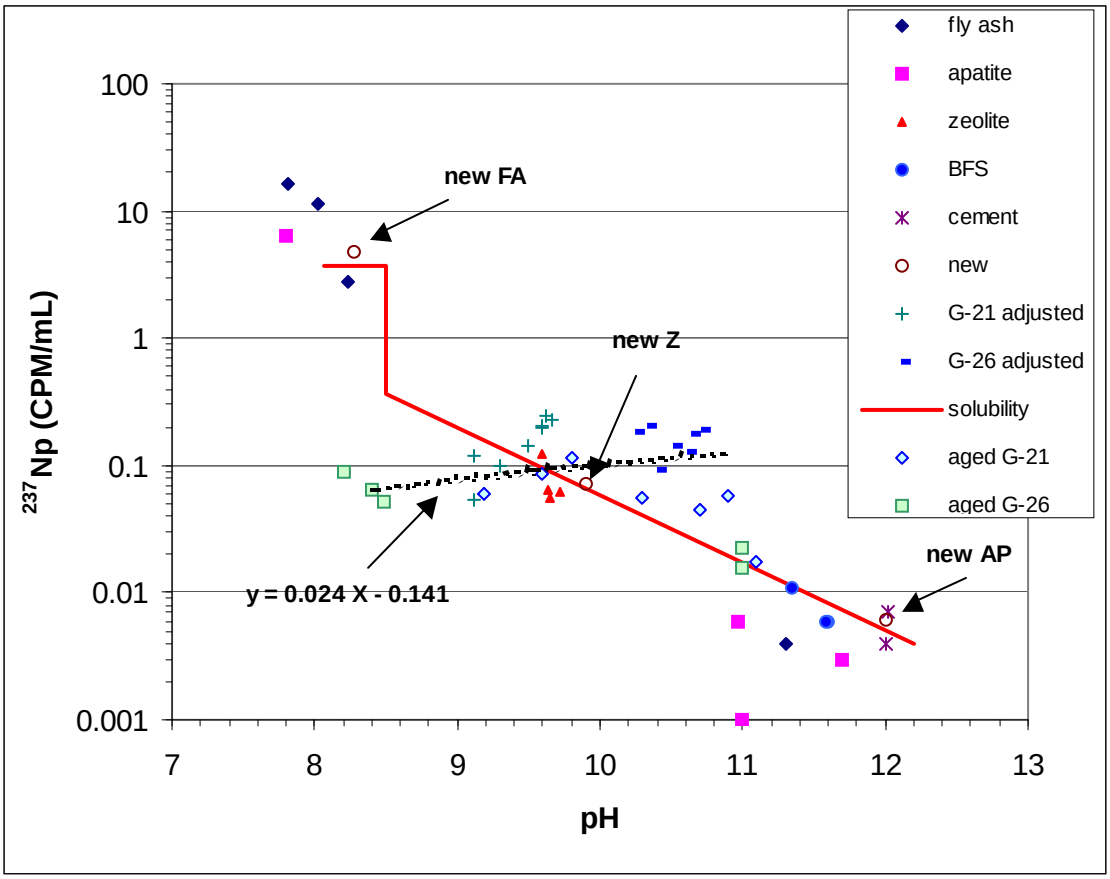

Figure 62. Concentrations of ^{237}Np in solution in contact with the various materials for all experiments . Three "new" experiments were run with zeolite (Z), Fly Ash (FA) and apatite (AP) were also run to check aging effects. The aged grouts that had received HCO_3 additions are also included and are indicated as G-21 and G-26 adjusted. The samples termed "aged G-21" and "aged G-26" are the 550 day samples without any additions of reagents. The dashed line indicates the relationship between pH and Np concentration used to estimate releases based on pH of the uranium column effluent.

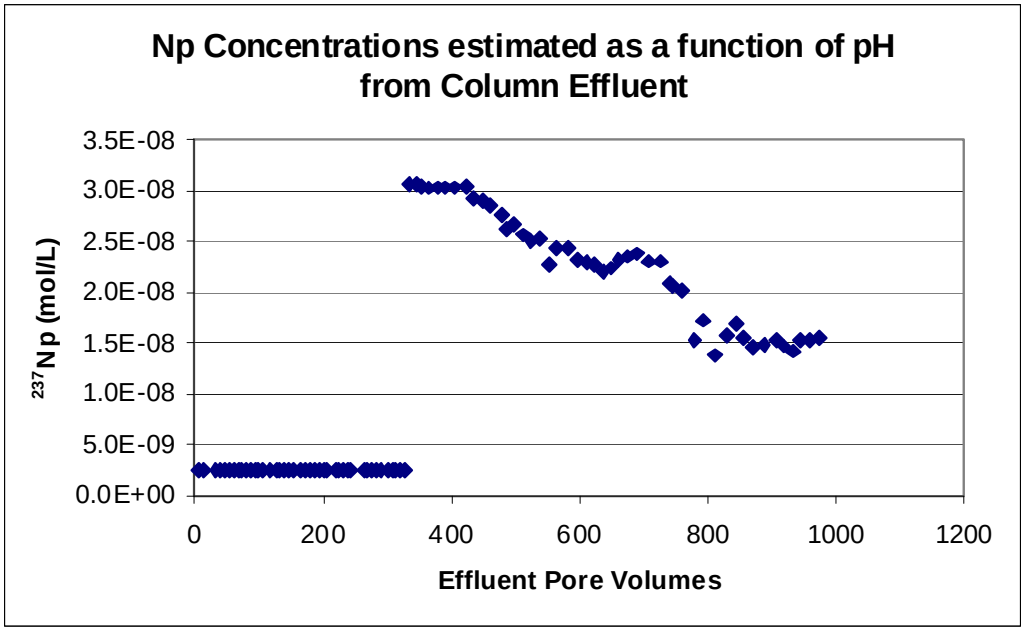

Figure 63. Calculated Np concentrations based on pH and pore volumes of effluent from the uranium column experiments.

References for Np

Traiy, I., A. Meijer, J. Conca, K. Kung, R. Rundberg, and E. Streitelmeier, 1996, Summary and Synthesis Report on Radionuclide Retardation for the Yucca Mountain Site Characterization Project, Los Alamos National Laboratory, YMP Milestone Report 3784.

Clark, D., S. Conradson, S Ekberg, N. Hess, M. Neu, P. Palmer, W. Runde, and C.D. Tait, 1996, EXAFS Studies of Pentavalent Neptunium Carbonato Complexes. Structural Elucidation of the Principal Constituents of Neptunium in Groundwater Environments, Journal of the American Chemical Society, Vol. 118, p. 2089-2090.

Clark, D. D. Hobart, and M. Neu, 1995, Actinide Carbonate Complexes and their Importance in Actinide Environmental Chemistry, Chemical Reviews, Vol. 95, p. 25-48.

Kaszuba, J. and W. Runde, 1999, The Aqueous Geochemistry of Neptunium: Dynamic Controls of Soluble Concentrations with Applications to Nuclear Waste Disposal, Environmental Science and Technology, vol. 33, p. 4427-4433.

Neck, V., J. Kim, and B. Kanellakopulos, 1992, Solubility and Hydrolysis Behaviour of Neptunium (V), Radiochimica Acta, vol. 56, p. 25-30.

Zhao, P., P. Allen, E. Sylwester and B. Viani, 2000, The partitioning of uranium and neptunium onto hydrothermally altered concrete, Radiochimica Acta, vol. 88, p. 729-736.

Itagaki, H, S. Nakayama, S. Tanaka, and M. Yamawaki, 1992, Effect of ionic strength on the solubility of neptunium (V) hydroxide, Radichimica Acta, vol. 58-59, p. 61-66.

Moore, R., K. Holt, H. Zhao, A. Hasan, N. Awwad, M. Glasser, and C. Sanchez, 2003, Sorption of Np (V) by Synthetic Hydroxyapatite, Radiochimica Acta, Vol. 91, p. 721-727.

Volkov, Y., S. Tomilin, G. Visyashcheva, and I. Kapshukov, 1979, Radiokhimiya, Vol. 21, p. 668.

Brady, P., H. Papenguth, and J. Kelly, 1999, Metal Sorption to Dolomite Surfaces, Applied Geochemistry, Vol. 14, p. 569-579.

Americium and Curium Results

Background

Because the chemical behavior of Am and Cm are very similar (Keller, 1971), we treat them together in this report. Am is present as Am(III) and Cm as Cm(III). Am and Cm may be incorporated into a variety of solid phases, but under the conditions considered here, the chemistry of these elements is dominated by hydrolysis and carbonate concentrations. At high pH and with no carbonate present one would expect $Am(OH)_3$ (Vitorge, 1992) and presumably a similar phase for Cm. The solubility of $Am(OH)_3$ is approximately 1.6×10^{-6} M in dilute NaOH (pH >10) and its solubility is similar in 2-5 M NaOH (Shilov, 1998). At pH 7, the solubility of $Am(OH)_3$ is reported as 3.2×10^{-4} M (Rai et al, 1983). As pH increases the concentration of Am decreases. Below pH 10 the concentration of Am is about 10^{-10} M (Rai et al., 1983) or $10^{-11.1}$M (Vitorge, 1992). While there may be some discrepancy about the solubility of $Am(OH)_3$, some of it stems from the difference in solubility of amorphous and crystalline Am hydroxide. The solubility product of crystalline $Am(OH)_3$ was determined to be log K_{sp} = -27.5 (Morss and Williams, 1994).

Americium (III) forms several carbonate compounds. $Am_2(CO_3)_3 \cdot x\ H_2O$ where x is 2 or 4 forms when $Am(OH)_3$ is contacted with sodium bicarbonate solution (Keller, 1971). $NaAm(CO_3)_2 \cdot 4H_2O$ and $Na_3Am(CO_3)_3$ also form when americium carbonate is treated with a sodium solution (Keller, 1971). At elevated pH values and moderate concentrations of carbonate one would expect $AmOHCO_3$ to be a stable solid (Vitorge, 1992). At lower pH or higher carbonate concentrations, $Am_2(CO_3)_3$ is stable (Vitorge, 1992). In the presence of carbonate two Am compounds have been observed, the carbonate $Am_2(CO_3)_3$ and the hydroxy-carbonate $AmOHCO_3$. They have solubility products (log K_{sp}) of –29.45 and –18.70 respectively under CO_2 partial pressures of both 1 % and 100 % (Runde et al., 1992). Kim et al, (1994) examined carbonate complexes $M(CO_3)^+$, $M(CO_3)_2^-$, and $M(CO_3)_3^{-3}$, where M = Cm (III) and Eu(III). Formation constants are similar to those for Am (III) indicating similar solubilities. Rorif et al., 2004) determined that enthalpies and therefore K_{sp} of the hexagonal and orthorhombic forms of lanthanide and Am hydroxycarbonates are different. The commonly

precipitated orthorhombic form of Am hydroxycarbonate has a log K_{sp} of –22.5 (±1.1), while the hexagonal form has a value of –25.5 (±1.1). The orthorhombic form is metastable and on aging appears to covert to the hexagonal form (Rorif, 2005). Ekberg et al., (2003) discuss the uncertainties in estimates of solubility products for these Am compounds. Both Am and Cm are expected to partition readily to calcite that forms as the grout weathers. Based on a value for the solubility product of Am carbonate of $K_{sp} = 10^{-33.1}$, Curti (1999) estimated that the partition coefficient for both Am and Cm into calcite is 200-1000, indicating strong uptake by calcite.

Still other solid phases may form from reactions between Am or Cm and grout components, not only the cementitious materials, but also the additives used in the grout. Another process that may exert some control on Am or Cm concentrations is adsorption onto solids within the grout. These may be additives such as the fluorapatite or zeolite that comprise 12 and 10 % respectively of the grouts, or they may be minerals, typically Ca-Al-Si materials, that form in the grout system as the cement sets. In addition, over time $CaCO_3$ minerals, such as calcite and aragonite, will form as a rind on the grout and as a fracture filling mineral. Based on an estimate by Curti (1999) Am and Cm will be incorporated into these secondary minerals, to a significant extent, as they precipitate.

Details for Am and Cm Experiments

Isotherm experiments were conducted separately using ^{241}Am and ^{244}Cm tracers. The Am experiments were run for 52 days, and the Cm experiments ran for 59 days. Concentrations of the tracers in the starting solution are given in Table 1. ^{244}Cm tracer was in the form of $Cm(NO_3)_4$ and contained (on alpha activity basis) 99.95% of ^{244}Cm. On a weight basis, the tracer contained 87.3% ^{244}Cm, 1.9% ^{245}Cm, and 10.5% ^{246}Cm. For the Cm isotherm experiments, samples were analyzed for gross alpha using 5 mL of sample dried on a planchette. For later experiments liquid scintillation counting was used, with 2 mL of sample to 17 mL of Ultima-Gold Cocktail. Detection limits for ^{244}Cm are estimated to be about 0.2 pCi/mL. For ^{241}Am, samples were counted on HPGe planar gamma detectors using Canberra electronics and software. The photopeak at 59.5 keV (36 % abundance) was used to analyze for ^{241}Am. Energy was calibrated with a

multitracer standard, and an aliquot of the ^{241}Am tracer. Count times were generally 1000 minutes, and an appropriate background spectrum was subtracted from each sample spectrum for quantification of count rate. For ^{241}Am, based on reference solution counts and the specific activity of the tracer (specific activity is 3.428 Ci/g of ^{241}Am), we calculate that 1 cpm/mL is 14 pCi/mL, 4.03 x 10^{-9} g/mL or 1.66 x 10^{-11} mol/L. The detection limit for a 1000 minute count is 0.05 cpm for a typical sample geometry, or 0.01 cpm/mL. For ^{241}Am this is 0.14 pCi/mL or 4.0 x 10^{-11} g/mL. Table 1 presents the activities and molarities of the Am and Cm tracers in the starting solutions of the "old" isotherm experiments and kinetics experiments used in this study.

Table 16. Activity and molarity of radionuclides in experiments

	Am-241		Cm-244	
	nCi/L	mol/L	nCi/L	mol/L
1	7.7	9.09 x 10^{-12}	13.7	7.86 x 10^{-12}
2	19.7	2.32 x 10^{-11}	137	7.86 x 10^{-11}
3	101	1.19 x 10^{-10}	683	3.91 x 10^{-10}
4	927	1.09 x 10^{-9}	1370	7.86 x 10^{-10}
5	1950	2.30 x 10^{-9}	2730	1.57 x 10^{-9}
Kinetics	467.0	5.52 x 10^{-10}	1380	7.92 x 10^{-10}

Am and Cm Isotherm Results

In no sample of the isotherm experiments were any counts from ^{241}Am observed. It had all been removed from solution to below the detection limit of approximately 0.14 pCi/mL. Since no Am was found in solution, the values of K_d calculated from these samples becomes a function of the starting concentration of the experiment. Results for both grouts combined are given in Table 17, where the highest value of K_d is the most appropriate for use in modeling. The presumed mechanism of Am removal from solution is formation of extremely low solubility hydroxides. Ewart et al, 1992, in a combined experimental and geochemical modeling study, give the solubility of Am in a cement/ blast furnace slag at pH 12 as about 5 x 10^{-11} mol/L and at pH 13 at about 10^{-11} mol/L.

From the speciation modeling, these concentrations are controlled by formation of $Am(OH)_3$ but at slightly lower pH values the Am concentration increased to 10^{-7} mol/L with the formation of carbonate and bicarbonate species.

Table 17. Estimated K_d Values of Am in both Grouts

Relative Activity	Start Activity cpm	End Activity cpm	K_d (mL/g)
200	696	< 0.1	>34,800
100	331	< 0.1	>16,550
50	36.2	< 0.1	>1810
10	7.04	< 0.1	>352
1	2.73	< 0.1	>137

For Cm, count rates of the samples were all below the detection limit of 0.08 pCi/mL. The MDL value was used to calculate the K_d values given in Table 18. This tracer contained significant counts of daughters, nevertheless essentially no activity was observed in the solutions indicating that the daughters too were carried out of solution as well as the Cm.

Table 18. Estimated K_d Values for Cm

	Grout 21			Grout 26		
Nominal Activity	Start pCi/mL	End pCi/mL	K_d (mL/g)	Start pCi/mL	End pCi/mL	K_d (mL/g)
200	2730	<0.08	>4,300	2730	<0.08	>4,300
100	1370	<0.08	>43,000	1370	<0.08	>43,000
50	680	<0.08	>210,000	680	<0.08	>210,000
10	137	<0.08	>430,000	137	<0.08	>430,000
1	13.7	<0.08	>850,000	13.7	<0.08	>850,000

Am and Cm Batch Experiments Results

Determine if Am and Cm, which have been sequestered in contact with the two grouts, returns to solution as the grouts age.

Results of resampling aged grouts are shown in Table 19 for ^{241}Am (aged 520 days) and ^{244}Cm (aged 596 days). Solutions from the two or three highest tracer concentration sample sets from the isotherm experiments were taken. Averaged results (most samples are in duplicate) and starting solution activities for Am and Cm are given in Table 19.

Table 19. ^{241}Am and ^{244}Cm (nCi/L) in Solution in Aged Grout Experiments

	Am-241			Cm-244		
	Start	**54 days**	**520 days**	**Start**	**59 days**	**596 days**
1	101	< 0.14	Not Sampled	683	< 0.08	< 0.2
2	927	< 0.14	< 0.14	1365	< 0.08	< 0.2
3	1950	< 0.14	< 0.14	2730	< 0.08	< 0.2

Am was counted by gamma spectroscopy and no photopeaks for ^{241}Am were observed in the background subtracted spectra; concentrations were less than 0.14 pCi/mL. For Cm, the 59 day counts were done with dried samples on planchettes for gross alpha counts while the later samples were analyzed by liquid scintillation. In either case results are at or below the detection limit. As shown in Figure 64, overall the count rates of the Cm samples were evenly distributed within ± 0.5 cpm/mL of 0 cpm/mL indicating they were at or below the detection limit. After aging, the count rates were very similar to those observed in our earlier short term experiments with these same samples. In both cases the count rates were very close to or below detection limits for all of the samples. No differences were observed between the two grout formulations for either tracer.

As the grout experiments aged they attained a range of pH values; for Am they varied from 7.9 to 10.28 and for Cm from 7.85 to 10.81. These differences are primarily due to some incursion of CO_2 and resultant carbonation of the samples, providing an effect similar to weathering in the environment. Each of these groups is a composite of samples

that started with different concentrations of tracer, as mentioned above. Independent of the starting concentrations, all of these count rates are similar, essentially below detection limits. In summary, while the pH of some samples was altered by aging, overall there was no release Am or Cm to solution.

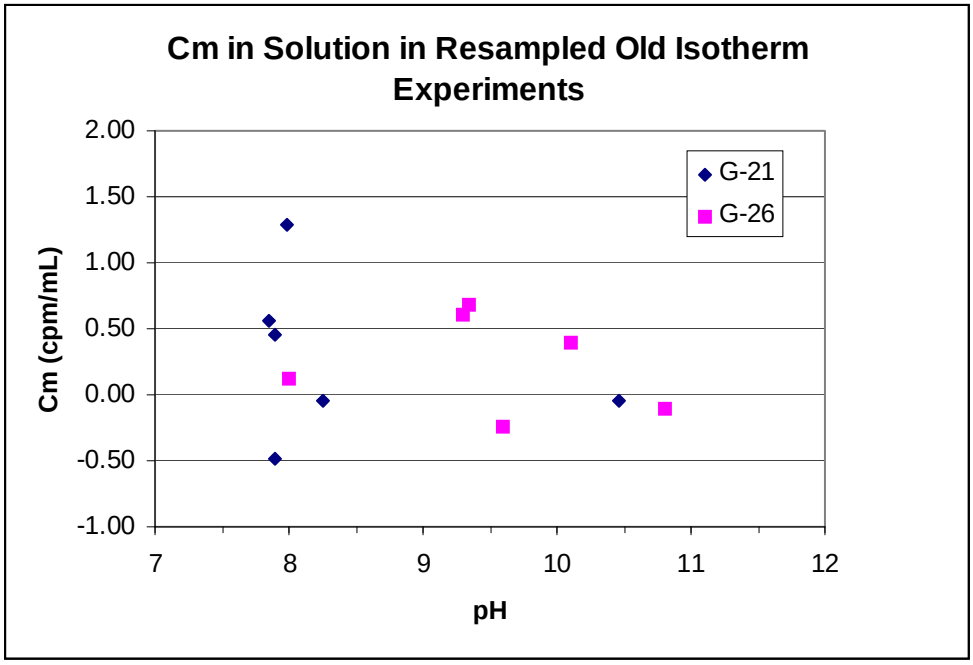

Figure 64. Resampling of aged Cm-grout samples showed that decreased pH as a result of carbonation had no effect on ^{224}Cm concentrations in solution.

Determine if Am and Cm, sequestered with the aged grouts, return to solution on contact with increasing concentrations of $KHCO_3$.

The effect of $KHCO_3$ addition to the solution in contact with each grout was determined beyond a HCO_3^- concentration equivalent to that of the West Valley groundwater. This is based on the assumption that in an open system, CO_2 ingress will persist. In addition, precipitation of calcite can be inhibited by a number of factors, allowing carbonate/bicarbonate concentrations to become elevated significantly beyond that expected. The proportion of carbonate/bicarbonate species will change as pH changes but the total quantity will be similar. Figure 65 shows how Am content and pH were

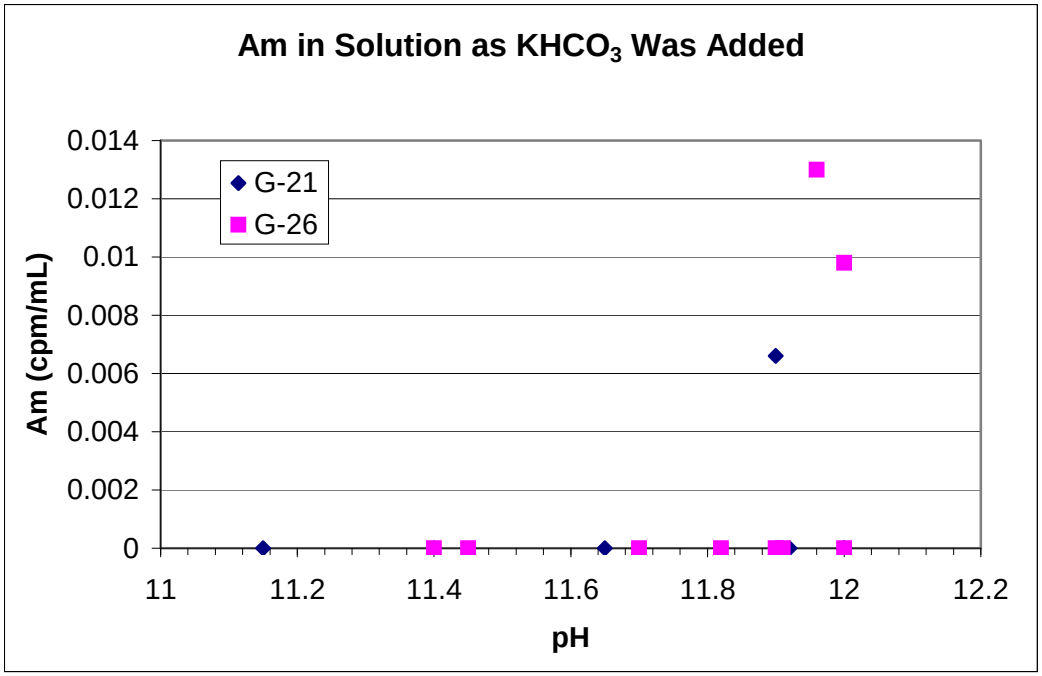

Figure 65. ^{241}Am concentrations in solution as a function of pH as $KHCO_3$ was added. These are aged grout experiments that subsequently received additions of $KHCO_3$.

changed by addition of $KHCO_3$ for each of the grouts. These experiments had aged 512 days before the start of additions and the pH of grouts 21 and 26 were 12.0 and 11.9 respectively. No ^{241}Am was observed over detection limits with the exception of 3 samples at low count rates. These slightly elevated samples occurred between sampling intervals 4 and 6 and subsequent samples returned to below detection limits. The original count rate at the start of the experiment was 165 cpm/mL or 2300 pCi/mL. The concentration of $KHCO_3$ was increased to 0.147 M (as added) over the course of 10 additions and sampling intervals. Changes in pH were not large and did not differ for each grout formula. It is unclear why the 3 samples were elevated (possibly colloidal material passed through the filters) but overall there was no increase in Am concentration as $KHCO_3$ was increased.

Figures 66 and 67 show results of a similar experiment for ^{244}Cm in contact with aged grouts, in terms of pH and $KHCO_3$ additions respectively. Concentrations of Cm are slightly elevated over the starting concentrations of both grouts with an increase between

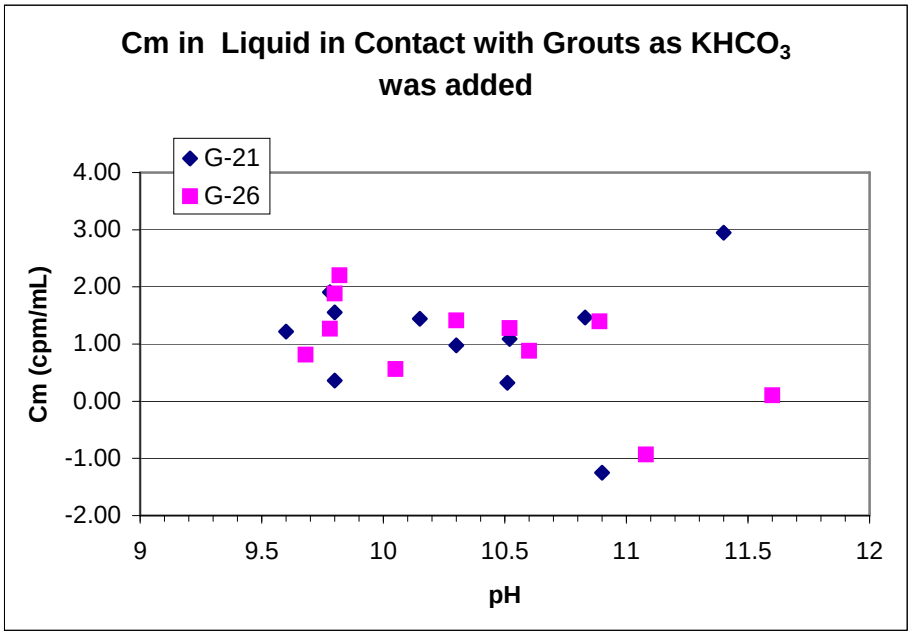

Figure 66. Effect of addition of $KHCO_3$ on release of Cm to solution.

1 and 2 cpm/mL. These concentrations, which seem to be steady state, are about 0.3 pCi/mL, slightly above the detection limit. That the count rates are elevated is substantiated by their positive distribution above 0 cpm. Recall that Cm count rates in the aged grout samples were distributed evenly about zero. After addition of $KHCO_3$, some beta activity was observed in the Cm samples, presumably the result of daughters or other radionuclide in the original tracer being released to solution. These count rates range from 4 to 15 cpm/mL.

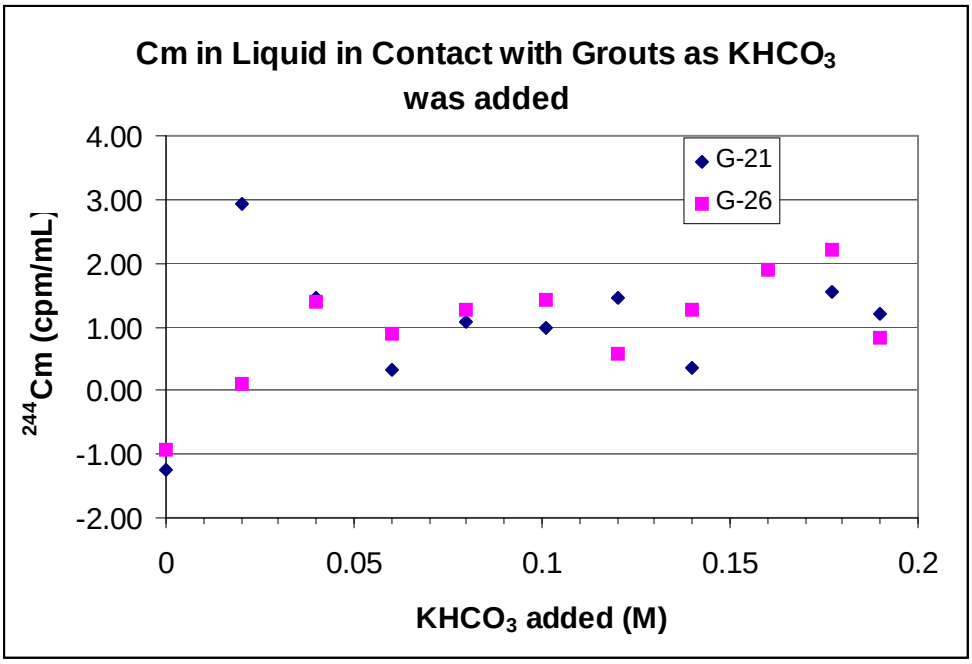

Figure 67. ^{244}Cm count rate as a function of the quantity of $KHCO_3$ in solution as it was added to aged grout experiments.

Determine the behavior of Am and Cm that have precipitated in a simulated grout pore water (without grout present), as the pH is lowered or $KHCO_3$ content is increased.

Figure 68 shows the aqueous concentrations of Am in simulated pore water control experiments in which pH or $KHCO_3$ were altered. In both experiments, ^{241}Am in the alkaline contact solution was undetectable under the initial condition of pH 12.3. In these two parallel experiments, aliquots of 1M $KHCO_3$ were added to one bottle of simulated pore water and 1M HNO_3 and NaOH were added to another to adjust pH. As $KHCO_3$ content increased, the ^{241}Am concentration generally remained below detection limits. This was so for most of the 10 intervals of $KHCO_3$ addition which resulted in a final added concentration of 0.147 M. Am did not return to solution even at high concentrations of $KHCO_3$ which resulted in pH values of 9.9.

The pH experiment started at pH = 12.3 and was lowered with HNO_3. No Am was observed in solution until the pH was between 9.9 and 8.3. As the pH decreased, the Am content increased so that at pH 7.2 the count rate was about 0.05 cpm/mL or 0.7 pCi/mL.

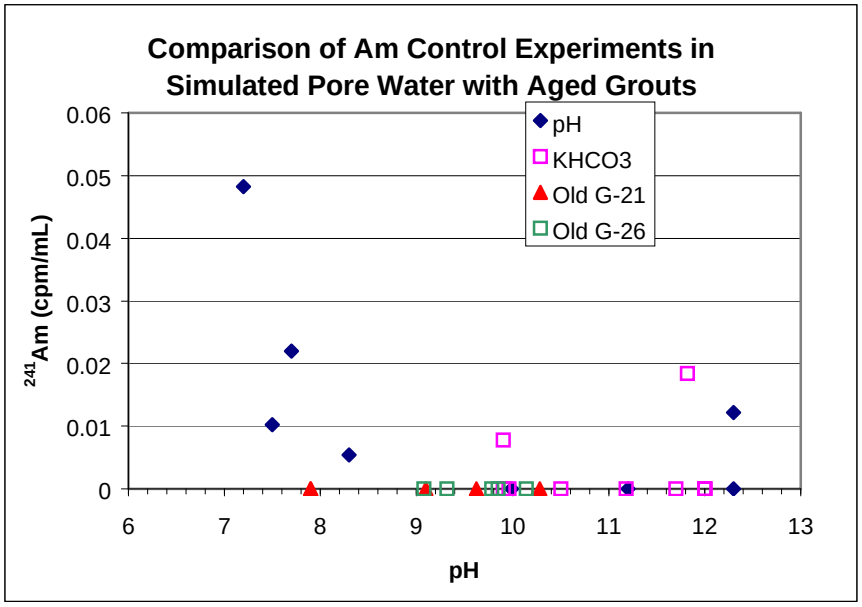

Figure 68. ^{241}Am count rate as a function of the quantity of $KHCO_3$ in solution as it was added.

The aged grout experiments are included with the results of the simulated grout pore water experiments in Figure 68. Even though the simulated pore water experiment resulted in elevated counts at low pH values, with grout present Am concentrations were below detection limits, even at a pH value of 7.8. This implies that the grout retains Am even at relatively low pH values. Because of their similar chemistry, it is expected that Cm would show very similar behavior. This is corroborated by the observation of essentially no counts in any of the aged grout experiments. It is evident that solubility, at least at pH values less than 9, is not the only process retaining Am or Cm in the presence of the grout.

Determine the behavior of Am and Cm in simulated grout pore water in contact with the components of the grout: portland cement, blast furnace slag, fly ash, zeolite, and fluorapatite.

Interactions of Am with individual components of the grout, as they are influenced by pH, are shown in Figure 69. No counts were observed for Am with the cement and blast furnace slag. These materials maintained high pH levels, keeping Am in the solid. Am

in contact with the zeolite and fly ash was not observed in solution above pH 11. Below that concentrations increased to a maximum of about 0.12 cpm/mL, or 1.7 pCi/mL. Below pH 9.2, it looks as if concentrations then decreased. Am in water in contact with apatite was first observed at pH 11.6 . The reason may be formation of a soluble complex of Am with a component of the fluorapatite, either fluorine or phosphate. In contrast, Am not found in solution at that pH in experiments without the apatite present. In summary, Am concentrations, and by analogy Cm concentrations, were low in contact with all of these materials (except the apatite additive) above pH 11. Am counts did increase slightly as the pH decreased below 11. Am, and presumably Cm form carbonate compounds that are important controls on their solubility. Calcite did form between pH 9 and 10 in uranium experiments and it also may have formed in these experiments incorporating Am.

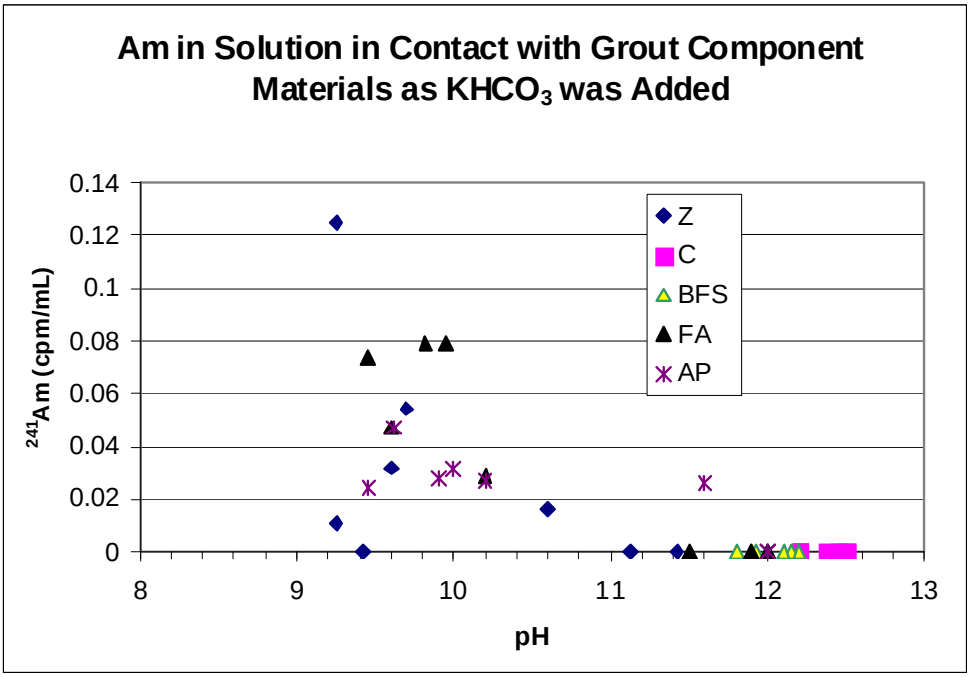

Figure 69. ^{241}Am concentrations in solution in contact with the grout components.

Determine the release mechanisms of Am and Cm from grout over long-times and estimate their leaching relative to pore volumes flowing through the grout.

Data from all experiments are shown on Figure 70, showing ^{241}Am cpm/mL as a function of pH. As shown earlier, in Figure 68, the experiments with simulated pore water resulted in no releases of ^{241}Am when $KHCO_3$ was added. In experiments where the pH was lowered with acid, Am was observed in solution only below pH 8.5. With the exception of the three grout kinetics experiment samples, the concentration of Am in solution was below our detection limits in all cases in which grout was present, even when the pH was low (7.9). Portland cement and blast furnace slag maintained high pH conditions and Am was below detection limits. Below pH 10.5 fly ash, zeolite and apatite, all had elevated ^{241}Am concentrations in solution. Addition of $KHCO_3$ did not result in Am returning to solution in the simulated pore water experiments, yet its addition did release Am from these materials. Colloidal material may be produced that incorporates Am and passes through the filters. More likely the cause is the formation of a soluble Am species in solution. Clark et al,(1995) show that $Am(CO_3)^{-2}$ becomes the dominant solution complex between pH 9 and 11 in modeling of well water interactions with Am at Yucca mountain. Curium in contact with grouts over long times was not found in solution, but addition of $KHCO_3$ did result in a small increase of about 0.3 pCi/mL which became steady state.

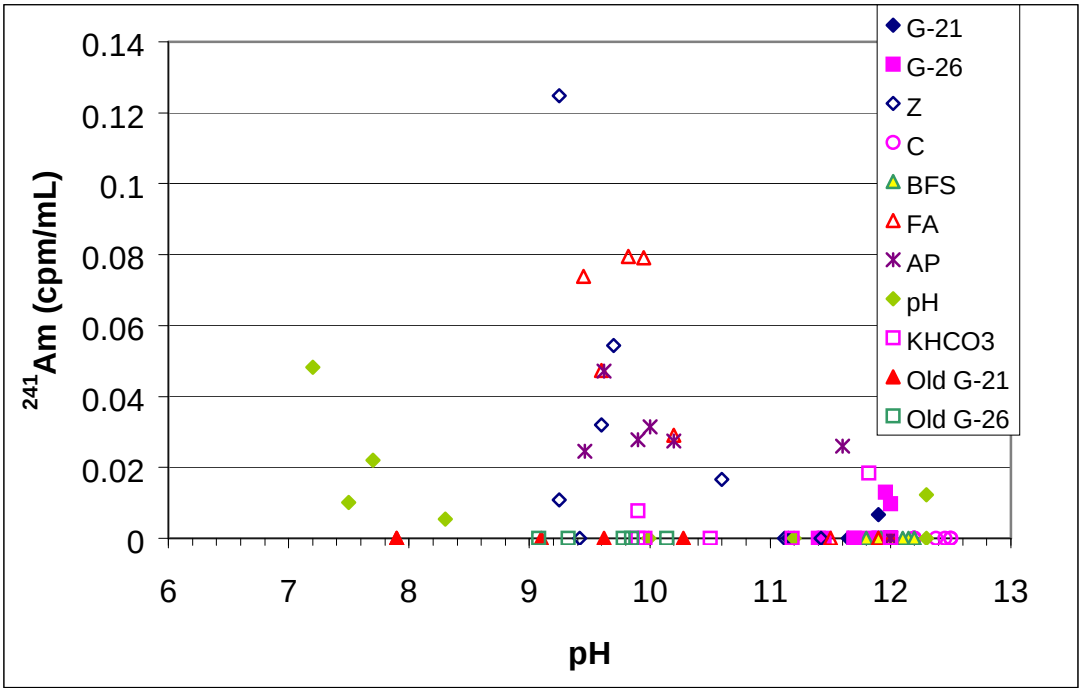

Figure 70. All experiments for Am.

An important implication of these data is that ^{241}Am and Cm that had aged with grouts and the short term test for Am in the simulated pore water, provided similar results until pH decreased below 9.

Thermodynamic modeling with Geochemists WorkBench was conducted for the solution composition used in the simulated pore water experiments. The "React" code was used and pH was incrementally adjusted from 12 to 8 to simulate the pH experiment. Results indicate that $Am(OH)_3$ was saturated and no discernable Am was in solution at pH values above 8.4. At that point $AmOHCO_3$ became saturated, and $Am(OH)_3$ was slightly undersaturated. At pH 8.0 $AmOH^{++}$ was in solution at a concentration of 2.2×10^{-8} M. This model conforms very closely to the results of the pore water pH experiment. When the $KHCO_3$ experiment was modeled (0.1 M HCO_3^- was added), $Am(CO_3)_3^{-3}$ began to enter solution at pH 11 reaching a maximum concentration at pH 10 and then diminishing to low concentrations by pH 8.5. The stable solid phase was $AmOHCO_3$, but interestingly no indication of the formation of $Am_2(CO_3)_3$ was given by the code. This profile of the solution concentration vs pH fits Am in solution rather well for the zeolite,

apatite and fly ash samples shown in Figure 70. That the thermodynamic modeling provided reasonable simulation of Am solubility constraints imparts some level of confidence that these experiments are giving useful information in a thermodynamically sound way, as opposed to being subject to a variety of transient states.

In the experiments containing grout, Am was rarely and inconsistently observed in solution. In general it was below detection limits. There is only one experimental point in which the pH of a grout sample drops low enough to indicate that the grout is providing additional retention beyond that of pH control. At pH 7.9 of the "old Grout-21" experiment the Am concentration is below detection. However at the same pH it is observable in the pH pore water experiment. This implies that solids other than $Am(OH)_3$ are controlling Am solubility in the grouts.

Effluent from the column experiments discussed in the uranium report ranged from pH 12 to approximately pH 8 in 900 – 1100 pore volumes. Over this pH range no Am was observed in solution when in contact with grouts, even after 596 days. In the pore water experiments, Cm was released as a result of $KHCO_3$ addition at very low concentrations that were just discernable. This occurred with the smallest addition of $KHCO_3$ and remained consistent as $KHCO_3$ additions continued, consequently we believe that low concentrations of Cm may be complexed with carbonate/bicarbonate. This is also the case for Am at pH ranges of 9 to 11 in the presence of some of the component materials used in the grouts.

References for Am and Cm

Clark, D. D. Hobart, and M. Neu, 1995, Actinide Carbonate Complexes and their Importance in Actinide Environmental Chemistry, Chemical Reviews, Vol. 95, p. 25-48.

Kim, J., R. Klenze, H. Wimmer, W. Runde, and W. Hauser, 1994, A study of the carbonate complexation of Cm (III) and Eu (III) by time resolved laser fluorescence spectroscopy, Journal of Alloys and Compounds, Vol. 213, pp. 333-340.

Brady, P., H. Papenguth, and J. Kelly, 1999, Metal Sorption to Dolomite Surfaces, Applied Geochemistry, Vol. 14, p. 569-579.

Curti, E., 1999, Coprecipitation of radionuclides with calcite: estimation of partition coefficients based on a review of laboratory investigations and geochemical data, Applied Geochemistry, Vol. 14, pp. 433-445.

Shilov, V. P., 1998, Probable Forms of Actinides in Alkali Solutions, Radiochemistry, Vol. 40, pp 11-16.

Rai, D., R.G. Strickert, D.A. Moore, and J. L. Ryan, 1983, Am(III) Hydrolysis Constants and Solubility of Am (III) Hydroxide, Radiochimica Acta, Vol. 33, pp. 201-206.

Runde, W., G. Meinrath, and J. Kim, 1992, A study of Solid-Liquid Phase Equilibria of Trivalent Lanthanide and Actinide Ions in Carbonate Systems, Radiochimica Acta, Vol. 58/59, pp. 93-100.

Vitorge, P. 1992, $Am(OH)_{3(s)}$, $AmOHCO_{3(s)}$, $Am_2(CO_3)_{3(s)}$ Stabilities in Environmental Conditions, Radiochimica Acta, Vol. 58/59, pp. 105-107.

Morss and Williams, 1994 radiochimica acta 66-7, p 89-93, 1994

Keller, C., 1971, The Chemistry of the Transuranium Elements, Verlag Chemie, Weinheim/Bergstr., Germany, 675 pp.

Rorif, F., J. Fuger, and J. F. Desreux, 2005, Thrmochemistry of selected trivalent lanthanide and americium compounds: othorhombic and hexagonal hydroxycarbonates, Radiochimica Acta, Vol. 93, pp. 103-110.

Ekberg, C., G. Meinrath, and B. Stromberg, 2003, A retraceable method to assess uncertainties in solubility estimations exemplified by a few americium solids, J. Chemical Thermodynamics, vol. 35, pp.55-66.

Isotherms for Fission Product Radionuclides

^{137}Cs Isotherms

Concentrations of ^{137}Cs in the tank wastes is given as 18 μCi/ mL. For our experiments, this activity would have been unworkable, but it is important to bracket the concentrations in the waste. Consequently, a small quantity of carrier Cs (non-radioactive) was added to the radionuclide tracers. The mass of cold Cs added was varied, controlling the total Cs concentration since the carrier free radionuclide comprised a very small mass of Cs. This allowed a wide range of concentrations in the isotherm experiments without excessive activity in the samples. The concentrations of Cs in the experiments were 10, 1.0, 0.5, 0.1, and 0.01 mg/L. The calculated activity in the waste (18 μCi/ mL), on a carrier free basis, is 0.2 mg/L. The experiments ran for 22 days.

Results of ^{137}Cs uptake on the grouts are shown in Figure 71. Both isotherms are linear over this concentration range, but there is a significant difference in uptake by the two grout formulations. The Cs K_d values for these materials are the slopes of the plots, 140 and 5.1 mL/g, for grout 21 and grout 26 respectively. Grout 21 sorbs about 5 times more Cs than grout 26. This can be attributed to the presence of the zeolite in the material instead of apatite. This is of interest because uptake of Cs by a zeolite is an adsorption process that presumably would be hindered by competing ions (e.g. K) that are present in relatively high concentrations in the grout. Nevertheless, the zeolite retains enough selectivity for Cs to actively sorb it after the grout had been made.

The difference in behavior between the two grout formulations was explored by determining the sorption of Cs onto the individual components of the grout. For the individual materials, isotherms were produced under conditions that are close to those within the grouts (e.g. pH and major competing ions by using the contact solution

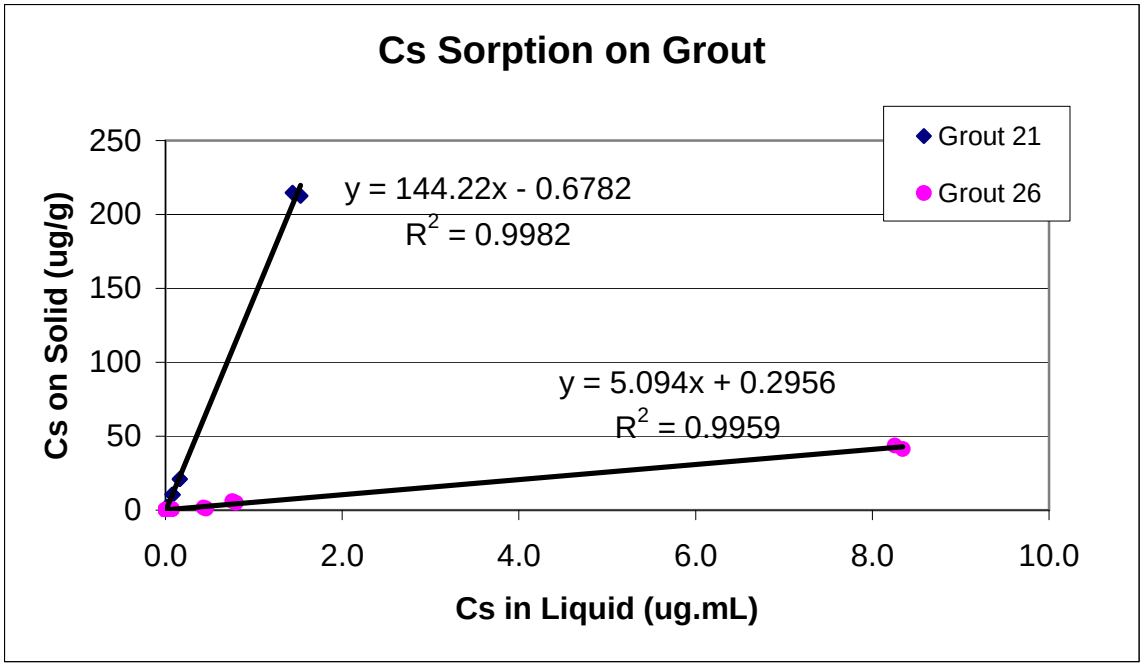

Figure 71. Isotherms for Cs on Grouts 21 and 26.

previously described). Log/log plots of concentrations of Cs on the solid vs steady-state concentrations in the liquid, were used to get parameters of the log transformation of the Freundlich isotherms as given in equation 2. The value of K_f is equivalent to K_d. Isotherms for the five grout components are shown as log/log plots in Figures 72-76. Their K_d values for Cs are given in Table 18 for the two grout formulations.

Table 18. K_d values for Cs

Material	K_d (mL/g)
Apatite	19
Cement	1
Fly ash	6
Zeolite	1500
Blast furnace slag	6
Grout 21	5
Grout 26	140

Of the component materials, only the zeolite has a significant K_d. Grout 21, which does not contain the zeolite, has a K_d of 5 mL/g which is typical of the materials that comprise it. Grout 26 contains 10% zeolite, and its K_d value is about 10% of the zeolite value. This implies that the zeolite does not loose its capacity to sorb Cs when it is incorporated into the grout even though there is mineral ingrowth and dissolution taking place, as it does in any cementitious material. Moreover, this result indicates that the testing regime (e.g. the composition of the contact solution) for the component materials must be an appropriate analog to conditions in the grout. The Cs K_d for apatite was 19 mL/g, which is similar to the value of 10 mL/g given in Table 2.1-1 (URS report, Conceptual Design Document, 2003). However, from that report the estimated K_d for the grout containing apatite was 280 while our measured value was 5 mL/g.

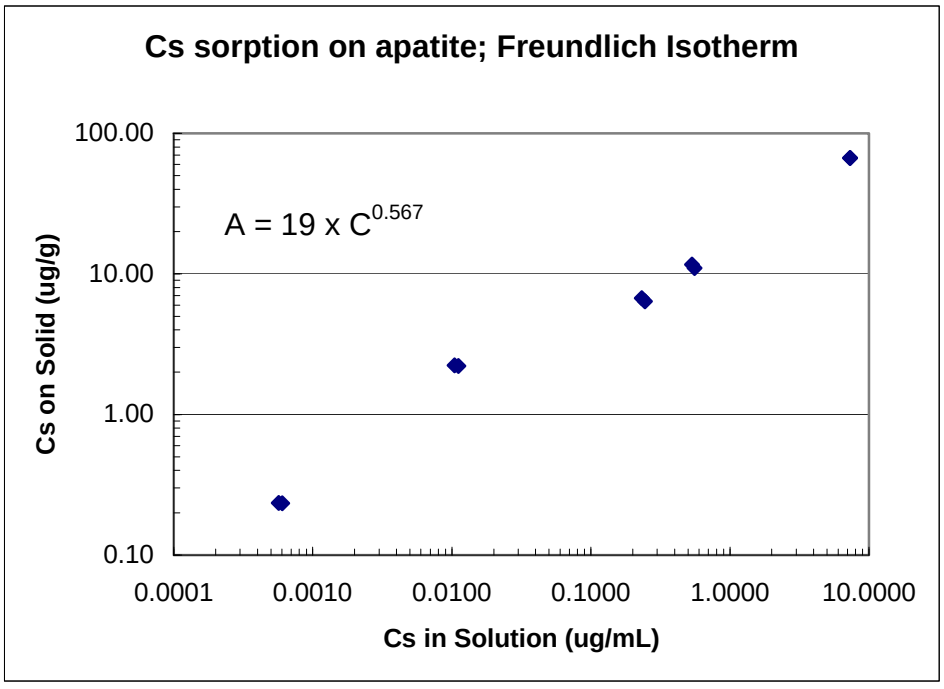

Figure 72. Freundlich Isotherm for Cs on apatite**.**

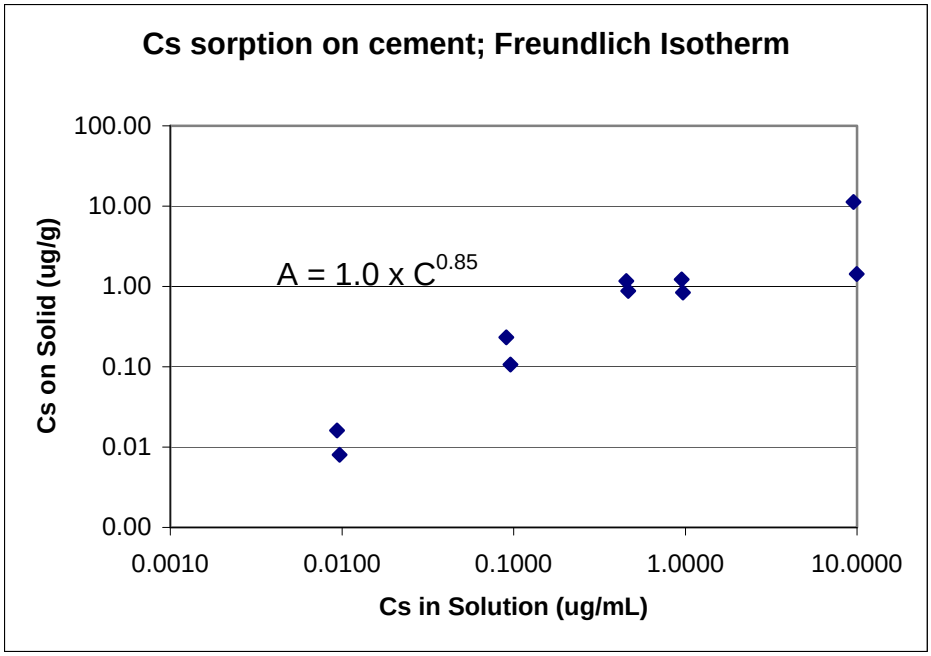

Figure 73. Freundlich isotherm for Cs sorption on cement.

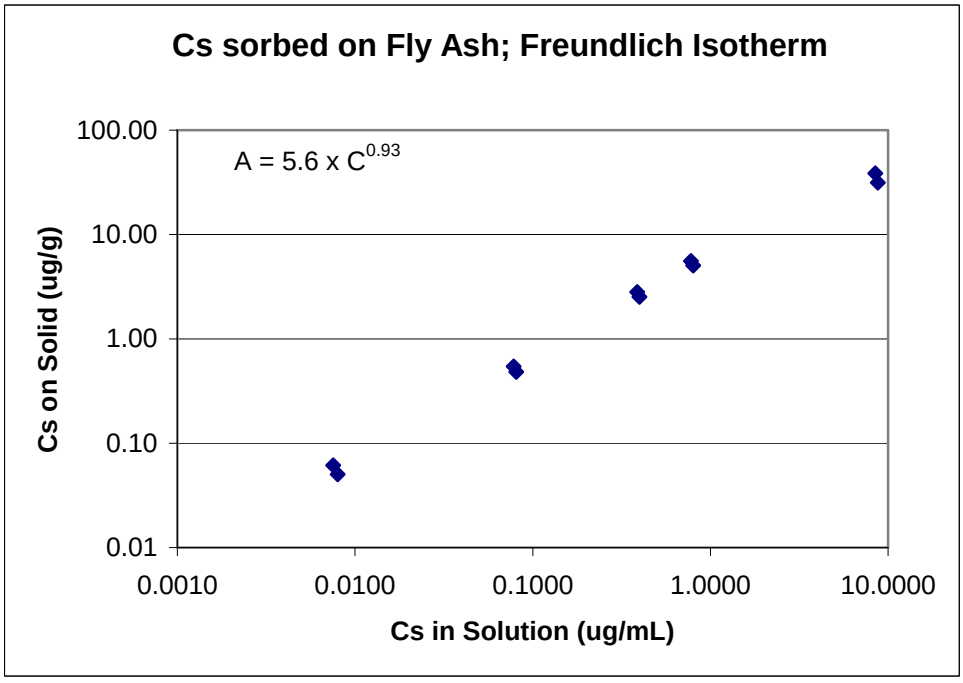

Figure 74. Freundlich isotherm for Cs sorption onto fly ash**.**

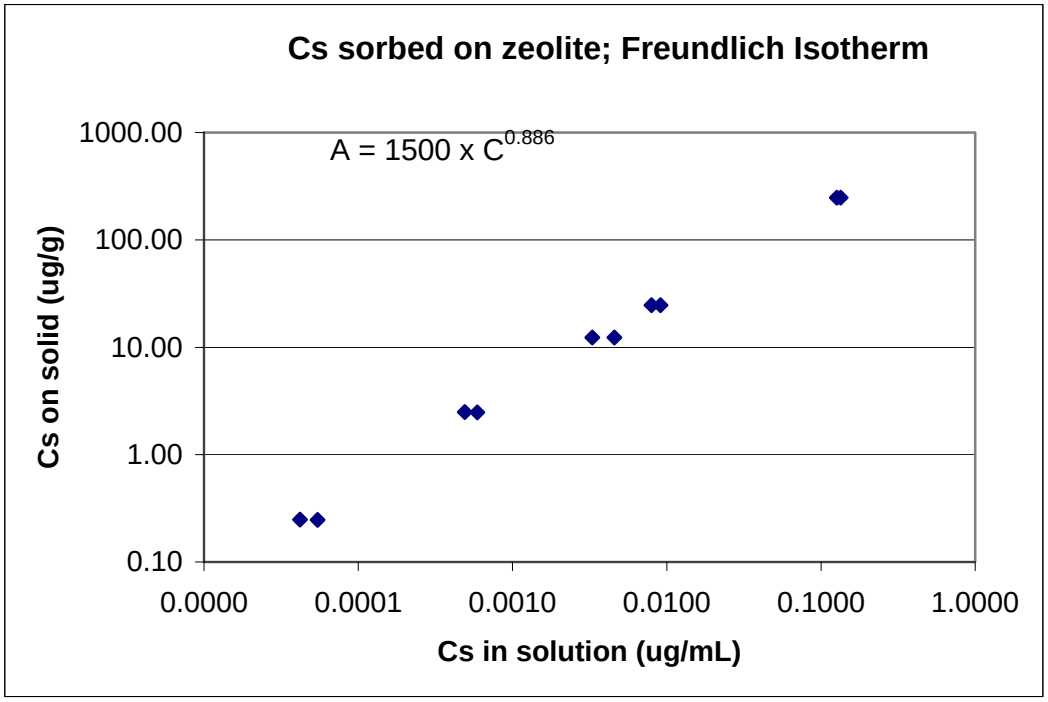

Figure 75. Freundlich isotherm for Cs sorption onto the zeolite. This material has the greatest partitioning for Cs of all materials tested.

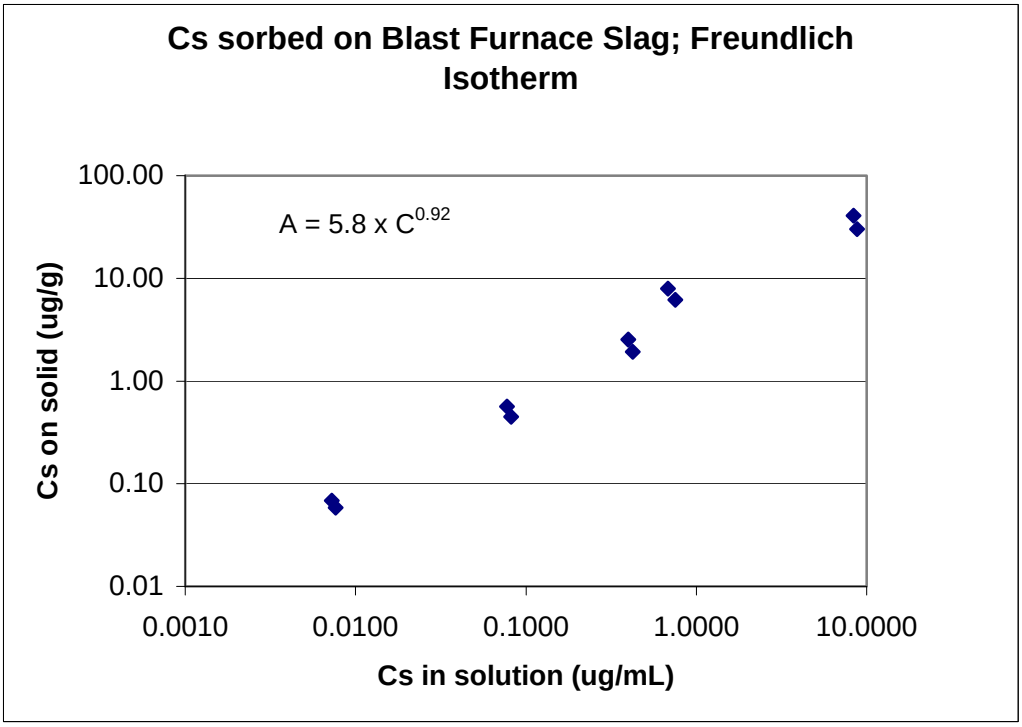

Figure 76. Freundlich isotherm for Cs sorption onto blast furnace slag.

Strontium Isotherms

For strontium sorption experiments ^{85}Sr tracer was used. This tracer had a specific activity of 50 Ci/g. Concentrations of contact solutions used in the isotherm experiments were: 0.055, 0.027, 0.014, 0.003, and 0.0003 μCi/mL. The grout isotherms ran for 29 days, while the isotherms for the component materials ran for 40 days. Based on sorption kinetics experiments with the two grout formulations, about 18 days is enough to reach steady state concentrations, as shown in Figure 77.

Figure 78 and Table 19 show that the zeolite component of the grout exhibited significantly greater uptake of ^{85}Sr than the other materials. This mineral, a clinoptilolite, is noted for its ability to sorb Sr. This capacity is preserved in the high pH, high Ca environment of the grout materials sorption experiments. This behavior extends to ^{85}Sr retention in the grouts, Figure 79, where the grout containing the zeolite has a higher K_d than the grout containing the apatite.

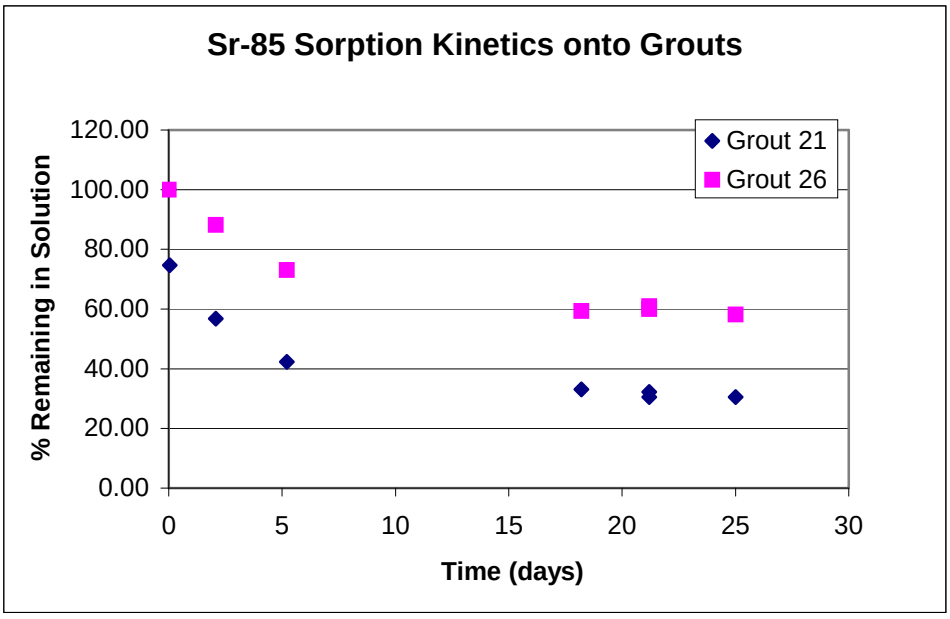

Figure 77. Uptake kinetics for Sr onto the two grouts showing that sorption is steady state by 18 days.

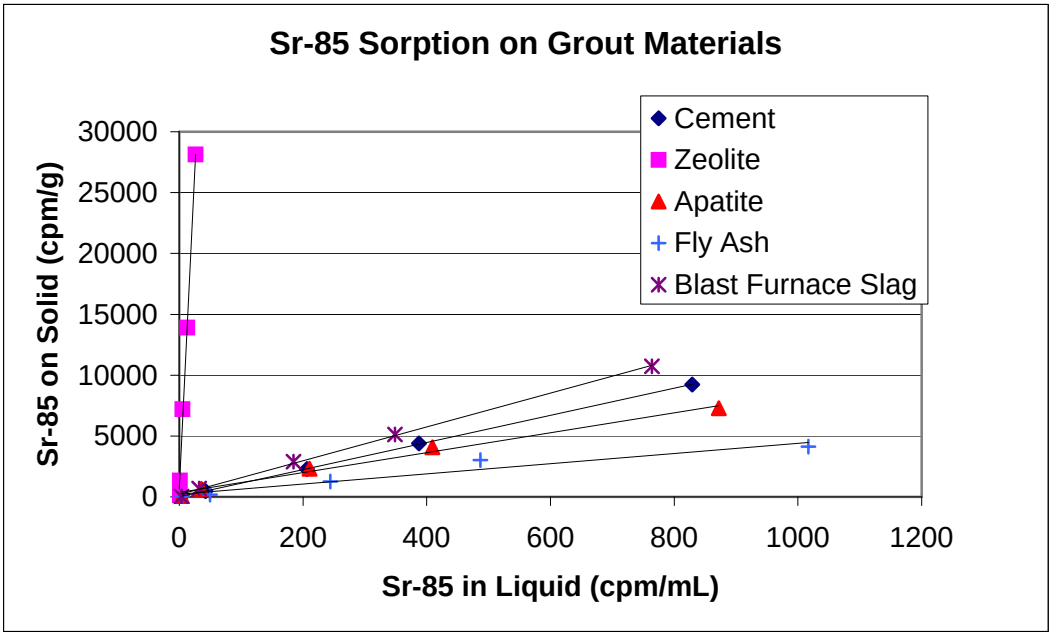

Figure 78. Isotherms for Sr-85 sorbed on the various grout components. Zeolite has the greatest partitioning for Sr.

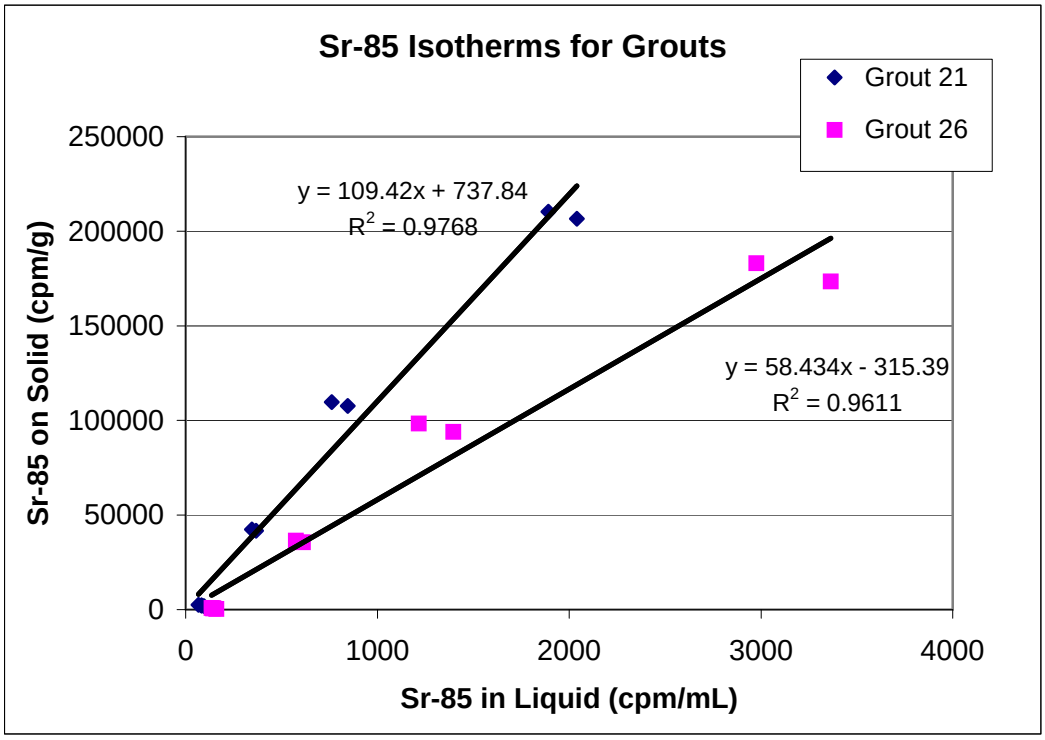

Figure 79. Isotherms for the two grouts, showing that Grout 21 sorbs about twice as much Sr as does Grout 26.

Table 19. K_d values for Sr

Material	K_d (mL/g)
Apatite	8.2
Cement	11.2
Fly ash	4.2
Zeolite	1050
Blast furnace slag	13.9
Grout 21	110
Grout 26	58

Iodine Isotherms

Iodine sorption isotherms were done using ^{125}I tracers with a specific activity of 10 Ci/g. The grout experiments ran for 31 days, while the grout component experiment ran for 67 days. Little, if any, uptake of iodine occurred on the grouts and concentrations were essentially steady state within a few days, as shown in Figure 80. The values for the kinetics experiment tend to be slightly over 100% for Grout 26, possibly indicating that the reference counts were a bit low. This effect may also be the result of anion exclusion from around negatively charged particles in solution.

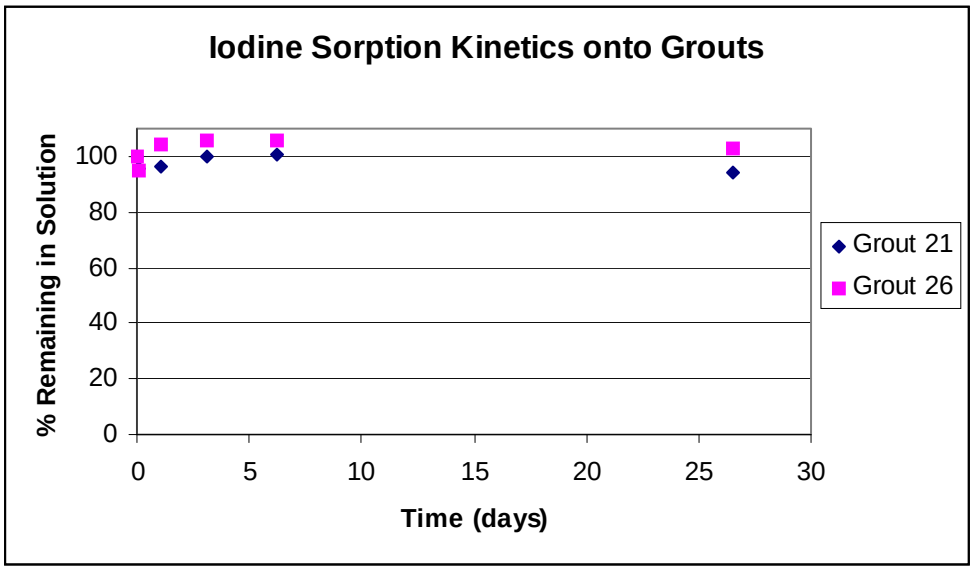

Figure 80. Iodine sorption kinetics onto the two grout materials showing the quantity of I remaining in solution.

Sorption of ^{125}I onto the grouts was very low although measurable values were obtained. As shown in Figure 81, the isotherms were linear with slopes (which equate to K_d) for Grouts 21 and 26 of 0.66 and 0.81mL/g, respectively. In most cases, uptake onto the various components of the grout was low. The exception was sorption onto cement, which was linear with a slope of 210mL/g. All other materials had slopes (K_d) of less than one. Isotherms for individual components are shown in Figures 82 and 83, and the K_d values from the isotherms are given in Table 20.

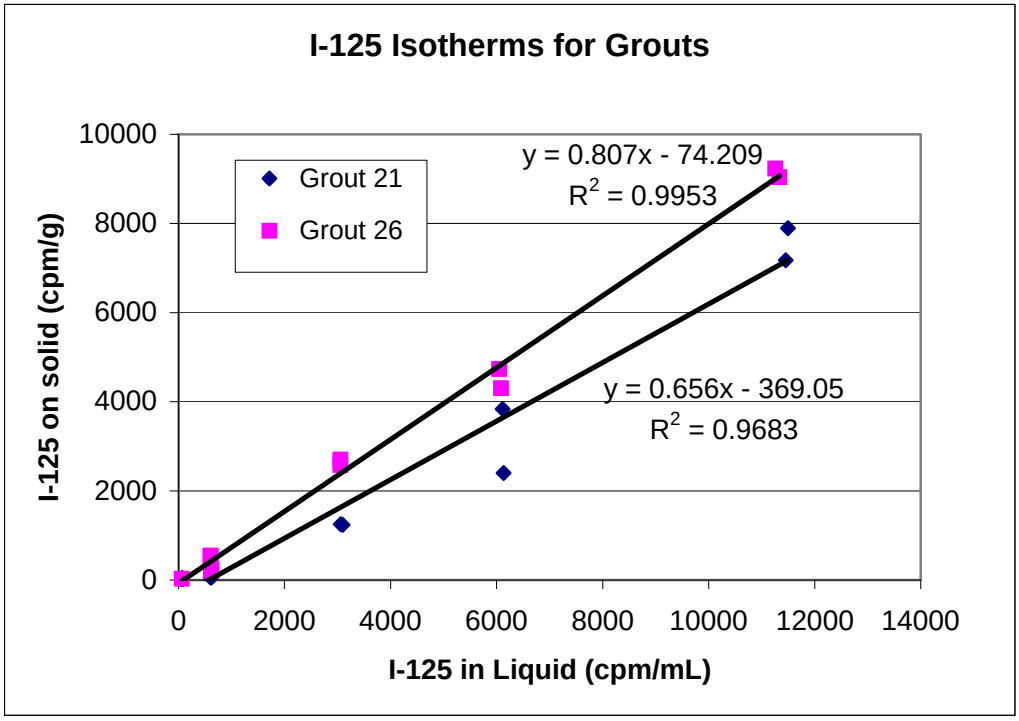

Figure 81. Isotherm for iodine onto grout materials, showing that there was very little uptake of iodine.

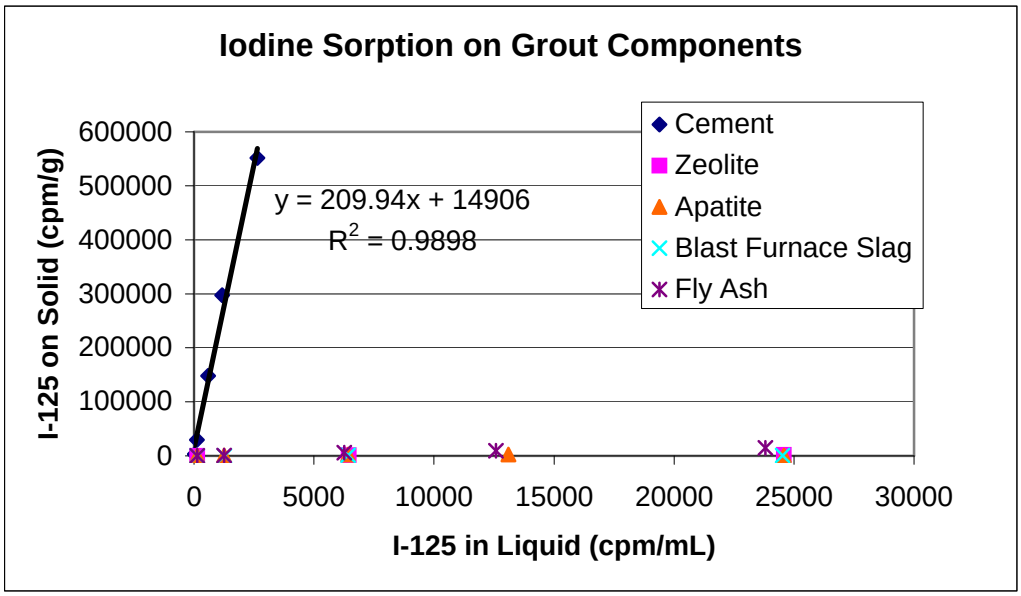

Figure 82. Isotherm for iodine sorbed onto grout component materials. Cement provided the greatest uptake of iodine.

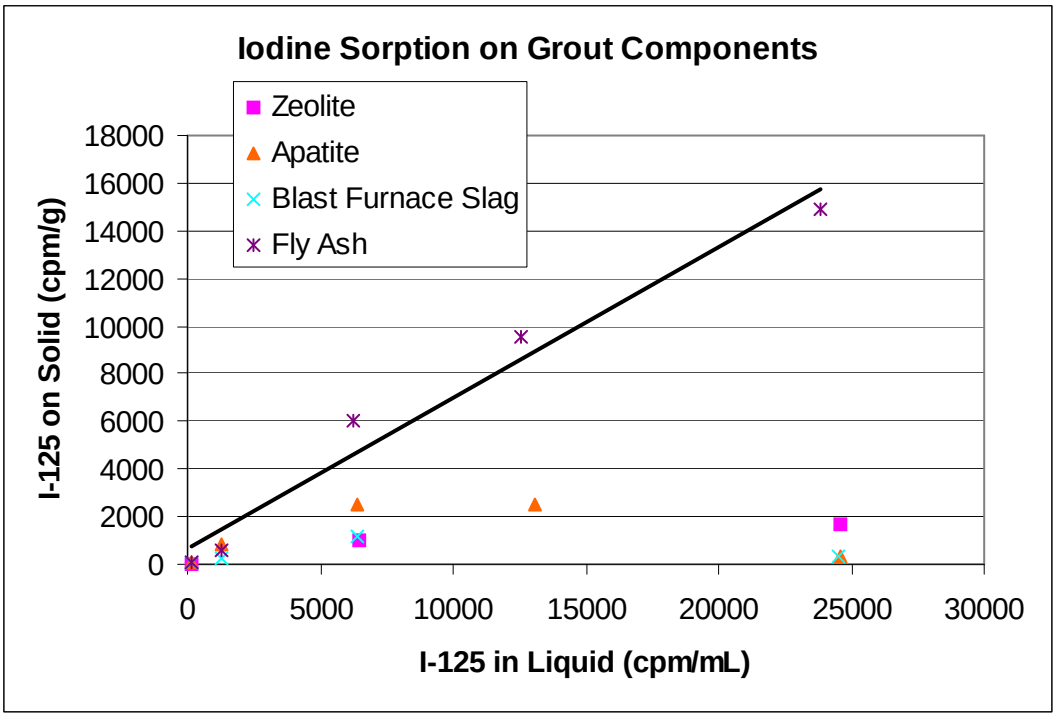

Figure 83. Isotherm showing uptake of iodine onto grout components. The plot for cement was removed to better show the relative partitioning of the other materials. After cement, fly ash provided the most uptake.

Table 20. K_d values for ^{125}I

Material	K_d (mL/g)
Apatite	Nil
Cement	210
Fly ash	0.63
Zeolite	Nil
Blast furnace slag	Nil
Grout 21	0.66
Grout 26	0.81

Technetium Isotherms

The tracer used was ^{99}Tc, as NH_4TcO_4, with a specific activity of 0.017 Ci/g. The grout sorption experiments ran for 43 days, while the component experiments sorbed for 51 days. Concentrations used in the isotherm experiments were: 0.055, 0.027, 0.014, 0.003, and 0.0003 μCi/mL. Uptake of ^{99}Tc by the two grouts was limited and reached steady state, as shown in Figure 84, after about 6 days. There was essentially no difference in uptake of ^{99}Tc by the two formulations, both with slopes less than 1, as shown in Figure 85 and Table 21. Most of the grout components showed little, if any, capacity to sorb Tc. The exceptions to this is, the blast furnace slag with a K_d of 12 mL/g, and the cement with a K_d of 2 mL/g.

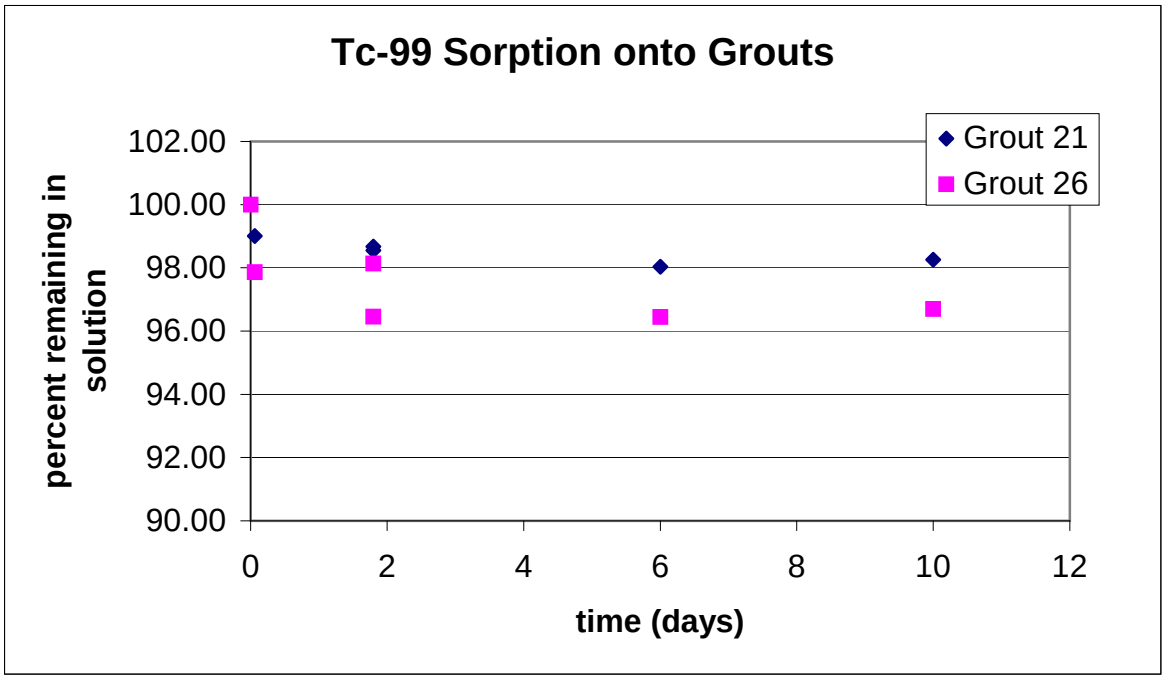

Figure 84. Sorption kinetics of Tc-99 onto grouts, showing that sorption was steady state after about 6 days.

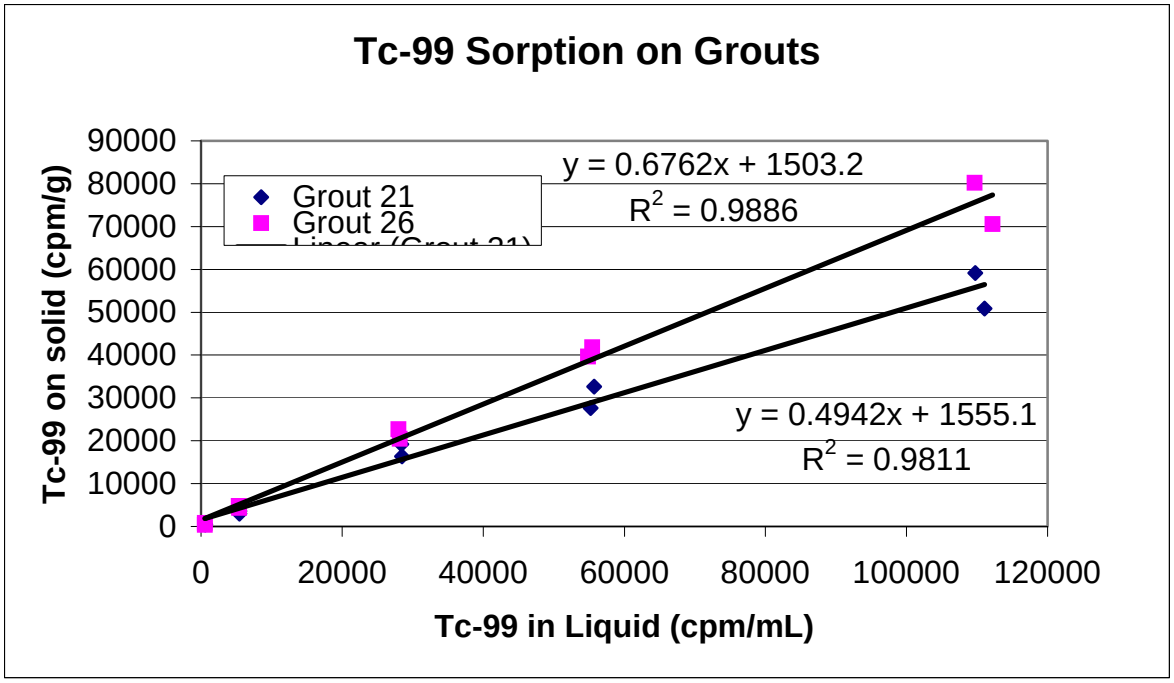

Figure 85. Isotherms for Tc-99 sorbed on grouts, indicating that little sorption takes place on these materials.

Table 21. K_d Values for ^{99}Tc

Material	K_d (mL/g)
Apatite	1.0
Cement	2.1
Fly ash	0.7
Zeolite	Nil
Blast furnace slag	12.2
Grout 21	0.5
Grout 26	0.7

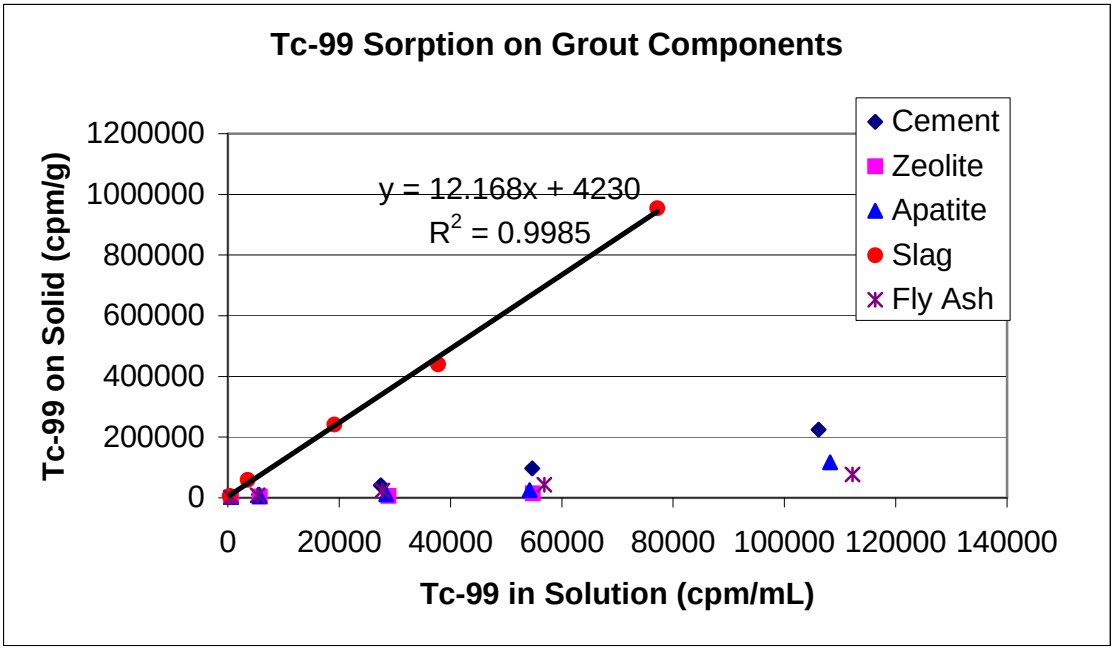

Figure 86. Isotherm for Tc-99 onto the grout component materials. The slag provided the greatest uptake of Tc.

Carbon Isotherms

A tracer of ^{14}C, as carbonate, was used to determine uptake of inorganic carbon. The tracer was 1 mCi from Isotope Products Laboratories which was diluted to give concentrations in the experiments of: 0.0545, 0.0273, 0.0136, 0.0027, and 0.00027 μCi/mL. The experiments ran for 189 days. Samples (2 mL) were analyzed by liquid scintillation counting . Results are shown in Figure 87 and in Table 22. There was relatively little ^{14}C remaining in solution. While the samples were very alkaline and this tends to retain ^{14}C, there can still be partitioning to the gas phase with subsequent loss from the system. It is unclear to what extent the experiments were influenced by this, but there is a reasonable trend in the data which implies that the data are reflecting sorption processes. The reference solutions, while preserved with NaOH, were seriously affected by vapor loss of ^{14}C and could not be used. Consequently, the starting concentrations were estimated based on the original tracer concentration and dilution factors for the experiments.

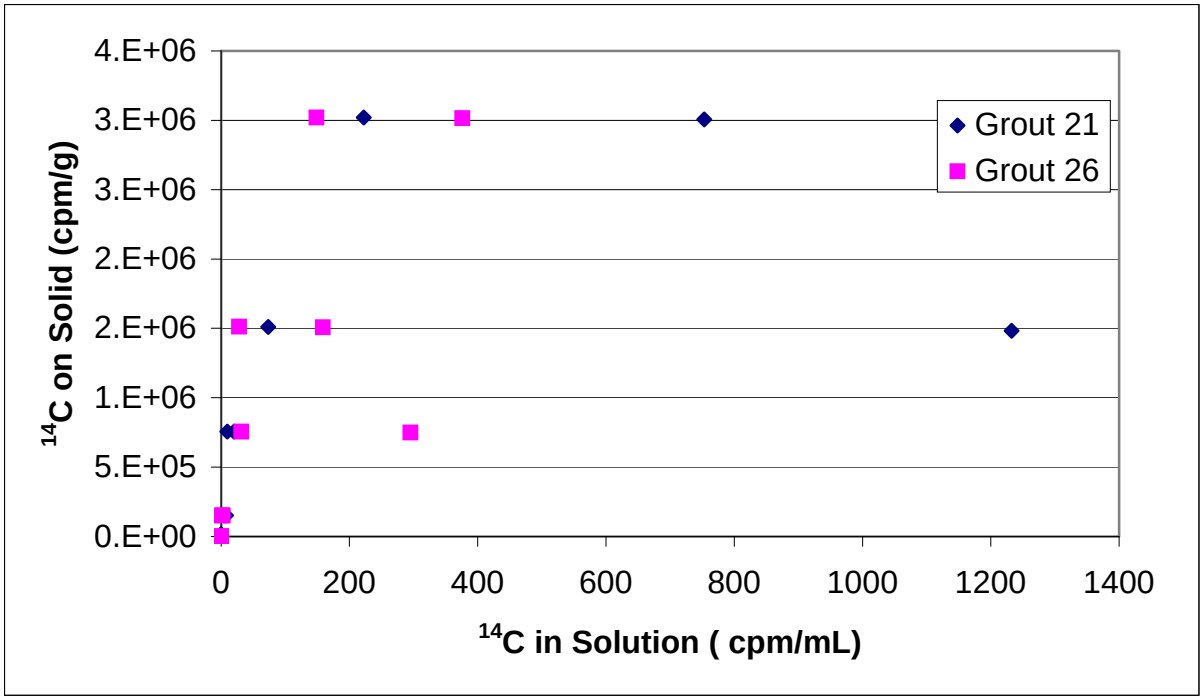

Figure 87. Partitioning of ^{14}C between the liquid and solid phases.

Table 21. Estimated K_d Values for ^{14}C

	Grout 21			Grout 26		
Nominal Activity	**Start cpm/mL**	**End cpm/mL**	**K_d (mL/g)**	**Start cpm/mL**	**End cpm/mL**	**K_d (mL/g)**
1	605	< 0.1	>150,000	605	< 0.1	150,000
10	6,050	6	27,000	6,050	1.5	126,000
50	30,200	15	58,000	30,200	160	13,000
100	60,500	650	11,000	60,500	92	32,000
200	121,000	480	8,800	121,000	262	14,000

Isotherms for RCRA and other Elements

Chromium Isotherms

The chromium tracer used was a solution of $K_2Cr_2O_7$. It was made at a concentration of 8800 mg/L which was pipetted into the experiments in aliquots ranging from 0.1 to 2 mL. For the lowest experiment concentration a dilution of the stock solution was made to 55 mg/kg and 1 mL was added to experiments. The actual experiment concentrations, measured by ICP, were: 310, 160, 80, 16.3, and 1.55 mg/L, which bracket the 160 mg/L in the waste. The grout experiments were run for 55 days. Figure 88 shows results of the Cr kinetics experiments with sorption being essentially complete within a few days.

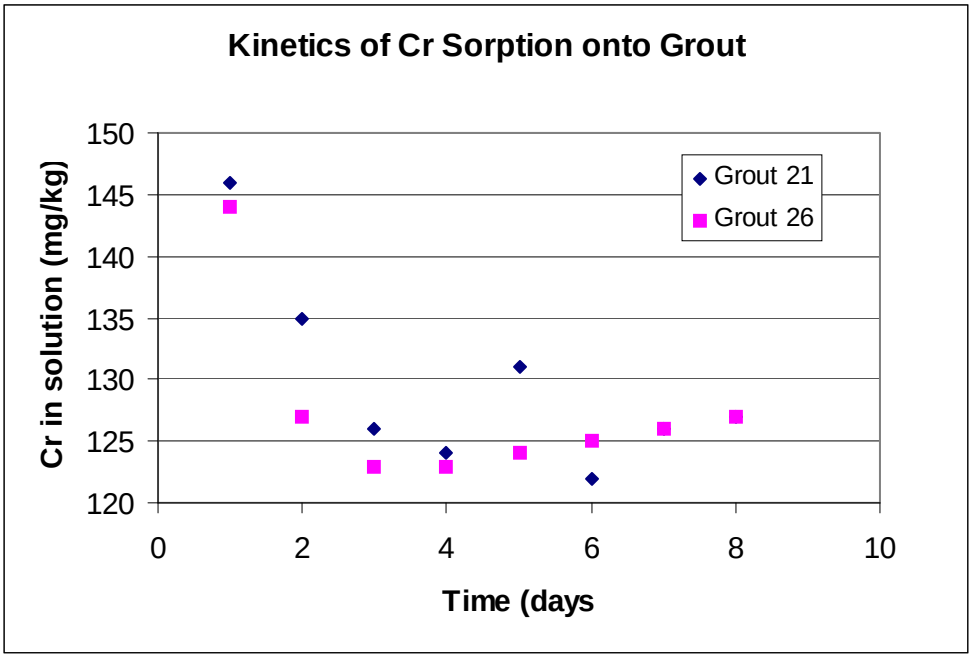

Figure 88. Uptake kinetics of Cr onto the grouts was complete by about 4 days. Some desorption may take place after that.

The grout isotherms, Figures 89 and 90, show non-linear sorption at the highest concentrations but they seem to be linear below about 400 to 600 mg/kg of sorbed Cr. For the linear sections of the plots, the slope (K_d) is between 6 and 7 mL/g for each material. Their capacity to retain Cr, based on the curvature of the slope, is estimated to be around 1200 mg/kg.

As shown in Figure 91, results of the component isotherms are quite interesting and unexpected. Sorption onto the cement component was greater by far than on the other materials. The K_d for this material was about 18 mL/g and uptake was linear to 7500 mg/kg indicating that significantly more Cr could be retained. The Blast Furnace Slag showed a lower capacity to sorb Cr and was non-linear, plateauing at about 2000 mg/kg, indicating that it could sorb no more Cr.

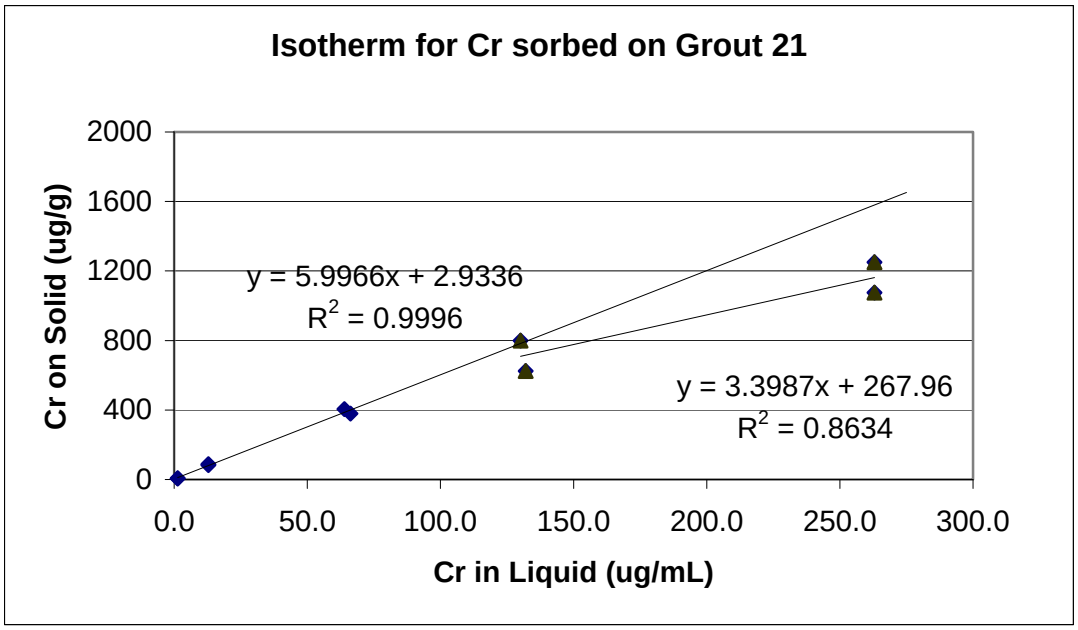

Figure 89. Isotherm for sorption of Cr onto Grout 21. This was non-linear with the early points indicating a K_d of about 6 mL/g.

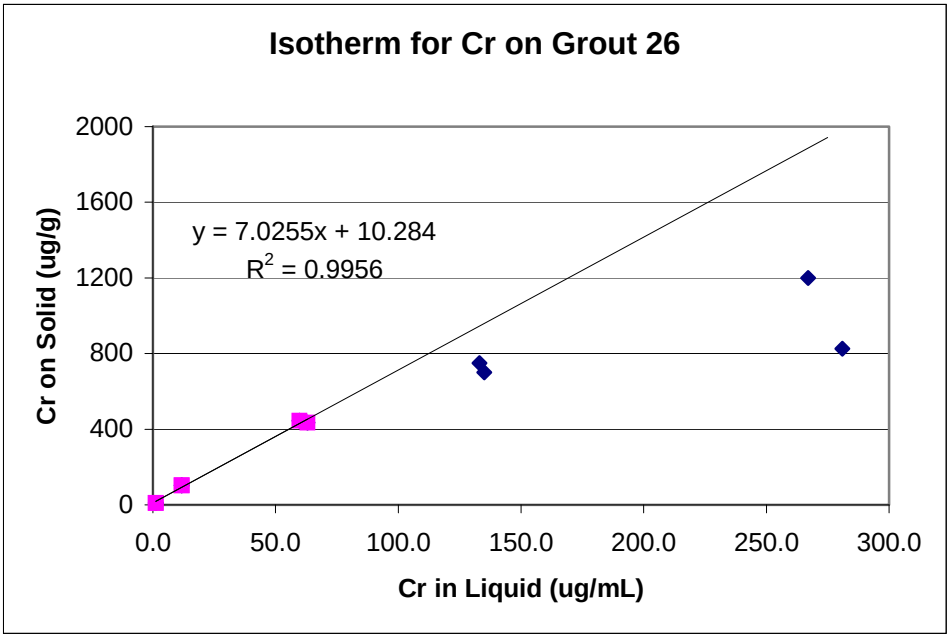

Figure 90. Isotherm for Cr onto Grout 26 was non-linear with the early points indicating a K_d of 7 mL/g.

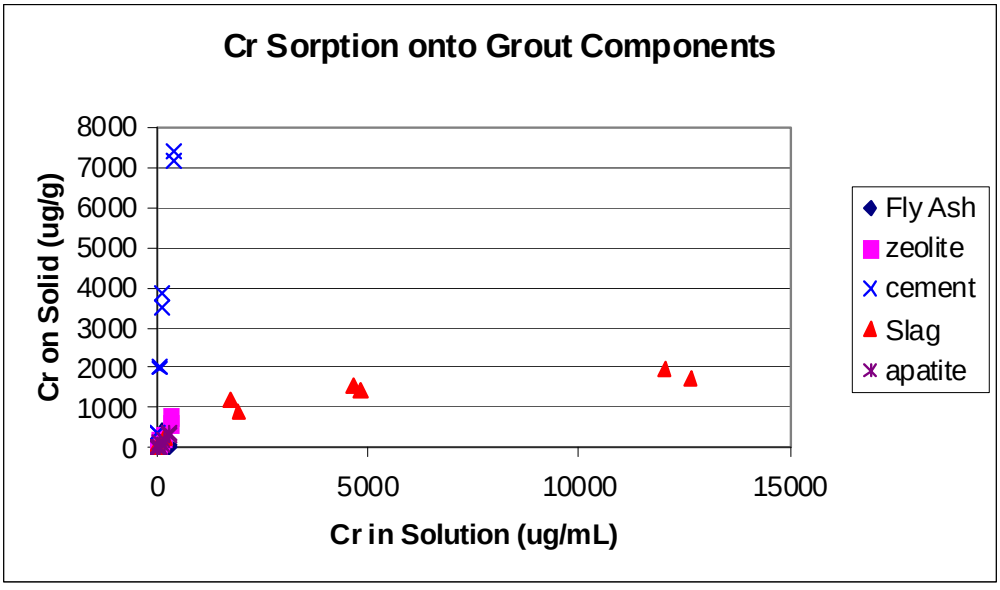

Figure 91. Sorption of Cr onto grout component materials was greatest for cement, followed by the blast furnace slag.

Vanadium Sorption onto Grouts

To determine sorption behavior of vanadium onto the two grouts, a 5500 mg/L solution was made from Na_3VO_4. This was diluted to give experiment concentrations of 0.93, 9.74, 49.7, 100, and 197 mg/L. The experiment ran for 57 days. For both grouts, uptake of V produced a non-linear isotherm as shown in Figures 92 and 93. Table 23 gives the K_d values calculated for the sets of batch experiments.

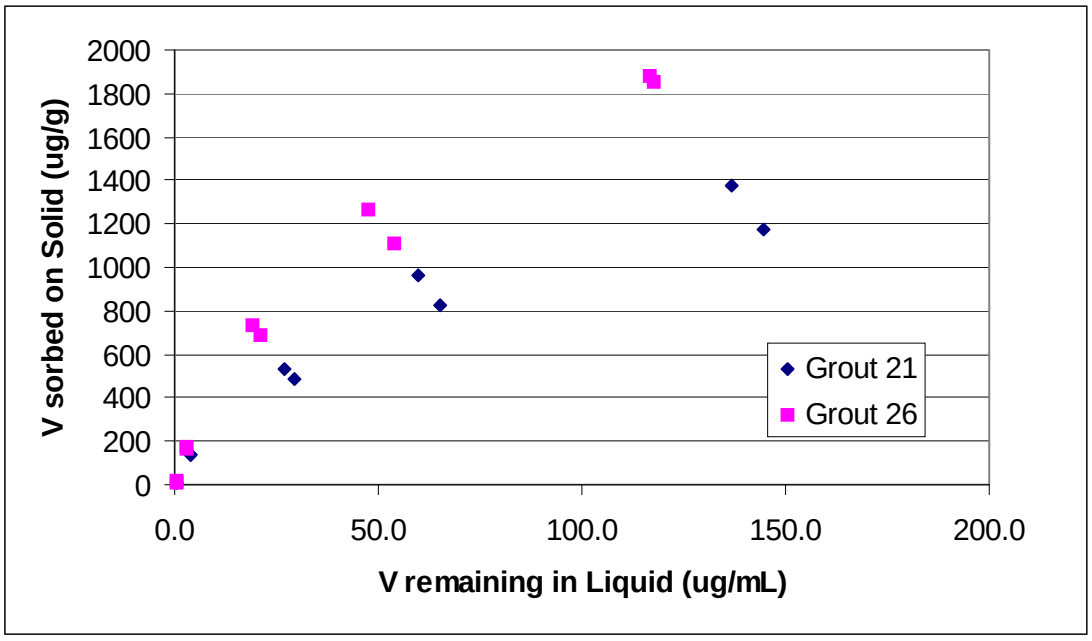

Figure 92. Isotherm for Vanadium sorption onto the two grout formulations.

Sorption of grout 26 was slightly greater than for grout 21. A Freundlich isotherm was generated by transforming vanadium concentrations to Log values. From these data, a linear regression (R^2 for both grout data sets was 0.97) gave the Freundlich parameters which are given on Figure 93, which is a Log/Log plot of these data. The K_d values are 46mL/g for Grout 26 and 28mL/g for Grout 21.

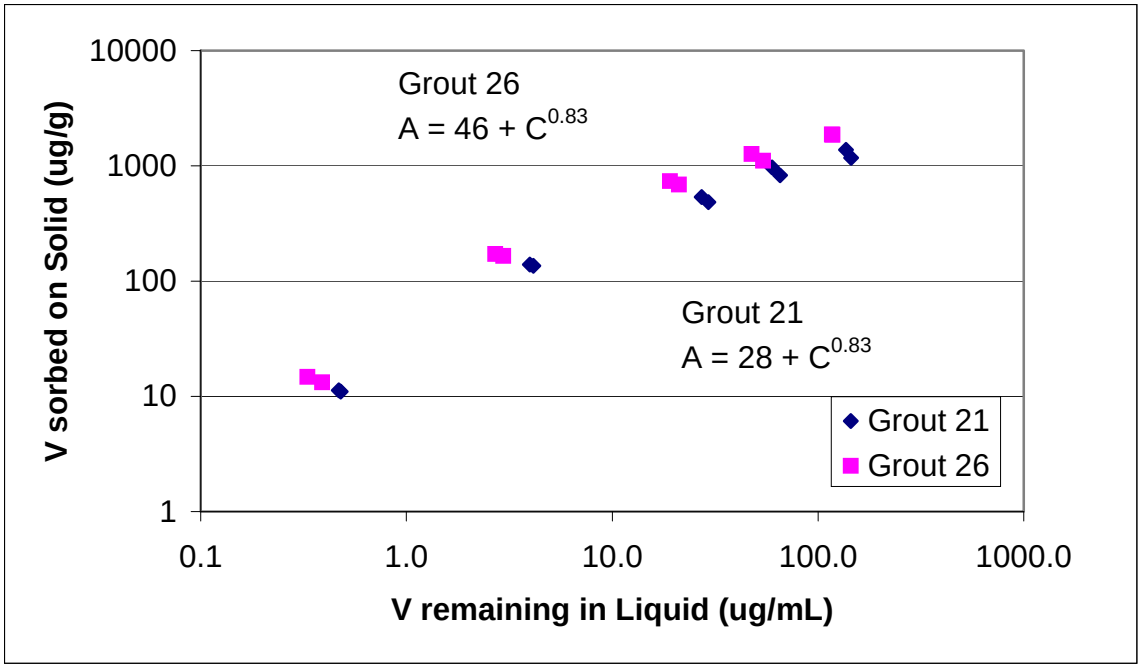

Figure 93. Freundlich isotherm for V sorption on the two grouts. The Freundlich equations are given.

Table 23.
Vanadium K_d calculated for each set

	Grout 21			Grout 26		
Nominal Activity	**Start V (mg/L)**	**End V (mg/L)**	**K_d (mL/g)**	**Start V (mg/L)**	**End V (mg/L)**	**K_d (mL/g)**
1	0.92	0.48	23	0.92	0.36	39
10	9.55	4.06	34	9.55	2.8	60
50	48.6	28.3	18	48.6	20	36
100	98.4	62.5	14	98.4	51	24
200	192	141	9	192	117	16

Cadmium Sorption onto Grouts.

For Cd uptake experiments, a 5500 mg/L solution of Cd was made using $CdCl_2$. In the experiments, the solution concentrations were 210, 106, 52, 10.4 and 0.58 mg/L. The experiment ran for 33 days, although the kinetics test showed that removal was very rapid, requiring only an hour for solution concentrations to be less than the detection limit of about 0.06 mg/L. No Cd was observed in solution in the isotherm experiments. Table 24 presents calculated K_d values based on the detection limit for Cd and on the mass removed from solution.

Table 24.
Cd K_d calculated for each set, based on Detection Limit and mass in experiments

	Grout 21			Grout 26		
Nominal Activity	**Start Cd (mg/L)**	**End Cd (mg/L)**	**K_d (mL/g)**	**Start Cd (mg/L)**	**End Cd (mg/L)**	**K_d (mL/g)**
1	0.58	0.06	>220	0.58	0.06	>220
10	10.4	0.06	>4300	10.4	0.06	>4300
50	53.7	0.06	>22,000	53.7	0.06	>22,000
100	106	0.06	>44,000	106	0.06	>44,000
200	214	0.06	>89,000	214	0.06	>89,000

Nickel Sorption onto Grouts

For Ni uptake experiments a 5000 mg/L solution of Ni was made using $NiCl_2$. Solution concentrations were: 175, 91.2, 45.6, 9.2, and 0.94 mg/L. The experiment ran for 16 days. Most samples were below detection limits of the ICP, about 0.1 mg/L. However, four samples did show detectable Ni with the highest at 0.9 mg/L. Results, averages of the replicates, are shown in Table 25. For those samples below the detection limit, K_d values were calculated based on the detection limit and the mass of Ni added to the experiment.

Table 25.
Ni K_d calculated for each set, most are based on Detection Limit and mass in experiments

	Grout 21			Grout 26		
Nominal Activity	**Start Ni (mg/L)**	**End Ni (mg/L)**	**K_d (mL/g)**	**Start Ni (mg/L)**	**End Ni (mg/L)**	**K_d (mL/g)**
1	0.94	0.1	>210	0.94	0.6	34
10	9.17	< 0.1	>2,300	9.17	< 0.1	>2,300
50	45.6	< 0.1	>11,000	45.6	< 0.1	>11,000
100	91.2	< 0.1	>18,000	91.2	< 0.1	>23,000
200	175	0.2	27,000	175	< 0.1	>44,000

Lead Sorption onto Grouts

Uptake experiments for Pb were conducted using a 7200 mg/L stock solution of $Pb(NO_3)_2$. In the experiments, the solution concentrations were 260, 131, 60, 12.7 and 1.7 mg/L. The experiment ran for 11 days, although the kinetics test showed that removal was very rapid, requiring only an hour for solution concentrations to be less than the detection limit of about 0.5 mg/L. No Pb was observed in solution in the isotherm experiments at a detection limit of about 0.2 mg/L. Table 26 gives estimated K_d values calculated from the detection limit and the mass of Pb added to the experiments.

Table 26.
Pb K_d calculated for each set, based on Detection Limit and mass in experiments

	Grout 21			Grout 26		
Nominal Activity	**Start Cd (mg/L)**	**End Cd (mg/L)**	**K_d (mL/g)**	**Start Cd (mg/L)**	**End Cd (mg/L)**	**K_d (mL/g)**
1	1.7	< 0.2	>190	< 0.2	1.7	>190
10	12.8	< 0.2	>1,600	< 0.2	12.8	>1,600
50	65.5	< 0.2	>8,200	< 0.2	65.5	>8,200
100	131	< 0.2	>16,000	< 0.2	131	>16,000
200	262	< 0.2	>33,000	< 0.2	262	>33,000

Silver Sorption onto Grouts

Uptake experiments for Ag were conducted using a 6875 mg/L stock solution of $AgNO_3$. In the experiments, the solution concentrations were 253, 126, 63, 12.6 and 1.22 mg/L. The experiment ran for 28 days, although the kinetics test showed that removal was very rapid, requiring only an hour for solution concentrations to be less than the detection limit of about 0.05 mg/L. No Ag was observed in solution in the isotherm experiments. Results are shown in Table 27, with K_d values based on the detection limit and the mass of Ag added to the experiments.

Table 27.
Ag K_d calculated for each set, based on Detection Limits and mass in experiments

	Grout 21			Grout 26		
Nominal Concentration	**Start Ag (mg/L)**	**End Ag (mg/L)**	**K_d (mL/g)**	**Start Ag (mg/L)**	**End Ag (mg/L)**	**K_d (mL/g)**
1	1.22	0.05	>590	1.22	0.05	>590
10	12.6	0.05	>6,300	12.6	0.05	>6,300
50	63.1	0.05	>32,000	63.1	0.05	>32,000
100	126	0.05	>63,000	126	0.05	>63,000
200	253	0.05	>130,000	253	0.05	>130,000

Barium Sorption onto Grouts

Uptake of Ba was measured on the two grout formulations. The 5300 mg/L stock solution of $BaCl_2$ was diluted to experiment concentrations measured at 0.9, 9.6, 49, 97, and 188 mg/L. The experiment ran for 56 days. Figure 94 shows that while most Ba was removed from solution, several mg/L of Ba remained. Consequently isotherm plots could be generated illustrating the K_d (around 1,600 mL/g) for Ba, based on slopes of the isotherms. Both grouts had similar behavior and the two regression lines overlie each other. Two points were excluded from the regression: those at X = 5 and 7.3. All other solution concentrations were below 3 mg/L, but with a detection limit of about 0.002 mg/L, Ba was readily detected. Values for K_d of the individual data sets are given in Table 28.

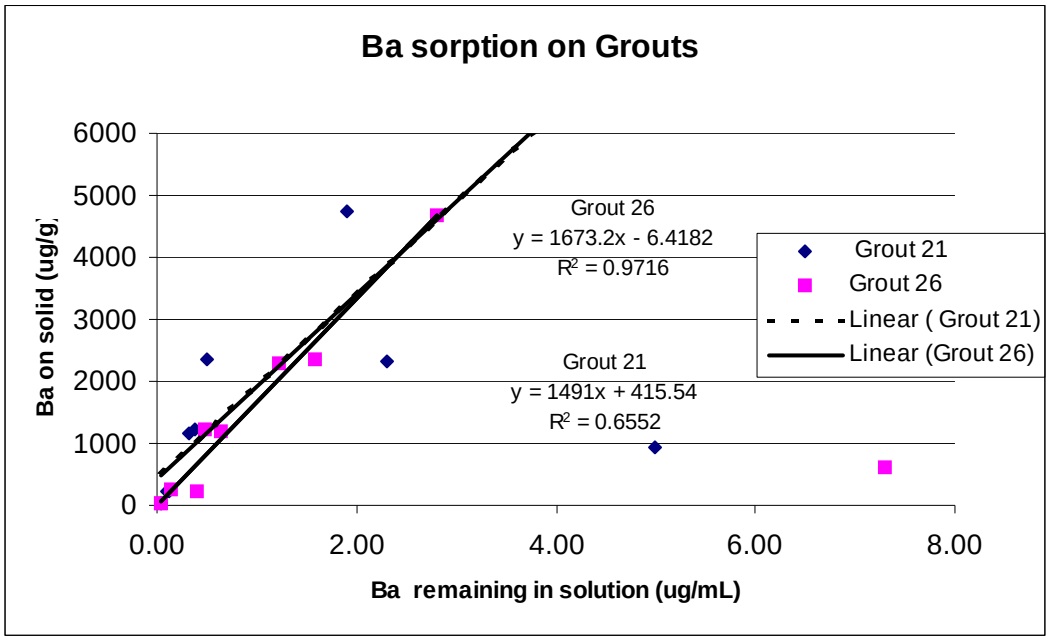

Figure 94. Isotherms for Ba sorbed on the two grout formulations. The regression lines for both grouts coincide. Two data points, at X=5 and X= 7.3 are removed from the regressions.

Table 28.
Ba K_d averages for each set

	Grout 21			Grout 26		
Nominal Concentration	**Start Ba (mg/L)**	**End Ba (mg/L)**	**K_d (mL/g)**	**Start Ba (mg/L)**	**End Ba (mg/L)**	**K_d (mL/g)**
1	0.82	0.05	390	0.85	0.05	450
10	9.7	0.12	2,000	9.8	0.26	1,200
50	47.9	0.36	3,400	48.8	0.56	2,200
100	95.4	1.4	2,800	94.4	1.40	1,700
200	188	3.5	1,700	186	5.0	1,100

Selenium Sorption onto Grouts

Sorption of Selenium on the two grout formulations was determined using a solution of Na_2SeO_4. A stock solution of 5200 mg/L Se was diluted to give experiment concentrations of 1.28, 10.6, 47.5, 96.1, and 190 mg/L. Results of a kinetics experiment, shown in Figure 95 indicated that the little sorption that took place was rapid. The experiment ran for 46 days before it was sampled. Sorption of Se was very low, consequently small differences in uptake and normal analytical variability resulted in a large degree of scatter in the data. Figure 96 shows that using linear regression, the slopes of the isotherms were 1.18 mL/g and 0.65mL/g respectively for grouts 26 and 21. The difference between the two is not significant. Table 29 presents averages of the duplicate data points and the K_d values calculated from them.

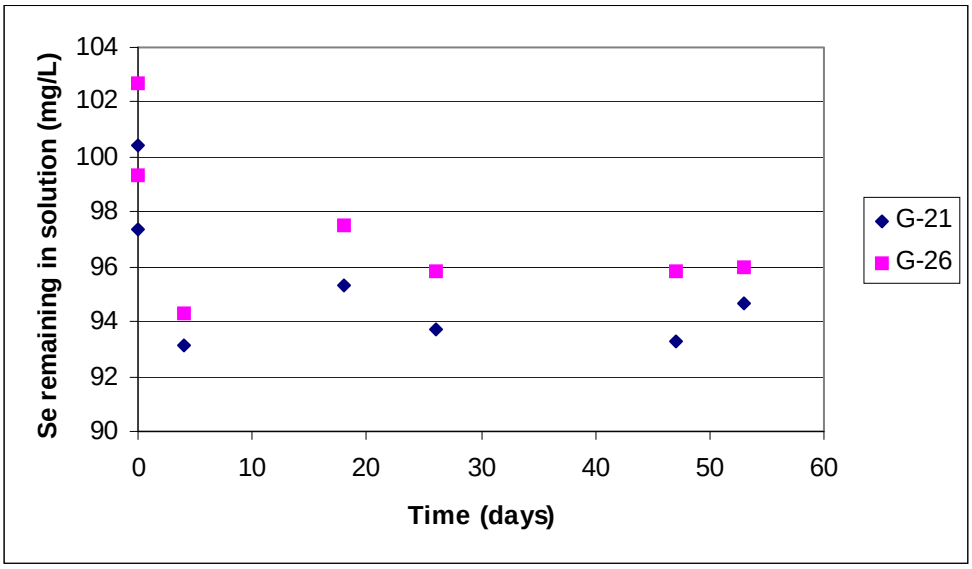

Figure 95. Sorption kinetics of Se on the two grout formulations.

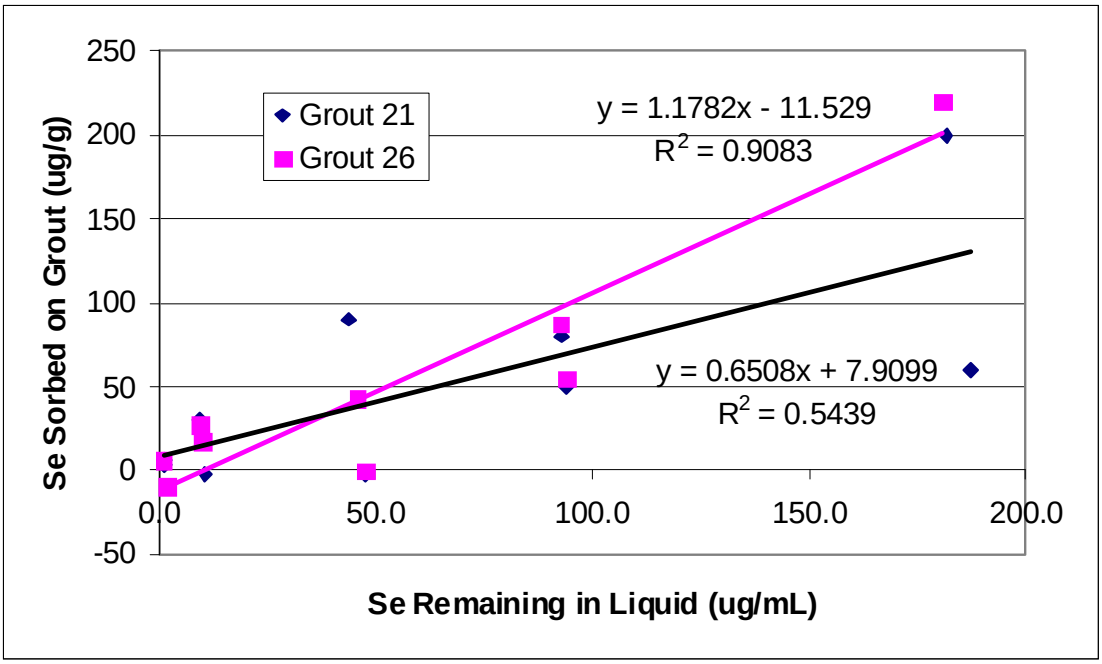

Figure 96. Isotherms for Se sorbed on the two grouts.

Table 29.
Se K_d averages for each set

	Grout 21			Grout 26		
Nominal Activity	**Start Se (mg/L)**	**End Se (mg/L)**	**K_d (mL/g)**	**Start Se (mg/L)**	**End Se (mg/L)**	**K_d (mL/g)**
1	1.28	1.08	4.6	1.28	1.36	0
10	10.6	10.1	1.5	10.6	9.7	2.4
50	47.5	45.8	1.0	47.5	46.6	0.5
100	96.1	93.5	0.7	96.1	93.2	0.8
200	190	184	0.7	190	181	1.2

Hg Sorption onto Grouts

Uptake experiments for Hg were run using mercury acetate $(HgC_2H_8O_2)_2$ from a 55 mg/L stock solution. This was diluted to concentrations of 36, 73, 264, 613, and 1405 μg/L in the experiments. Sorption was complete in less than 25 days and the experiment ran for 74 days. No Hg was observed in the isotherm solutions at a detection limit of about 2 ng/L for a 0.4 mL sample. A Milestone Instruments Direct Mercury Analyzer was used for analysis. Results are shown in Table 30, with K_d values based on the detection limit and the mass of Hg added to the experiments.

Table 30.
Hg K_d calculated for each set, based on DL and mass in experiment

Grout 21			Grout 26		
Start Hg (ng/L)	**End Hg (ng/L)**	**K_d (mL/g)**	**Start Hg (ng/L)**	**End Hg (ng/L)**	**K_d (mL/g)**
36	2.0	>430	36	2.0	>430
73	2.0	>890	73	2.0	>890
264	2.0	>3,300	264	2.0	>3,300
613	2.0	>7,600	613	2.0	>7,600
1405	2.0	>18,000	1405	2.0	>18,000

TCLP Testing of Grouts

Four grout samples, for TCLP testing, were made containing contaminant elements of interest. The grout formulations, 21b and 26a, were made in 250 gram batches. Each was made with a high loading as well as a low loading of contaminants. The grouts were produced as described earlier and the contaminants were added as an aqueous mixture, taking the place of some of the water in the grout mixtures. The surrogate waste was made with major ion composition as shown in Table 31.

Table 31. Major Ion Composition of Surrogate Waste

Component	Concentration mg/L (mM)	Component	Concentration mg/L (mM)
Ca	9.2 (0.23)	NO_3	5500 (88.7)
CO_3	7980 (133)	CrO_4	560 (4.8)
K	360 (9.2)	Li	25 (3.6)
Na	15000 (652)	SO_4	596 (6.2)
NO_2	11200 (243)	pH	10.3

The surrogate waste was made up to 950 mL then small aliquots of solutions containing the various elements of interest were added and the total volume brought to one liter. The contaminant concentrations are given in Table 32. One set of grouts were made to contain a low loading of the waste, another had a higher loading. Quantities of surrogate waste in each 250 g batch are given in Table 33. These samples aged for about one month and were sent to General Engineering Laboratories (Charleston, SC) for TCLP testing. Standard SW-846 methods were used, with most analyses done by ICP-OES. Results are shown in Table 34, along with detection limits for each element.

Table 32. Concentrations of Elements of Interest in Surrogate Waste

Element	Concentration mg/L	Element	Concentration mg/L
Ag	1.0	V	1.0
As	1.0	Tl	2.0
Ba	1.0	Sb	6.1
Be	1.0	Pb	5.5
Cd	1.0	Ni	5.0
Se	1.0	Hg	0.5

Table 33. Quantities of Surrogate Waste Added to Grouts

Grout	High Loading (g)	Low Loading (g)
21b	20.0	3.87
26a	21.26	4.11

Most elements were found at either very low concentrations or were not detected at all: in this case they are given as the detection limit in Table 34. The following were below detection limits: Cd, Pb, Hg, Ni, Ag, and Tl. All were found at concentrations below 0.2 mg/L, with the exception of Ba which, at about 1.2 mg/L, was still far below TCLP limits of 100. No elements were found to exceed, or even approach, the TCLP limits.

The release of most of the RCRA elements to the TCLP solution is likely controlled by pH. A few, such as V, Cr and As, seem to show a waste loading effect which would indicate that they are not solubility limited. The grouts containing higher loadings, in these cases, leached a little more of these elements. There is no systematic difference in performance between the two grout formulations.

Table 34. TCLP Results (mg/L)

Element	G-21 High Loading	G-21 Low Loading	G-26 High Loading	G-26 Low Loading	Detection Limit
Sb	0.102	0.060	0.039	0.060	0.035
As	0.115	0.084	0.069	0.065	0.024
Ba	1.220	1.230	1.000	1.090	0.004
Be	0.006	0.003	0.003	0.003	0.003
Cd	0.004	0.004	0.004	0.004	0.004
Cr	0.054	0.031	0.029	0.026	0.007
Pb	0.038	0.027	0.027	0.027	0.027
Hg	0.0005	0.0005	0.0005	0.0005	0.0005
Ni	0.015	0.015	0.015	0.015	0.015
Se	0.044	0.034	0.069	0.080	0.034
Ag	0.012	0.012	0.012	0.012	0.012
Tl	0.100	0.100	0.100	0.100	0.100
V	0.128	0.107	0.142	0.123	0.006